FINITE ELEMENT ANALYSIS OF SUPPORTED EXCAVATIONS IN CLAY

Merih SÖZER

December, 1986

Boğaziçi University

FINITE ELEMENT ANALYSIS OF SUPPORTED EXCAVATIONS IN CLAY

by

MERİH SÖZER

B.Sc.in C.E., Istanbul Technical University,1986

Submitted to the Institute for Graduate Studies in Science and Engineering in Partial Fulfillment of the Requirements for the Degree of

Master of Science

in

Civil Engineering

Boğaziçi University

December, 1986

ACKNOWLEDGEMENTS

I would like to emphasize my sincere gratitude to those who assisted me during the development and the preparation of this study, primarily to my thesis supervisor Prof.Dr. H.Turan Durgunoğlu for his invaluable criticisms, recommendations and orientations.

I am indebted to the Staff of Boğaziçi University Civil Engineering Department for their generous help and constructive criticizms.

I am also indebted to all Boğaziçi University Computer Center personnel for making facilities avilable to me.

Istanbul, December,1986 MERİH SÖZER

ABSTRACT

In this study, various soil mechanics problems are investigated using the computer program developed by Clough and Duncan (1969). By this program, both incremental analyses and gravity turn-on analyses can be provided. Moreover, different construction procedures can also be realized, such as fill construction, excavation, material alteration,water level changes, structural elements construction.

In the second chapter, general idea of incremental soil-structure interaction problems is given. Meanwhile, stress-strain behaviour of soil which is assumed to be non-linear, stress dependent throughout the computer program is explained in detail. Additionally, the techniques for obtaining the parameters which are necessary to perform the computer program are discussed. The behaviour of interface elements are studied in this chapter.

In the third chapter, different soilmechanics problems are analyzed by using the options of computer program. In the fourth chapter, a supported excavation problem which is a project of excavation system of Istanbul Metro is analyzed in order to predict system behaviour.

The manual of computer program is presented in appendix.

ÖZET

Bu çalışmada, çeşitli zemin mekaniği problemleri Duncan ve Clough (1969) tarafından geliştirilmiş bilgisayar programı kullanılarak incelenmiştir. Bu program ile inşaat safhalarının etkisi incelenebilmekte ve ayrıca inşaat safhaları ele alınmadan analiz yapılması sağlanabilmektedir. Buna ek olarak, dolgu inşaatı, kazı, malzeme değişimi, su seviyesi değişimleri, yapı elemanları inşaatı gibi çeşitli inşaat uygulamaları gerçekleştirilebilmektedir.

İkinci bölümde, yapı-zemin etkileşim problemlerinin genel olarak esası verilmiştir. Bu sırada, lineer olmayan ve gerilmeye bağlı zeminlerin gerilme-şekil değiştirme bağıntıları detaylı olarak anlatılmıştır. Ayrıca, bilgisayar programı için gerekli zemin parametrelerinin elde edilmesinde kullanılan teknikler de verilmiştir. Arayüz elemanlarının davranışları da bu bölümde gösterilmiştir.

Üçüncü bölümde, çeşitli zemin mekaniği problemlerinin analizi bilgisayar programının seçenekleri kullanılarak yapılmıştır. Dördüncü bölümde, İstanbul Metrosunun iksali kazı sisteminin analizi sistem davranışının tahmini için gerçekleştirilmiştir.

Bilgisayar programının bilgi girişi ek'te verilmiştir.

LIST OF FIGURES

LIST OF FIGURES (Cont'd)

LIST OF FIGURES (Cont'd)

LIST OF TABLES

LIST OF SYMBOLS

Greek Letters

α	coefficient of Linear thermal expansion
α_A	arctangent of coefficient of lateral earth pressure at rest
δ_s	relative shear displacement
δ_η	relative normal displacement
$\{\delta\}$	nodal point displacements vector
Δ_η	relative normal displacement
Δ_s	relative shear displacement
$\Delta\sigma_x$	change in horizontal stress
$\Delta\sigma_y$	change in vertical stress
ΔT	change in temperature
Δu	change in pore pressure
ε_x	horizontal strain
ε_y	vertical strain
γ	unit weight of soil
γ_ω	unit weight of water
ν	Polsson's ratio
ν_{ult}	ultimate value of Polsson's ratio
ϕ	angle of internal friction
ϕ'	effective angle of internal friction
ϕ_d	drained value of angle of internal friction

LIST OF SYMBOLS (Cont'd)

σ_1	major principal stress
σ_1	effective major principal stress
σ_3	minor principal stress
σ_3	effective minor principal stress
$\sigma(1), \sigma(2), ..$	stress at the center of an element
$\{\sigma\}_e$	stress vector for interpolation elements
$(\sigma_1-\sigma_3)_f$	principal stress difference at failure
$\{\sigma\}_n$	stress vector for element nodal points
σ_x	horizontal stress
σ_x'	effective horizontal stress
σ_y	vertical stress
σ_y'	effective vertical stress
$(\sigma_1-\sigma_3)_{ult}$	maximum principal stress difference predicted by hyperbolic stress-strain relationship
τ	shear stress
τ_f	shear stress at failure for interface element
τ_{xy}	shear stress on x-y plane
τ_{ult}	shear stress at failure predicted by hyperbolic load-displacement curve for interface element
ψ_A	arctangent of incremental coefficient of lateral earth pressure at rest

English Letters

a	reciprocal of initial tangent modulus or initial tangent stiffness
$a_1, a_2..$	interpolation coefficients
$\{a\}$	vector of interpolation coefficients
a_v	rate of change of void ratio with change in pressure
b	reciprocal of ultimate principal stress difference or ultimate shear stress on an interface.

LIST OF SYMBOLS (Cont'd)

c	cohesion
c'	effective cohesion
C	lumped constant for all constant terms in consolidation modulus equation
D_r	relative density
e	void ratio
e_o	initial void ratio
E	Young's modulus
E_i	initial tangent modulus
E_t	tangent modulus
E_{ur}	unloading-reloading modulus
{F}	force vector for guadrilateral element nodal points
FUEL(I)	future level of phreatic line at specified interval
{H}	8x12 matrix defining guadrilateral boundary geometry
HTB	new y coordinate on top of backfill
k_n	normal stiffness, interface element
k_s	shear stiffness, interface element
k_{si}	initial tangent shear stiffness, interface element
k_{st}	tangent shear stiffness, interface element
[K]	general stiffness matrix
K_j	coefficient of proportionality between interface initial shear stiffness and power function of interface normal stress
K_m	coefficient of proportionality between initial tangent modulus and power function of minor principal stress
K_o	coefficient of lateral earth pressure at rest
$K_o\Delta$	incremental coefficient of lateral earth pressure at rest

LIST OF SYMBOLS (Cont'd)

K_{ur}	coefficient of proportionality between unloading-reloading modulus and power function of minor principal stress
[m]	element coordinate matrix
M_B	bulk modulus
M_D	deviatoric modulus
n	exponent for stress-dependent modulus relationship
[n]	coordinate matrix of the nodes of element
NMlTYP	material type number for backfill type 1
p_a	atmospheric pressure
p'	effective pressure in consolidation test
{P}	nodal point forces vector
PREL(I)	present level of phreatic line at specified interval
R_f	correlation factor
R_x	horizontal nodal force
R_y	vertical nodal force
S	stress level
u	tangential nodal displacement
v	normal nodal displacement
x	horizontal coordinate
XIL	horizontal distance between nodal points I and L
XJL	horizontal distance between nodal points J and I
XKJ	horizontal distance between nodal points K and J
XLK	horizontal distance between nodal points L and K
XW(I)	horizontal distance of phreatic line to the end of specified interval
y	vertical coordinate
XIJ	vertical distance between nodal points I and J

LIST OF SYMBOLS (Cont'd)

YJK	vertical distance between nodal points J and K
YKL	vertical distance between nodal points K and L
YLI	vertical distance between nodal points L and I
YAVG	averaged vertical distance of center of gravity of an element

TABLE OF CONTENTS

TABLE OF CONTENTS (Cont'd)

TABLE OF CONTENTS(Cont'd)

I. INTRODUCTION

Almost all, civil, environmental, transportation, structural and geotechnical engineers are intimately concerned with soil mechanics concept. This is because nearly all the construction endeavors of those engineers are concerned with soil behaviour, since either the soil is used as a construction material or a structure is placed upon it. Thus, the study of soil mechanics is of considerable economic importance in terms of above mentioned engineering branches, since soil is the most readily available construction material at any site. On the otherhand, the behaviour of soil is still understood by experience rather than engineering methods in many respect. Namely, experience is still a dominant factor in the solution of soil mechanics problems. This is largely attributed to the quite complex structures of soils and the errors due to the assumptions made for simulating the soil parameters.

The most general purpose method of analyses of soil mechanics problems is the Finite Element Method. In this study, the Finite Element Method is utilized considering construction sequences and assuming nonlinear, stress dependent soil

behaviour (Clough and Duncan,1969). This way, general soil mechanics problems can be solved both efficiently and accurately instead of using graphical and other analytical techniques. Furthermore, the importance of experience is decreased by providing adequately representative soil parameters. Those parameters should be sufficient in number to represent all aspects of soil behaviour as in the case of the parameters of nonlinear hyperbolic stress-strain behaviour. In some problems, the dominant factor may be construction sequences and real representation of those is to be simulated. This technique also considers the construction sequences. Accordingly the Incremental Finite Element Method provides great facilities in tackling with different soil mechanics desing problems and shortcomings of methods at hand are eliminated.

By using the Incremental Finite Element Method, fill construction, excavation, water level changes, construction of structural elements and boundary water pressures or any other external loads can be taken into account in different orders. This method was successfully applied by Clough and Duncan (1969) in the design of Port Allen and Old River Locks, and later also in many other projects. Hence, very efficient tool for designing the soil mechanics problems has been introduced.

II. METHODS OF ANALYSIS

2.1 INTRODUCTION

In this chapter, the finite element theory and its applications in the solutions of soil mechanics problems are introduced briefly. Then, the computer program developed by G.W. Clough and J.M.Duncan (1969) which is used in this study is presented with all features in detail. Particularly, attention is given to simulate various construction stages such as gravity turn-on, incremental exavation, water pressure loading, fill or concrete placement, temperature loading of structural material.

At the succeeding paragraphs, material types and formulations used in the computer program are introduced in terms of both theory and application. Assuming, the soil behaves non-linearly, the stress-strain behaviour of soil elements on primary loading and on unloading and reloading is described. The behaviour of interface elements used between the soil and the various construction materials is also summarized.

2.2 FINITE ELEMENT METHOD

The basis for the finite element method has been described by Clough (1960). In this method, a continum is represented as an assemblage of the finite elements assumed to be connected only at the nodal points located along the boundary of the elements. The nodal point displacements $\{\delta\}$ are the basic unknowns of the system and are related to the prescribed nodal forces $\{P\}$ by a general stiffness matrix $[K]$. This relationship is expressed as

$$[K] \cdot \{\delta\} = \{P\} \qquad (2.1)$$

The general stiffness matrix $[K]$ is an assemblage of the stiffnesses of the individual finite elements, combined by a process known as the direct stiffness technique. Solving for the unknown displacements requires solution of the set of the the simultaneous equations described by equation (2.1), an operation that necessititates the use of a high speed computer because realistic system typically involve several hundred degrees of freedom.

Equilibrium in the finite element method is quaranteed only for the nodal point forces, local equilibrium conditions along the boundaries of the elements may not be satisfied. Generally, across element boundaries, only displacement compatibility is assumed, and discontinulties in stress and strain will occur.

Element stiffnesses are derived on the basis of an assumed displacement pattern within an element. For two-dimensional

plane elements, Clough(1960) derived an element stiffness using a linear displacement function, and Felippa(1966) developed element stiffnesses for quadratic and cubic displacement functions. The assumed displacement patterns control the number of nodes needed for an element because the number of nodes must be consistent with the degree of the assumed displacement pattern, and must be sufficient to insure displacement compatibility between elements.

Most commonly, triangular or(rectangular elements are used, but more general shapes , such as arbitrary quadrilaterals with curved boundaries, have been considered (see Ergutoudis, et al., (1968)). Wilson (1963) has shown that the most satisfactory results for general application of finite-element method are obtained by use of quadrilateral elements composed of an assemblage of triangular elements.

As a summary, the simple algorithm for the finite element method is described in figure (2.1).

In conventional finite element theory due to the experience obtained from lock structures, some modifications were done by G.W.Clough and J.M.Duncan (1969) for representing soil behaviour. By this modifications, the soil interface behaviour described more conveniently. Those are summarized below.

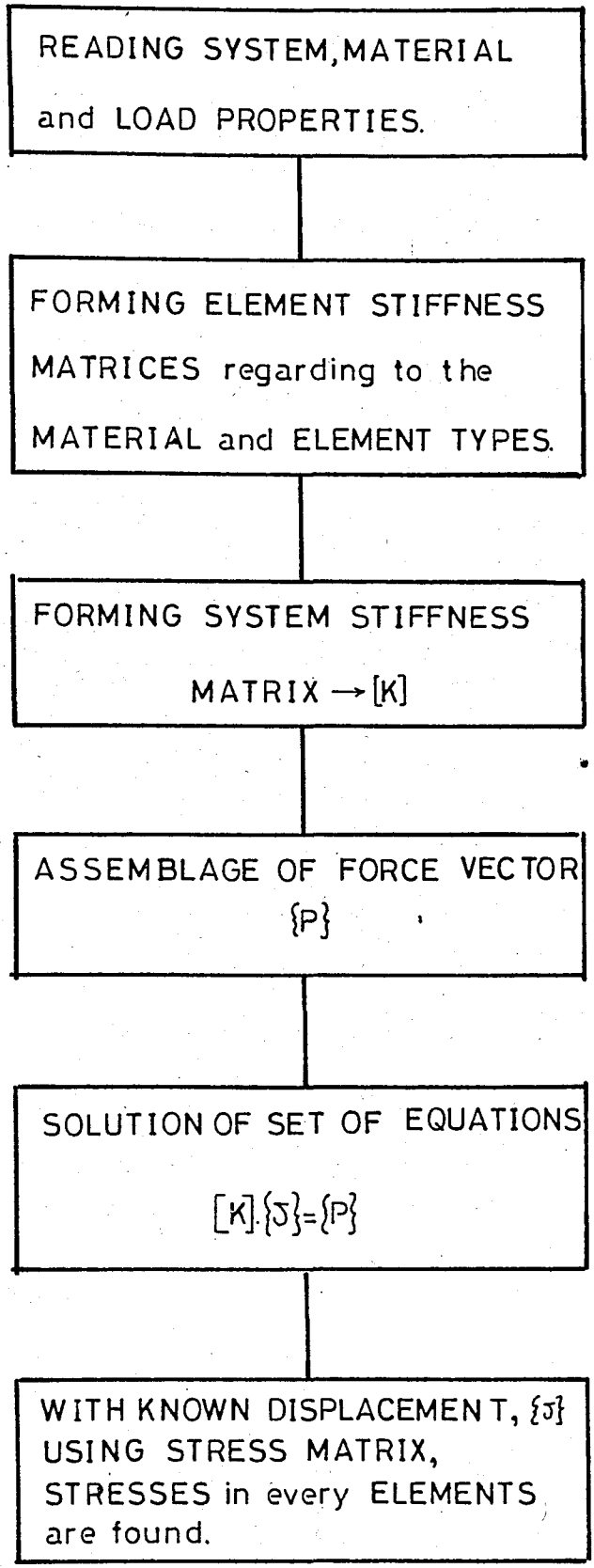

FIGURE (2.1)
ALGORITHM for the Finite Element Method

A. Element Failure

It was noted that failure was occuring in localized areas of the finite element mesh. In order to better represent the behaviour of these localized areas after failure, three constitutive equations relating stresses and strains were formulated.

The constitutive equations for plane strain initially employed were;

$$\begin{bmatrix}\sigma_x\\ \sigma_y\\ \tau_{xy}\end{bmatrix} = \frac{E}{(1+\nu).(1-2.\nu)} \begin{bmatrix}(1-\nu) & 0 & 0\\ 0 & (1-\nu) & 0\\ 0 & 0 & \frac{(1-2\nu)}{2}\end{bmatrix} \begin{bmatrix}\varepsilon_x\\ \varepsilon_y\\ \tau_{xy}\end{bmatrix} \qquad (2.2)$$

It has been shown by Woodward (1966) that these equations may also be formulated in terms of a modulus related to the behaviour of a soil under the action of deviatoric stresses, the deformation modulus, M_D, and a modulus related to the behaviour of a soil under the action of hydrostatic stresses, the bulk modulus, M_B. This formulation given by Woodward(1966) yields the constitutive equations in the following form :

$$\begin{bmatrix}\sigma_x\\ \sigma_y\\ \tau_{xy}\end{bmatrix} = \begin{bmatrix}M_B + M_D & M_B - M_D & 0\\ M_B - M_D & M_B + M_D & 0\\ 0 & 0 & M_D\end{bmatrix} \cdot \begin{bmatrix}\varepsilon_x\\ \varepsilon_y\\ \gamma_{xy}\end{bmatrix} \qquad (2.3)$$

in which M_D is the deformation modulus and M_B is the bulk modulus. By employing this formulation a failed element was

assigned a reduced deformation modulus value, and thereby a reduced resistance to shear, but the value of bulk modulus was not reduced so that the element still offered resistance to hydrostatic stresses. The deformation modulus was calculated as shown in Equation (2.4) using the values of tangent modulus and Poisson's ratio for primary loading or unloading-reloading, whichever was appropriate.

$$M_D = \frac{1}{2} \cdot \left(\frac{E_t}{1+\nu}\right) \qquad (2.4)$$

Thus, the deformation modulus varied in the same manner as E_t for primary loading and E_{ur} in unloading-reloading.At failure, both E_t and E_{ur} were assigned very small values so that the calculated deformation modulus value was also small. The bulk modulus value was assumed to be constant for a given minor principal stress value in primary loading and unloading-reloading. This assumption was based upon the observation that volume changes during shear of specimens in laboratory triaxial tests with constant values of σ_3 are small, and the void ratio of the test specimens after shear is very nearly the same as that before shear. Therefore, the deformation under the influence of hydrostatic stresses before and after shear would be abaut the same, and the bulk modulus values would not be expected to vary with shear stress, but only with confining pressure.

The bulk modulus value was assumed to vary with confining pressure in the same manner as the initial tangent modulus and the unloading-reloading modulus. A similiar type of stress-

dependency has been determined for the bulk modulus by Vesic and Clough(1968) and Domaschuk and Wade(1969). The equation employed to calculate the Bulk Modulus was,

$$M_B = \frac{1}{2} \cdot \frac{E}{(1+\nu).(1-2.\nu)} \qquad (2.5)$$

in which E was E_i during loading and E_{ur} during unloading-reloading.

The resulting behaviour for the soil elements at moderate stress levels, which represented most of the elements in the analysis, using new formulation of equation (2.3) was the same as when using original formulation of equation (2.2). However, at failure, the behaviour of a soil element was more consistent with actual soil behaviour under these conditions than was obtained using the original formulation.

B. Interface Element Normal Stresses

For the interface elements, it was noted that around the junction of vertical and horizontal boundaries the calculated value of normal stress were somewhat erratic. It was found by Clough and Duncan (1969) that more consistent pattern of normal stresses on the interface could be obtained from the adjacent two-dimensional elements. These more consistent pattern of normal stresses were then employed in the calculation of shear stiffness values for the interface elements and a more reasonable behavioral pattern was found to result.

C. Overshoot of Allowable Interface Shear Strength

It was also noted by Clough and Duncan (1969) for the interface elements that the value of shear stress developed on the interface during any one increment would sometimes "overshoot" the allowable shear stress by a large amount. To correct this behaviour, the increment of analysis was repeated with forces applied at the nodes of the interface element representative of the allowable shear stress on the element.

After incorporating these modifications into the procedure, more convenient way of finite element analyses for soils is realized., by Clough and Duncan (1969).

2.3 APPLICATION OF FINITE ELEMENT THEORY TO SOIL MECHANICS

The application of the finite element method to continuous structures was introduced by Clough(1960). Subsequently, by extending the method, a variety of complex structural and soil and rock mechanics problems have been treated, many of which are described by Zienkewicz and Cheung (1967).

The development of the finite element method has greatly facilitated the theoretical analysis of stresses and displacements in soil. Factors such as material anisotropy and non-homogeneity and irregular problem geometry and loading conditions can be considered, Moreover, the method has been extended to include the effects of local yield by considering nonlinear and elasto-plastic behaviour.

Due to its broad aspects and complexity, the soil-structure interaction and incremental finite element analyses problems are considered to be the most versatile soil mechanics subject in which many kinds of simulations can be realized. Therefore, soil-structure interaction problems are the most sophisticated case of the finite element method in soil mechanics. Various kinds of problem have been simulated so far are :

- Analysis of earth banks during earthquakes-Idriss and Seed (1967)
- Incremental analyses of earth dams-Clough and Woodward (1967)
- Analyses of layered pavement systems-Duncan, Moniswith and Wilson (1969)
- Footing and retaining wall analyses-Girijavallabham and Reese (1967)

- Analyses of jointed rock behaviour-Goodman, Taylor and Bekke (1968)
- Analyses of slopes in soil-Dunlop, Duncan and Seed (1968)
- Three dimensional analyses of arch dams and their foundations-Ergatodis, Irons and Zienkiewicz (1968)
- Underground powerhouse analyses with "no tension" rock material-Zienkiewicz, Valliappan and King (1968)
- Response of earth dams to travelling seismic waves-Dibaj and Penzien (1969)
- Nonlinear analysis of stresses and strains in soils-Duncan and Chang (1969)
- Analysis of soil movements around a deep excavation-Duncan and Chang (1969)

2.4 USED COMPUTER PROGRAM

Initially, the program used in this study was written to apply the procedure for the finite element analysis of reinforced concrete U-frame lockstructures and to apply it to the analysis of Port Allen and Old River Locks.

The procedures developed (Clough and Duncan, 1969) involve the use of incremental finite element analyses with nonlinear, stress-dependent, inelastic soil stress-strain behaviour. The soil stress-strain parameters required for these analyses may be determined from the results of triaxial compression tests on the soil or from the results of direct-shear and consolidation tests. The reinforced concrete is treated as a linear-elastic material characterized by a sustained modulus

which may be determined from the results of creep tests. The properties of the interface between concrete and soil are expressed in terms of a non-linear, stress-dependent,stress-strain relationship.

Application of the program to the analyses of Port-Allen and Old-River locks showed that the procedures gave results in good agreement with the results of extensive instrumentation program on these structures. With the values obtained from the program, internal moments and shears in structural elements as well as structural deflections , external pressures and soil movements can be calculated.

The incremental construction or loading may consists of excavation, fill or concrete placement, water pressure changes on pervious soil elements, boundary water pressure loading on impervious elements and temperature loading of structural material. The stress-strain behaviour of soil elements may be linear or non-linear with hyperbolic, stress dependent stress-strain behaviour on primary loading or stress-dependent strees-strain behaviour on unloading and reloading.Material behaviour may be drained or undrained or some materials are drained while others undrained.

Interface elements may be used to allow relative displacements on the boundary between two adjacent two-dimensional elements. Interface elements may be set to "inactive",assumed to be not present, or "active", allow relative displacements. Those elements have bilinear stress-strain behaviour.

The program SOIL-STRUCT developed by Clough and Duncan

(1969) and used in this study consists of subroutines which realize the arbitrary incremental analyses and controlled by the main-deck. The main deck, namely main part of the program, reads the input and directs the program in a specified subroutine. The subroutines are summarized below,

1. Subroutine-INITIAL calculates initial stresses for all elements, displacements for all nodal points, modulus values for two-dimensional elements and stiffness values for interface elements.

2. Subroutine-STRSTF assembles the general stiffness matrix for the entire structure, adds in concentrated loads at the nodal points, adds in loads due to boundary pressures and modifies the system stiffness matrix for boundary conditions.

3. Subroutine-QUAD generates the element stiffness matrix for each two-dimensional elements, formulates the constitutive equations, and if specified, generates element loadings due to gravity or temperature changes.

4. Subroutine-JTSTF generates the element stiffness matrix for each interface elements.

5. Subroutine-EXCAV, if excavation is specified, interpolates for the stresses on the excavation boundary, adds loads due to equivalent nodal forces on the excavation boundary and assigns minimal stiffness values to excavated interface and two-dimensional elements.

6. Subroutine-EQNDFO calculates equivalent nodal forces for excavation boundary stresses or water pressure changes on the boundaries of an element.

7. Subroutine-SEEP calculates new pore pressures at the nodes of an element and distributes equivalent nodal loads obtained for the water pressure changes. This subroutine is used for the previous-soil elements.

8. Subroutine-BUILD is used for the fill and concrete placement. It assigns appropriate material types and initial modulus values to backfill and concrete elements and activates interface elements.

9. Subroutine-BANSOL solves the simultaneous equations obtained from the system stiffness matrix and the system load vector for nodal point displacements.

10. Subroutine-STRESS calculates incremental stresses, adds stresses, and prints stresses for two-dimensional elements. Moreover, displacements are also cumulated.

11. Subroutine-JSTRESS calculates and prints stresses for one-dimensional interface elements.

12. Subroutine-MODCAL checks interfaces and two-dimensional elements for failure and calculates modulus values and stiffness values for interface and two-dimensional elements respectively.

In the following sections the essence of subroutines, namely theories and applications used are described.

A. GRAVITY TURN-ON ANALYSES

The essence of gravity turn-on analyses is to ignore construction sequence, and then apply gravity forces throughout the medium employing constant values of modulus and the poisson's ratio. In many soil-structure interaction problems, the types of loading of principal importance are those due to gravity and water-pressures. Many finite element programs contain options for simulating gravity and water pressure loading on linear-elastic material. Hence, if appropriate modulus values could be chosen to represent the behaviour of the lock and the surrounding soils, analyses could be conducted very conveniently using standard program options.

Determination of modulus values for soils for use in a Linear-elastic analyses is made difficult by the number of factors which influence the stress-strain behaviour of a soil. Representation of all of these factors as they occur in a field-problem by a laboratory test on an "undisturbed specimen" is seldom achieved. However, even if the soil and testing conditions were ideally representative of the in-situ conditions, it is very difficult to select a single modulus value to represent soil stress-strain behaviour, because the behaviour of soils is essentially non-linear.

The shortcomings of gravity turn-on analyses in simulating actual construction procedures have been discussed by Goodman and Brown (1966), Clough and Woodward (1967), and Dunlop,Duncan and Seed (1968). Basically, the drawbacks lie in the difficulties in accommodating general initial stress conditions, the necessity

for neglegting the effects of stress history on material properties, and inaccuracles in calculated deflections. Because gravity turn-on analyses do not correctly represent the sequence of loading which occurs during construction, it might be anticipated that these analyses would not correctly represent the soil-structure interaction.

However, in the view of simplicity of gravity turn-on analyses, it was consired to be worthwhile to examine the effectiveness of this procedure by the two dimensional finite element program developed by Professor E.L. Wilson of the University of California, Berkeley. In the program, the slip on the interface between the structural material and the soil was not considered.

The validity of the gravity turn-on approach is tested by Clough and Duncan (1969) for Port-Allen lock using various material property assumptions to determine if reasonable values for the material properties could be chosen to give calculated results that agreed with the observed results.

According to results obtained from this study, the linear-elastic, gravity turn-on analyses do not correctly represent a satisfactory approach to the analyses of the incremental-soil-structure interaction problems, and it is difficult to select a correct modulus value for soils. This approach is used, in SOIL-STRUCT computer program, only in the calculation of initial stresses and displacement. After initial calculations, incremental analyses assumes the non-linear behaviour of soils.

B.INCREMENTAL EXCAVATION

Dunlop,Duncan and Seed (1968) have shown that the excavation problems can be solved by finite element technique applying stresses to the nodal points of the excavation surface. In this technique, stresses created by excavation are determined, then equivalent nodal loads for these stresses acted equally but in opposite sense to these nodal points. Since the stresses applied to the excavation boundary are equal in magnitude but in opposite sense to the initial stresses, the excavation boundary becames stress-free. Excavated elements are assigned a minimal stiffness, to prevent any interaction with the rest of the elements during excavation.

In the finite element technique, stresses generally are found at the center of the elements, but the excavation boundary between the elements, stresses should somehow be converted to the nodal points of the finite elements. Dunlop, et al, (1968) determined the stresses on the boundary by averaging the stresses in pairs of adjacent elements on opposite sides of the boundary. Equivalent nodal loads were then calculated assuming that these stresses were constant along the boundary between adjacent nodal points. This procedure was shown to be very accurate, provided the elements on either side of the excavation boundary were rectangular and of equal size.

Chang(1969) later on developed a similiar technique for elements of unequal size. Nodal forces on the boundary were calculated using only the stresses in the element directly above the boundary. The nodal forces were then corrected in

accordance with an assumed gravity stress gradients within the elements.

Both the stress averaging technique developed by Dunlop, et al., (1968) and the gravity gradient technique developed by Chang (1969) were designed to meet the needs of specific applications.

A more general technique for finding equivalent nodal loads of excavation boundaries is accomplished with the aid of interpolation formula. By this formula, unknown stresses of boundary points are calculated from the known center stresses of the element. The interpolation function is in the form of polynomial which is expressed as following (Clough and Duncan, 1969).

$$\sigma = a_1 + a_2.x + a_3.y + a_4.xy \qquad (2.6)$$

where σ is the nodal stress to be interpolated, x and y are the coordinates of the nodal point and a_1, a_2, a_3 and a_4 are interpolation coefficients. This equation (2.6) is an incomplete quadratic expansion which accounts for non-linearity in the stress variation by means of the "xy" term.

In the most general form of the excavation problem, the excavation of a quadri-lateral element creates four excavation boundaries, and Equation 2.6 is used to determine the stresses at all four noads of the element. Furthermore, assuming linear variations of stresses between the calculated stress values at the nodes, a complete stress distribution may be defined on the boundaries around the element. Such stress distribution

for an arbitrary quadrilateral is shown in Fig. 2.2

Equivalent nodal loads obtained from boundary stress-distribution, are then applied to the excavation boundary.

In order to use equation 2.6 to find stresses at the nodes of an element excavated, three sets of the interpolation coefficients are calculated (for σ_x, σ_y, τ_{xy},) using the known stresses in the element excavated and the stresses of other three adjacent elements. For a given stress, σ (which can be σ_x, σ_y or τ_{xy}) the unknown interpolation coefficients are expressed as,

$$\sigma(1) = a_1 + a_2.x_1 + a_3.y_1 + a_4.x_1.y_1 \qquad (2.7)$$

$$\sigma(2) = a_1 + a_2.x_2 + a_3.y_2 + a_4.x_2.y_2 \qquad (2.8)$$

$$\sigma(3) = a_1 + a_2.x_3 + a_3.y_3 + a_4.x_3.y_3 \qquad (2.9)$$

$$\sigma(4) = a_1 + a_2.x_4 + a_3.y_4 + a_4.x_4.x_4 \qquad (2.10)$$

where $\sigma(1)$ is the stress of element 1, $\sigma(2)$ is the stress of element 2 and so on. These equations can be rewritten in matrix form as,

$$\{\sigma\}_e = [m].\{a\} \qquad (2.11)$$

where $\{\sigma\}_e$ is the vector of known stresses for elements 1,2,3 and 4, [m] is the coordinate matrix for elements 1,2,3 and 4, and {a} is the vector of interpolation coefficients. Here, the unknown vector of interpolation coefficient can be written as

$$\{a\} = [m]^{-1}, \{\sigma\}_e \qquad (2.12)$$

After that, using the vector of interpolation coefficients, the stresses at each node of the element to be excavated can be obtained.

$$\{\sigma\}_n = [n]. \{a\} \qquad (2.13)$$

where [n] is the coordinate matrix of the nodes of the element to be excavated.

Combining equations (2.12) and(2.13), all procedure can be stated in a single formula as follows.

$$\{\sigma\}_n = [n] \cdot [m]^{-1}.\{\sigma\}_e \qquad (2.14)$$

Consequently, nodal stresses of the element to be excavated has been written in terms of the stresses at the center of four adjacent elements. In other words, the values of σ_x, σ_y, and τ_{xy} at the nodes of an element to be excavated can be defined in terms of the center point stresses of that element and three adjacent elements.

According to Clough and Duncan (1969) once the nodal stresses have been evaluated, the equivalent nodal forces may be established for the element as shown at the boundary J-K of the element of the quadrilateral shown in Fig.(2.2). The equivalent vertical nodal force at node J depends on the magnitude of σ_y and τ_{xy} at nodes I,J. and K.Using the principle of virtual work, and assuming linear variations between the calculated nodal stress values,the vertical force at node J

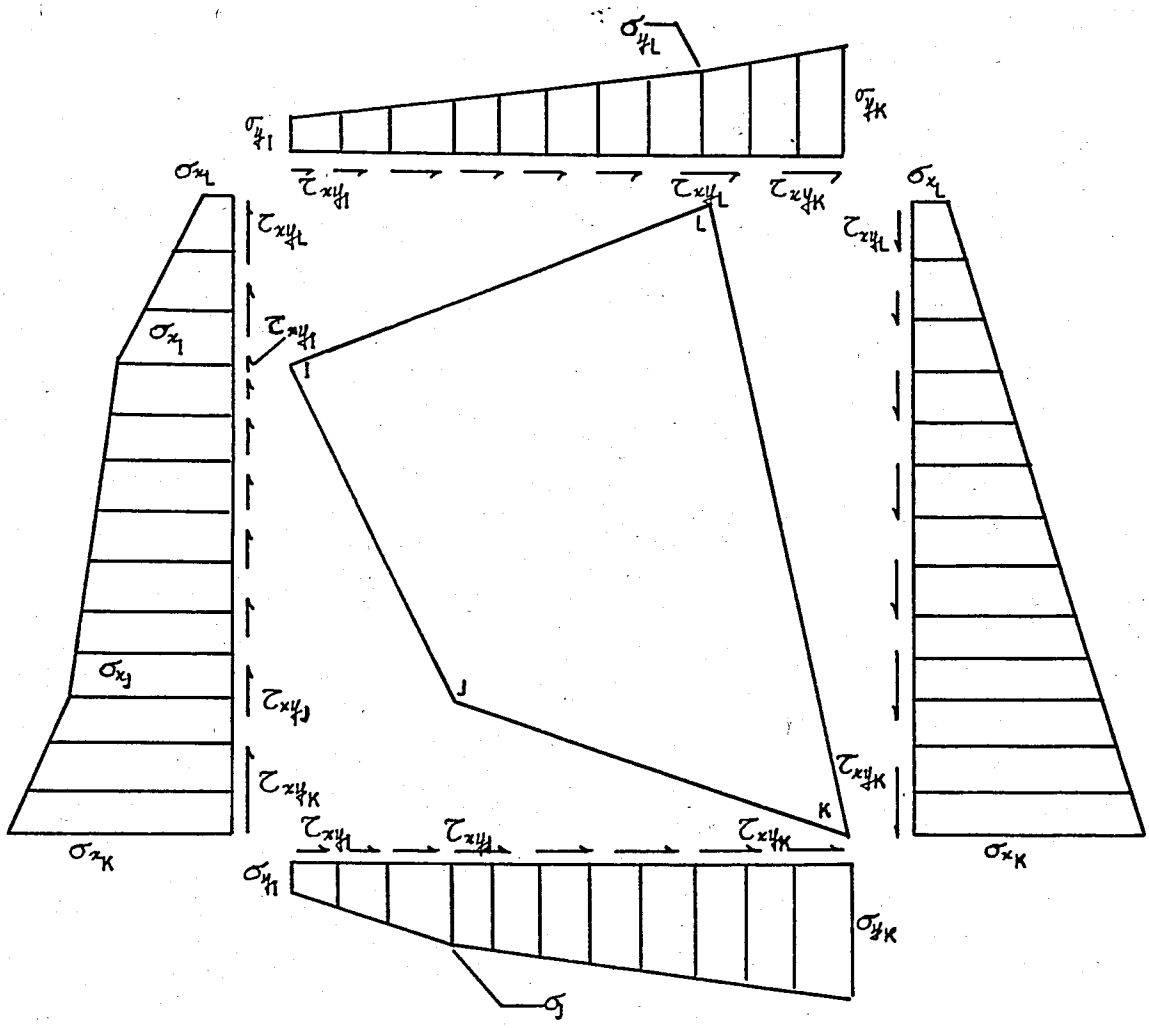

$YIJ = y_I - y_j$
$YJK = y_j - y_K$
$YKL = y_K - y_L$
$YLI = y_L - y_I$

$XJI = x_j - x_I$
$XKJ = x_K - x_j$
$XKL = x_L - x_K$
$XIL = x_I - x_L$

Note: All Stresses and Gradients Assumed Positive as Shown.

FIGURE(2.2)

Arbitrary Quadrilateral Element and Boundary Stress Distribution(After Clough and Duncan, 1969)

can be written as,

$$R_y^J = \frac{1}{6} * \left[(XJI) * \sigma_{yI} + 2 * (XJI + XKJ) * \sigma_{yJ} + (XKJ) * \sigma_{yK} \right.$$

$$\left. + (YIJ) * \tau_{xyI} + 2 * (YIJ + YJK) * \sigma_{xyJ} + (YJK) * \tau_{xyK} \right] \qquad (2.15)$$

This treatment is repeated for all forces of the nodal points of an element, and written in matrix form as follows.

$$\{F\}_n = [H] * \{\sigma\}_n \qquad (2.16)$$

where $\{F\}_n$ is the 8x1 vector containing all element nodal forces, $[H]$ is an 8x12 matrix defining element boundary geometry and $\{\sigma\}_n$ is a 12*1 vector of nodal stresses. The equation in expanded form is written in equation (2.17) (Clough and Duncan, 1969) The all manipulations done so far can be gathered in a single equation using the expression to obtain nodal point stresses.

$$\{F\}_n = [H] * [n] * [m]^{-1} * \{\sigma\}_e \qquad (2.18)$$

In most of the cases, there is no need to apply all eight of the nodal loads, since equivalent nodal loads need only be applied to those nodes which are the boundary of both an exacavated and intact element.

In order to chose elements for interpolation equations, one element should be the element which is excavated and the other three element should be as near as possible to the excavated element. On the other hand, centers of those three

$$\begin{Bmatrix} R_x^I \\ R_y^I \\ R_x^J \\ R_y^J \\ R_x^K \\ R_y^K \\ R_x^L \\ R_y^L \end{Bmatrix} = \frac{1}{6} \cdot \begin{bmatrix} 2(YLI)+2(YIJ) & YIJ & 0 & YLI & 0 & 0 & 0 & 0 & 2(XJI)+2(XIL) & XJI & 0 & XIL \\ 0 & 0 & 0 & 0 & 2(XIL)+2(XJI) & XJI & 0 & XIL & 2(YLI)+2(YIJ) & YIJ & 0 & YLI \\ YIJ & 2(YIJ)+2(YJK) & YJK & 0 & 0 & 0 & 0 & 0 & XJI & 2(XJI)+2(XKJ) & XKJ & 0 \\ 0 & 0 & 0 & 0 & XJI & 2(XJI)+2(XKJ) & XKJ & 0 & YIJ & 2(YIJ)+2(YJK) & YJK & 0 \\ 0 & YJK & 2(YJK)+2(YKL) & YKL & 0 & 0 & 0 & 0 & 0 & XKJ & 2(XKJ)+2(XLK) & XLK \\ 0 & 0 & 0 & 0 & 0 & XKJ & 2(XKJ)+2(XLK) & XLK & 0 & YIJ & 2(YIJ)+2(YKL) & YKL \\ YLI & 0 & YKL & 2(YKL)+2(YLI) & 0 & 0 & 0 & 0 & XIL & 0 & XLK & 2(XLK)+2(XIL) \\ 0 & 0 & 0 & 0 & XIL & 0 & XLK & 2(XLK)+2(XIL) & YLI & 0 & YKL & 2(YKL)+2(YLI) \end{bmatrix} \begin{Bmatrix} \sigma_{x_I} \\ \sigma_{x_J} \\ \sigma_{x_K} \\ \sigma_{x_L} \\ \sigma_{y_I} \\ \sigma_{y_J} \\ \sigma_{y_K} \\ \sigma_{y_L} \\ \tau_{xy_I} \\ \tau_{xy_J} \\ \tau_{xy_K} \\ \tau_{xy_L} \end{Bmatrix}$$

EQUATION (2.17)

(After Clough and Duncan, 1969)

elements should not lie on a vertical or horizontal line in which case the matrix [m] becomes singular, and no result is obtained. In the areas of very high stress-gradients, it is desirable to chose an interpolation function with more than four terms, however the procedure described herein is still applicable. An example for selecting interpolation elements is given in figure 2.3.

The equations simulating incremental exavation are derived such that total stress case is assumed. Therefore, those equations are valid for the soil in dry. However, by substituting effective stresses for total stresses in equation (2.6) through equation(2.18), excavation under water can be simulated.

Generally, excavations in practice are accomplished by several increments as in the case of fill placement. But if the material is assumed to be linear, number of increments simulating excavation does not change the result. One another important fact is to choose correct mesh for excavation problems. In order to obtain reasonable values, mesh should be finer in the vicinity of vertical-horizontal excavation boundaries where stress gradients are very large and stresses are small.

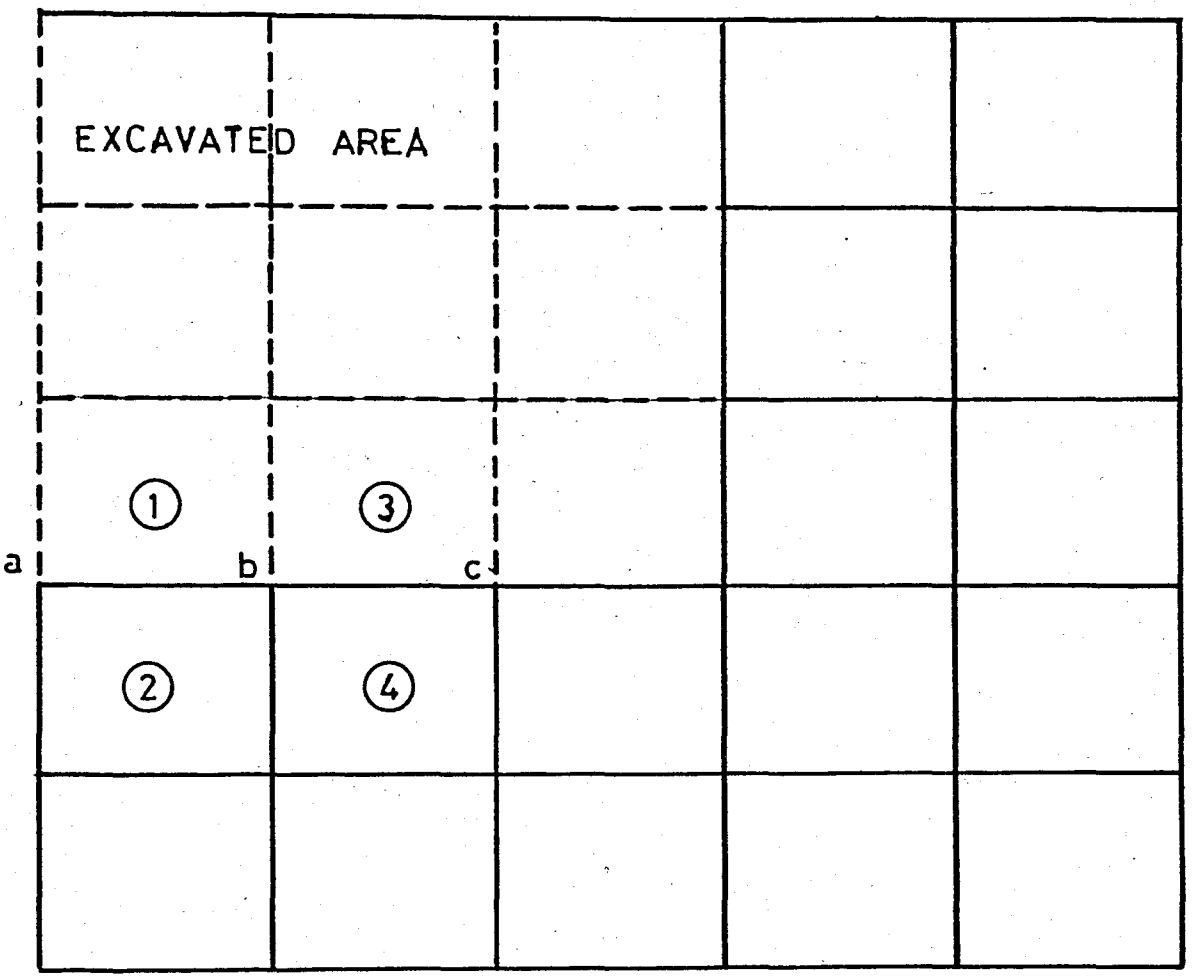

① ② ③ ④ -Interpolation Elements for boundary segment a-b-c

FIGURE(2.3)

Determining Boundary Stresses for Excavation by Interpolation(After Clough and Duncan,1969)

C. INCREMENTAL WATER PRESSURE LOADING

According to Clough and Duncan (1969), changes in water pressure produce incremental loading which may cause changes in effective stresses and thereby affect the behaviour of soil masses. It is, therefore, important to be able to simulate the effects of water pressure changes on a soil mass. Impervious material, such as concrete, and pervious materials, such as sand, behave differently when subjected to changes in water pressure. A change in water pressure on one side of impervious material produces boundary pressure loading which was taken into account in SOIL-STRUCT by an option called "Boundary Pressure Loading". A change in water pressure on one side of a pervious material, however, results in development of seepage through the material, and the excess head is dissipated in the material. This type of loading in SOIL-STRUCT considered by an option called "Seepage Loading." Here, loading is appropriately represented as a distributed load, which in the finite element analyses may be represented as a load distributed equally to the nodes of each element. The type of loading appropriate for a clay with low permeability would depend upon the amount of time allowed for seepage to develop through the clay. If the loading rate is rapid and a steady seepage condition does not develop, the clay may be loaded by boundary pressure loading. On the other hand, if the loading rate is very slow, the clay may be loaded by a distributed loading.

Chang(1969) developed a procedure for calculating nodal point forces to represent the effect to dewatering. The water

pressure change at the centroid of an element was assumed to represent a uniform change in pressure around the element. Equivalent nodal point forces that are calculated from this uniform loading and applied to the nodes of the element. Although the procedure developed by Chang(1969) gave good results for the cases he analyzed, it has been found that using uniform water pressure changes around the element based on the mid-point water pressure changes could lead to inaccuracies if the actual pressure changes were nonuniform or if the element is a nonrectangular guadrilateral.

The variation of water pressures around an element may be accounted for in the loading of finite element mesh by considering the water pressure changes at each node of an element and assuming a linear variation of the water pressure changes between the nodal points. An arbitrary quadrilateral subjected to linearly varying water pressure changes on each side is shown in Fig2.4.Because the loading shown in simply a special case of the boundary stress loading used for excavation,equation (2.17) may be used to evaluate the equivalent nodal forces. This equation can be rewritten for water pressure loading as in equation (2.19).

If the loading on an element is to be distributed as a body load, the horizontal and vertical forces are summed and divided by four. By realizing these operation in equation (2.19), the following equation is obtained (Clough and Duncan, 1969)

$$\begin{bmatrix} R_X \\ R_Y \end{bmatrix} = \frac{1}{8} \begin{bmatrix} YLI+YIJ & YIJ+YIK & YJK+YKL & YKL+YLI \\ XIL+XJI & XJI+XKJ & XKJ+XLK & YLK+XIL \end{bmatrix} \cdot \begin{bmatrix} \Delta U_I \\ \Delta U_J \\ \Delta U_K \\ \Delta U_L \end{bmatrix} \qquad (2.20)$$

$$\begin{Bmatrix} R_x^I \\ R_y^I \\ R_x^J \\ R_y^J \\ R_x^K \\ R_y^K \\ R_x^L \\ R_y^L \end{Bmatrix} = \frac{1}{6} \begin{bmatrix} 2(YLI)+2(YIJ) & YIJ & 0 & YLI \\ 2(XLI)+2(XJI) & XJI & 0 & XIL \\ YIJ & 2(YIJ)+2(YJK) & YJK & 0 \\ XJI & 2(XJI)+2(XKJ) & XKJ & 0 \\ 0 & YJK & 2(YJK)+2(YKL) & YKL \\ 0 & XKJ & 2(XKJ)+2(XLK) & XLK \\ YLI & 0 & YKL & 2(YKL)+2(YLI) \\ XLI & 0 & XLK & 2(XLI)+2(XLK) \end{bmatrix} \begin{Bmatrix} \Delta u_I \\ \Delta u_J \\ \Delta u_K \\ \Delta u_L \end{Bmatrix}$$

EQUATION(219)
(After Clough and Duncan,1969)

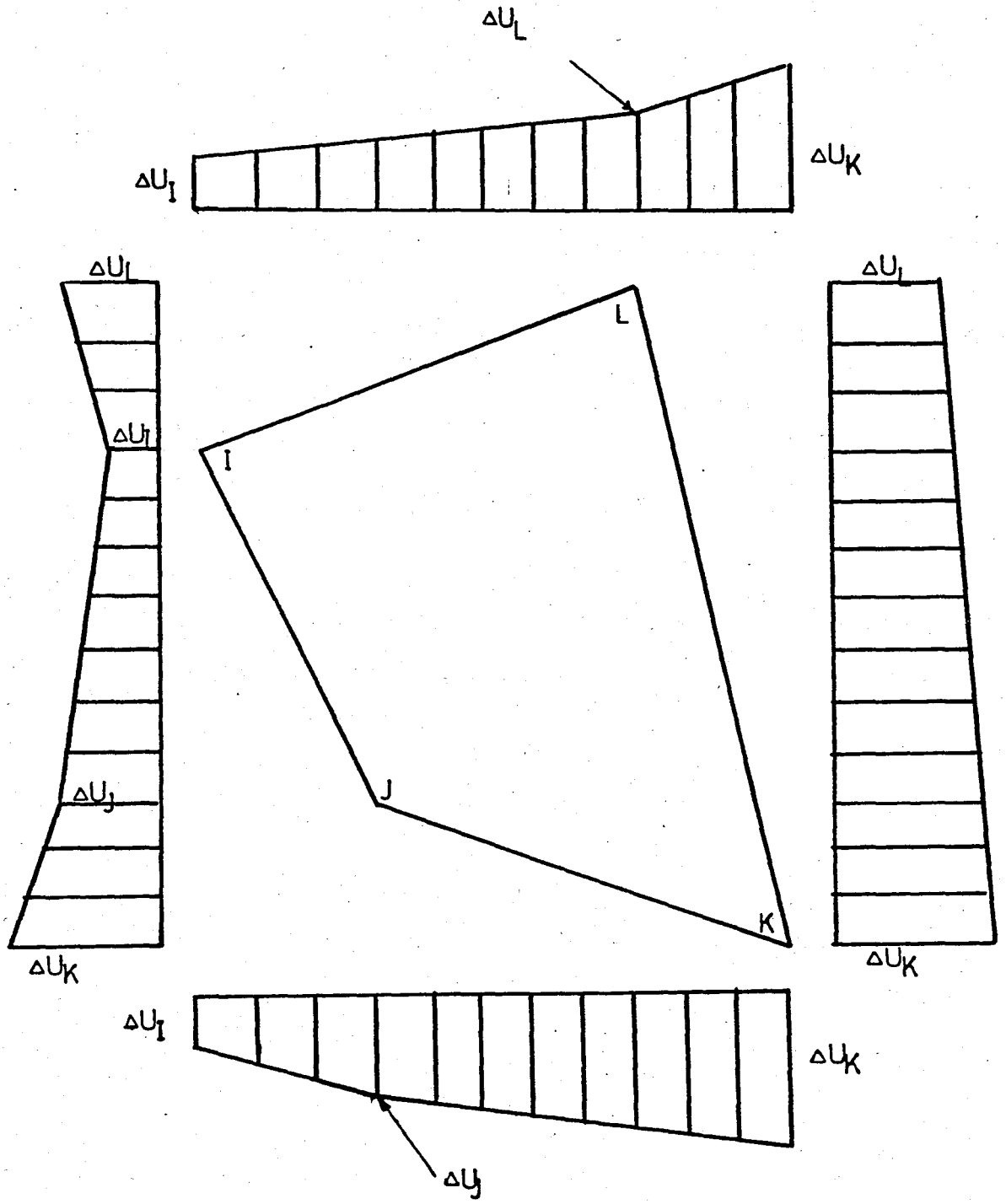

FIGURE(2.4)
Arbitrary Quadrilateral Element and Boundary Water Pressure Distribution(After Clough and Duncan,1969)

An example of the distributed type of loading due to a simple ground water lowering is shown in Fig.2.5. As can be seen in this figure, while the water pressure changes on elements 2 and 3 are different, the net element loading is the same, namely, four vertical forces equivalent to (γ_ω *Element Area)*$\frac{1}{4}$. For element 4, although there is a large change in water pressure on all sides of the element, there is no net loading because the element was not subject to any differential water prussure changes. If the water level was subsequently raised to its original level, equal but opposite nodal loads to those shown in Fig. 2.5 should be applied to simulate the rise of water level.

In SOIL-STRUCT, the changes of porepressure in a nodal point can be specified in two ways;

a) Indicating the increment or decrement of pore pressure at every nodal points when defining the coordinates of those points.

b) Using the phreatic-line concept.

In case b, the changes of pore pressures is calculated automatically by the program. Here, the phreatic line is divided into parts, and those parts are represented by their rightmost x-coordinates, new level of phreatic line and present level of phreatic line. An example of seepage phreatic line is given in Fig.2.6

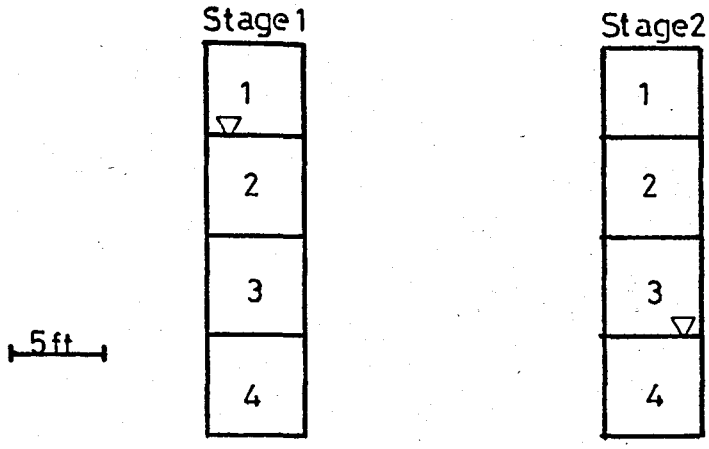

ELEMENT	1	2	3	4
ΔU on Element, Feet of Water	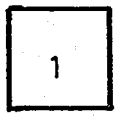	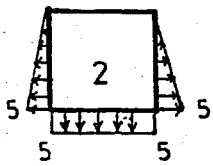	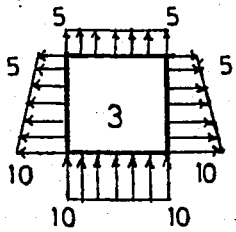	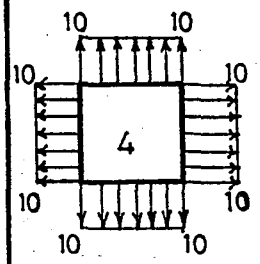
Equivalent Nodal Loads Lbs	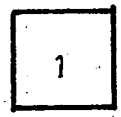	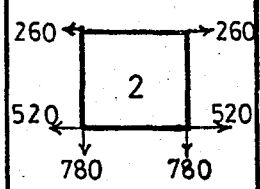	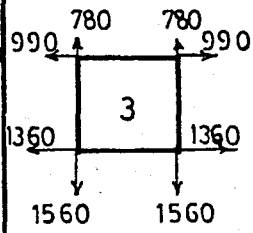	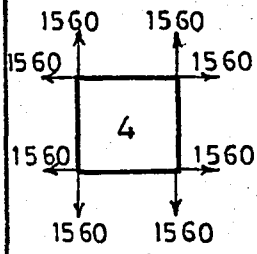
Distributed Loading on Element, Lbs	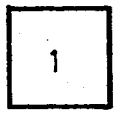	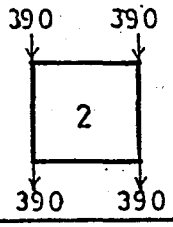	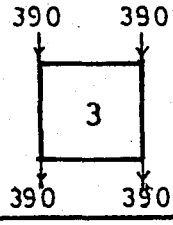	

FIGURE(2.5)

Example of Water Pressure Loading on pervious Soil Element (After Clough and Duncan,1969)

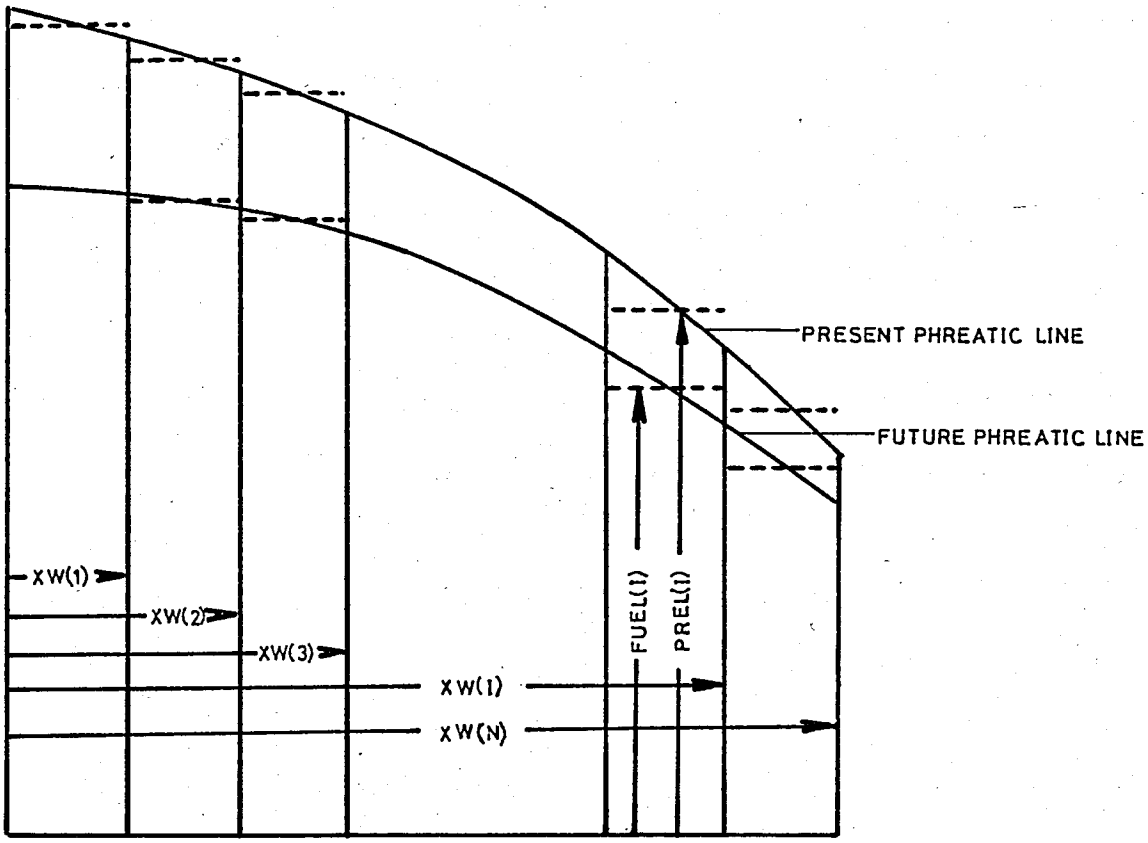

FUEL(I) - FUTURE LEVEL OF PHREATIC LINE IN Ith INTERVAL
PREL(I) - PRESENT LEVEL OF PHREATIC LINE IN Ith INTERVAL

FIGURE(2.6)

Representation of Pore Pressure Using Changes of Seepage Phreatic Line.

D. PLACEMENT OF CONCRETE OR FILL MATERIAL

King (1965) applied the finite element method to the incremental construction of a concrete gravity-dam, and Clough and Woodward(1967) employed similiar techniques to simulate the incremental construction of earth dams. In the approach developed by King, a structure is considered to be build in small layers. Upon initial placement, each layer is assumed to behave as a dense liquid, i.e., to have weight but no ability to resist shear. Subsequently, upon placement of the next layer, the previous layer is assumed to behave as a solid. King (1965) justified the "dense liquid" assumption on the basis that concrete is liquid when placed and hardens before placement of the next layer. Clough and Woodward(1967) showed that the "dense liquid" approach was also appropriate for earth fill because the weight of a lift of earth fill is first applied when the fill is dumped from a hauling unit in a loose uncompacted form. Subsequent compaction of a lift of earth fill "hardens" the layer before placement of the next lift.

The dense liquid technique developed by King (1965) for simulation of concrete and backfill placement for the other structures. When structural material and soil backfill has common boundary in the finite element mesh using the dense liquid approach developed by King (1965) would require that a "liquid" soil backfill layer be placed next to a "hardened" concrete layer. The modulus ratio between those two materials could be as high as 10^9, and even after the soil layer has hardened, the modulus ratio would be about 10^8.

Thus, it is apparent that the top of a soil layer deflect more than the adjacent concrete layer. To allow for relative movement between these dissimiliar materials in incremental analysis, interface elements of the type described by Goodman, et al., (1968) were used between the backfill and concrete. The details of the behaviour of this element are given in section (2.6). By assuming a frictionless interface element between a newly placed "liquid" backfill layer and the "hardened" concrete, free relative movement was allowed between these materials in a manner consistent with the assumption of a "liquid" backfill layer.

Placement of concrete and fill material is accomplished through the subroutine "BUILD" in "SOIL-STRUCT". When specifiying the build-up option, the elements added, number of active elements, zero displacements of the newly placed layer,number of structural elements and backfill type I elements, new Y coordinate on top of backfill should be indicated.

In Subroutine"Build", for the interface elements normal and shear stiffnesses are found. Simultaneously σ_x values are calculated. Here, the normal stiffness of interface element is assigned to 10^8 and the shear stiffness of that element is assigned to 10. Importantly, the interface element should be in contact with the NBlTYP element only as a backfill material.

For structural element, the area is calculated then multiplied by the unit weight of structural material. This value is distributed to all nodes of the element evenly in a vertical direction. In soil elements, $\sigma_y = \gamma*(HTB-YAVG)$ and $\sigma_x=\sigma_y*K_o$

are calculated and the subroutine MODCAL is used to check the modulus of the soil element.

E. ANALYSIS OF THE EFFECTS OF INCREMENTAL TEMPERATURE CHANGES

Since the program SOIL-STRUCT has been written to verify the effectiveness of finite element theory by considering the actual problem of lock structures, the temperature option was added. Seasonal temperature variations cause deflections of reinforced concrete structures, and thereby produce changes in pressures between the structure and the surrounding soil. Techniques for calculating equivalent nodal loads to simulate incremental temperature changes were developed by Sandhu,et al., (1967) for the linear strain element. The equivalent nodal loading is determined from the stresses in a completely restrained element subjected to temperature change. These loads are applied to the element nodes and the change in stress due to temperature change is determined by superimposing the stresses developed under complete restraint, which are calculated using simple equations of mechanics, and the stress due to the equivalent nodal loading.

For plane strain, the stresses due to temperature change in a completely restranied structure are,

$$\Delta\sigma_x = \Delta\sigma_y = \frac{E.\alpha.\ \Delta T}{(1+\nu).(1-2\nu)} \qquad (2.21)$$

in which E is the modulus of elasticity, ν is the Poisson's ratio, α is the coefficient of thermal expansion, and ΔT is the average temperature change in an element.

Temperature change is considered in the program by specifying the values of temperature changes on nodal points. This is indicated when giving the coordinates of nodes as an input.

2.5 STRESS-STRAIN BEHAVIOUR OF MATERIALS

In utilizing the computer-program SOIL-STRUCT, the correct representation of material properties should be achieved. Since many factors, such as density, water content, drainage conditions, stress history, confining pressure and shear stress influence the stress-strain behaviour of soil, field conditions must be simulated as much as possible. This can be done using appropriate sampling procedures and suitable testing. In general, three characteristics of the stress-strain behaviour of a soil are as follows :

- stress-dependency,
- non-linearity,
- inelasticity.

These characteristics are shown in Fig.2.7, a hypothetical plot of stress-strain curves for two compression tests on soil samples subjected to different confining pressures.

The stress dependency is obvious in the effect of confining pressure, a steeper stress-strain curve is being obtained for the higher confining pressure than for the lower confining pressure. The non-linearity of the stress-strain behaviour can be seen in the Figure 2.7 that stress does not increase linearly with increasing value of strain. The third property, inelasticity, can be seen regarding at the unloading-reloading curve. After the unloading is completed, some inelastic deformation remains. Here, one more important property is seen that the unloading curve is steeper than the primary loading curve. The reloading curve is similiar to the unloading

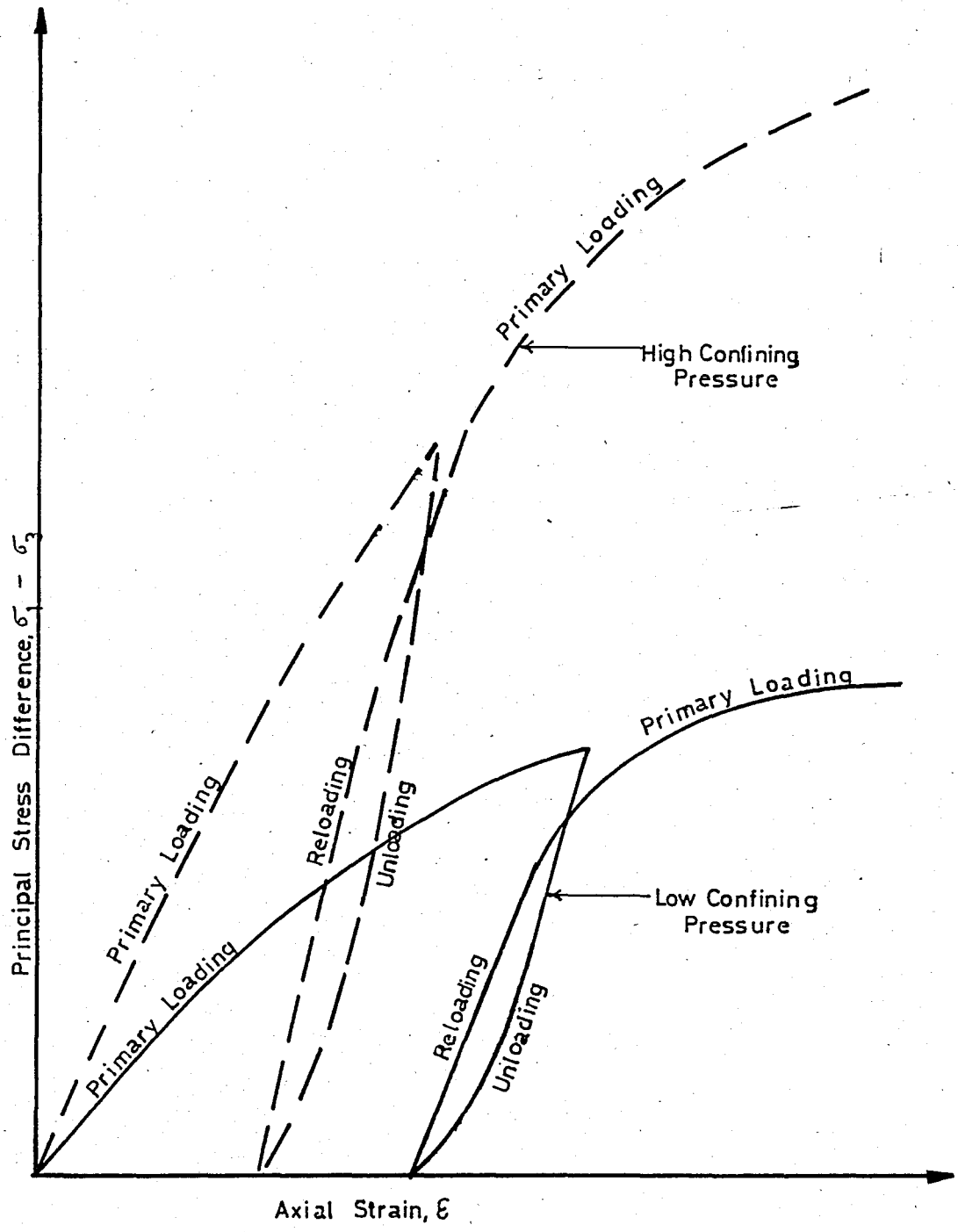

FIGURE(2.7)

Typical Stress-Strain Curves for Cyclic Loading of a Soil Sample(After Duncan and Chang,1969)

curve, but when the value of principal stress difference is reached where unloading was begun, the path of the primary loading curve is resumed.

With the development of electronic computers, the analyses of soil structures with above mentioned characteristics has become feasible. These characteristics were incorporated into a simplified, practical analytical formulation by Duncan and Chang (1969).

A. NONLINEARITY

Konder and his coworkers have shown that the non-linear stress-strain curves of both clay and sand may be represented by hyperbolae with a high degree of accuracy. This hyperbolic equation proposed by Konder(1963) and Konder and Zelasko(1963) was

$$(\sigma_1-\sigma_3) = \frac{\varepsilon}{a+b*\varepsilon} \qquad (2.22)$$

in which "σ_1" and "σ_3" are the major and minor principal stresses; "ε" is the axial strain; and "a" and "b" are the constants whose values are determined experimentally. Both of these two constants "a" and "b" have physical meanings. As shown in Figure 2.8, "a" is the reciprocal of the initial tangent modulus, E_i, and "b" is the reciprocal of the asyptotic value of stress difference which the stress-strain curve approaches at infinite strain $(\sigma_1-\sigma_3)_{ult}$. To sum up, "a" and "b" depend on soil type and stress-state respectively.

Typical Hyperbolic Stress-Strain Curve

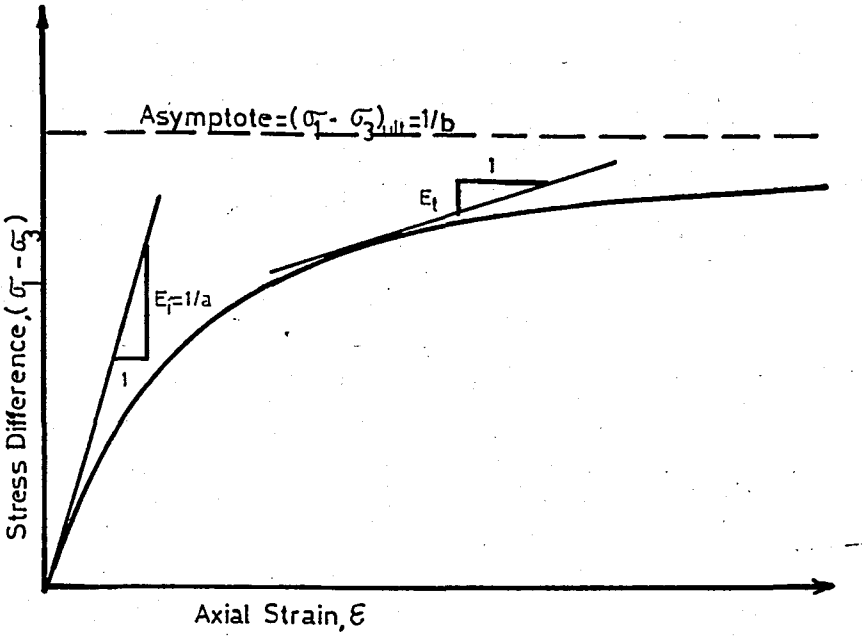

FIGURE(2.8)
Typical Hyperbolic Stress-Strain Curve
(After Clough and Duncan,1969)

Transformed Linear Hyperbolic Plot

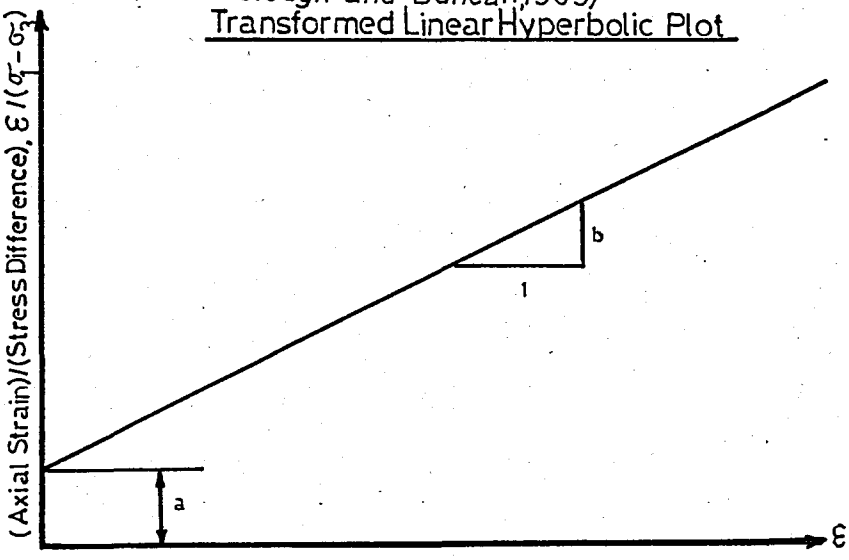

FIGURE(2.9)
Transformed Linear Hyperbolic Plot
(After Clough and Duncan,1969)

Kondner and his coworkers showed that the values of the coefficients "a" and "b" may be determined most readily if the stress-strain data are plotted on transformed axes, as shown in Figure(2.9).When equation (2.22) is rewritten in the following form

$$\frac{\varepsilon}{(\sigma_1-\sigma_3)} = a + b \cdot \varepsilon \qquad (2.23)$$

it may be noted that "a" and "b" are the intercept and the slope of the resulting straight line. By plotting stress-strain data in the form shown in Figure (2.9), it is easy to determine the values of the parameters "a" and "b" corresponding to the best fit between a hyperbola and the test data.

When this is done it is commonly found that the asymptotic value of $(\sigma_1-\sigma_3)$ is larger than the compressive strength of the soil by a small amount. This would be expected, because the hyperbola remains below the asymptote at all finite values of strain. The asymptotic value may be related to the compressive strength by means of a factor R_f as shown by

$$(\sigma_1-\sigma_3)f = R_f \cdot (\sigma_1-\sigma_3)_{ult} \qquad (2.24)$$

in which $(\sigma_1-\sigma_3)_f$ is the compressive strength, or stress difference at failure; $(\sigma_1-\sigma_3)_{ult}$ is the asymptotic value of stress difference; and R_f is the failure ratio, which always has a value less than unity. For a number of different soils, the value of R_f has be found to be between 0.75 and 1.00, and

to be essentially independent of confining pressure.

By expressing the parameters "a" and "b" in terms of the initial tangent modulus value and the compressive strength, Equation (2.22) may be rewritten as

$$(\sigma_1-\sigma_3) = \frac{\varepsilon}{\left[\frac{1}{E_i} + \frac{\varepsilon \,.Rf}{(\sigma_1-\sigma_3)f}\right]} \qquad (2.25)$$

This hyperbolic representation of stress-strain curves developed by Kondner has been found to be a convenient and useful means of representing the nonlinearity of soil stress-strain behaviour.

In order to obtain an expression for the tangent modulus, Duncan and Chang (1969) differentiated equation (2.22) to obtain the following equation :

$$E_t = \left[1 - \frac{Rf.(\sigma_1-\sigma_3)}{(\sigma_1-\sigma_3)f}\right]^2 .E_i \qquad (2.26)$$

in which the term $(\sigma_1-\sigma_3)/(\sigma_1-\sigma_3)f$ was termed the stress level. The stress level was defined in terms of the Mohr-Coulomb strength parameters, $\emptyset$ and c, as,

$$\frac{\sigma_1-\sigma_3}{(\sigma_1-\sigma_3)f} = \frac{\sigma_1-\sigma_3}{\sigma_3.[\tan^2(45+\emptyset/2)] + 2c.\tan(45+\emptyset/2)} \qquad (2.27)$$

B. STRESS-DEPENDENCY

The tangent modulus value and the compressive strength of soils have been found to vary with the confining pressure employed in the tests (Clough and Duncan, 1969). But this is not valid for the case of unconsolidated-undrained tests on saturated soils.

Experiment studies by Tanbu have shown that the relationship between initial tangent modulus and confining pressure may be expressed as

$$E_i = K.p_a.\left(\frac{\sigma_3}{p_a}\right)^n \qquad (2.28)$$

in which E_i is the initial tangent modulus; σ_3 is the minor principal stress; p_a is atmospheric pressure expressed in the same pressure units as E_i and σ_3; K is a modulus number; and n is the exponent determining the rate of variation of E_i with σ_3; both K and n are pure numbers. Values of the parameters K and n may be determined from the results of a series of tests by plotting the values of E_i against σ_3 on logarithmic scales and fitting a straight line to the data as shown in Figure (2.10). The values shown in Figure (2.10) were determined from the results of drained triaxial tests on a rockfill material used for the shell of Furnas Dam, and a silt from the foundation of Cannonsville Dam reported respectively by Casagrande, and Hirscfeld and Poulos.

Assuming that σ_3 does not change, the relationship between compressive strength and confining pressure may be expressed in terms of the Mohr-Coulomb failure criterion as

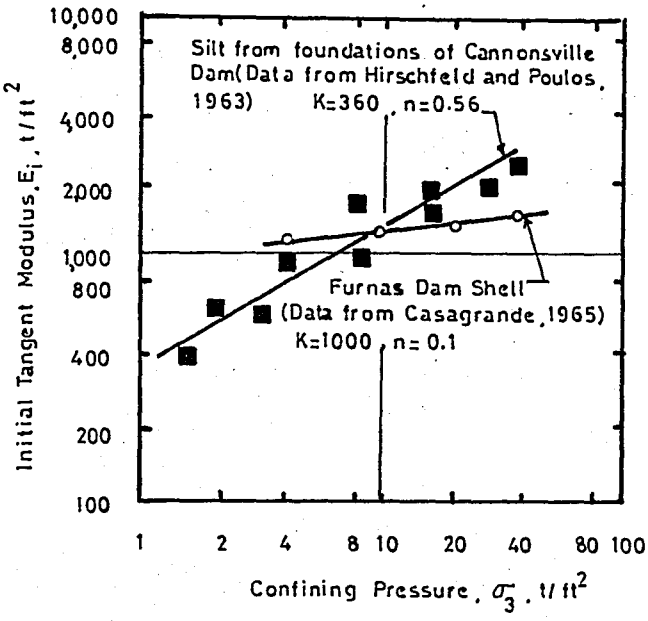

FIGURE (2.10)

Variations of Initial Tangent Modulus with Confining Pressure under Drained Triaxial Test Conditions(After Duncan and Chang, 1969)

$$(\sigma_1-\sigma_3)f = \frac{2c.\cos\phi + 2.\sigma_3.\sin\phi}{1-\sin\phi} \qquad (2.29)$$

in which c and ϕ are the Mohr-Coulomb strength parameters.

Using equations (2.26) and (2.28), the resulting equation for E_t becomes,

$$E_t = \left[1 - \frac{R_f.(\sigma_1-\sigma_3)}{(\sigma_1-\sigma_3)f}\right]^2 .K_m P_a \left(\frac{\sigma_3}{P_a}\right)^n \qquad (2.30)$$

This expression for tangent modulus may be employed very conveniently in incremental stress analyses, and the essential portion of the stress-strain relationship in SOIL-STRUCT. It can be employed for either effective stress analyses or total stress analyses. For effective stress analyses, drained test conditions, with σ_3', constant throughout, are used to determine the values of the required parameters. For total-stress analyses unconsolidated-undrained tests, with σ_3 constant throughout, are used to determine the parameter values.

It should be pointed out that the stress-strain relationship described has been derived on the basis of data obtained from standard triaxial tests in which the intermediate principal stress is equal to the minor principal stress, because in most practical cases only triaxial test data are available. However, this same relationship may be used for plane strain problems in which the intermediate principal stress is not equal to the minor principal stress, if appropriate plane strain test results are available. For cases in which three dimensional stresses and strains are involved, it may be derirable to include a failure criterion or a stress-strain

relationship of soils for the effects of the value of the intermediate principal stress.

The usefullness of equation (2.30) lies in its simplicity with respect to two factors.

1. Because the tangent modulus is expressed in terms of stresses only, it may be employed for analyses of any arbitrary initial stress conditions.

2. The parameters involved in this relationship may be determined readily from the results of laboratory tests. The amount of effort required to determine the values of the parameters K,n and R_f is not much greater than that required to determine the values of c and $\emptyset$.

Another very important case is how to treat the unloading of soil mechanics problems. Duncan and Chang (1969) have shown that the behaviour of a soil on unloading and reloading may be adequately represented by a single modulus value which was defined by the slope of a line connecting the upper and lower ends of the hysteresis loop formed during loading and unloading. (see Figure (2.15)). This modulus was found to vary with confining pressure as,

$$E_{ur} = K_{ur} \cdot p_a \left(\frac{\sigma_3}{p_a} \right)^n \qquad (2.31)$$

where E_{ur} is the unloading modulus and K_{ur} and n are constants for a given soil type. It can be seen that the form of equation (2.31) is the same as that found for the initial tangent modulus shown in equation (2.28). Data by Holubec (1968) and Chang(1969) have shown the exponent, n, in equation (2.31)

and the exponent for the E_i relationship with σ_3 of equation (2.28) are the same, but that the value of K_{ur} is greater than the value of K_m.

C. NONLINEAR STRESS ANALYSES

Non-linear, stress-dependent stress-strain behaviour may be approximated in finite element analysis by assigning different modulus values for each element into which the soil is subdivided for purposes of analysis. The modulus value assigned to each element are related to the stresses and strain within each element. Because the modulus values depend on the stresses and the stresses in turn depend on the modulus values, it is necessary to make repeated analyses to insure that the modulus values and the stress conditions correspond for each element in the system.

Two techniques for approximate nonlinear stress analyses are shown in Figure (2.11 a-b). By the iterative procedure, shown Figure (2.11a), the same change in external loading is analyzed repeatedly. After each analysis the values of stress and strain within each element are examined to determine if they satisfy the suitable nonlinear relationship between stress and strain. If the values of stress and strain do not correspond, a new value of modulus is selected for that element for the next analysis. This kind of procedure is used in the program Soil-Struct. It has been also applied to analyses of the load-settlement behaviour of a footing on sand Girijavallabhan and Reese (1967) and to analyses of pavements by Duncan, Monismith and Wilson (1968).

On the other hand, by the incremental procedure, shown Figure (2.11 b), the change in loading is analyzed in a series of steps, or increments. Here, the essence of this procedure

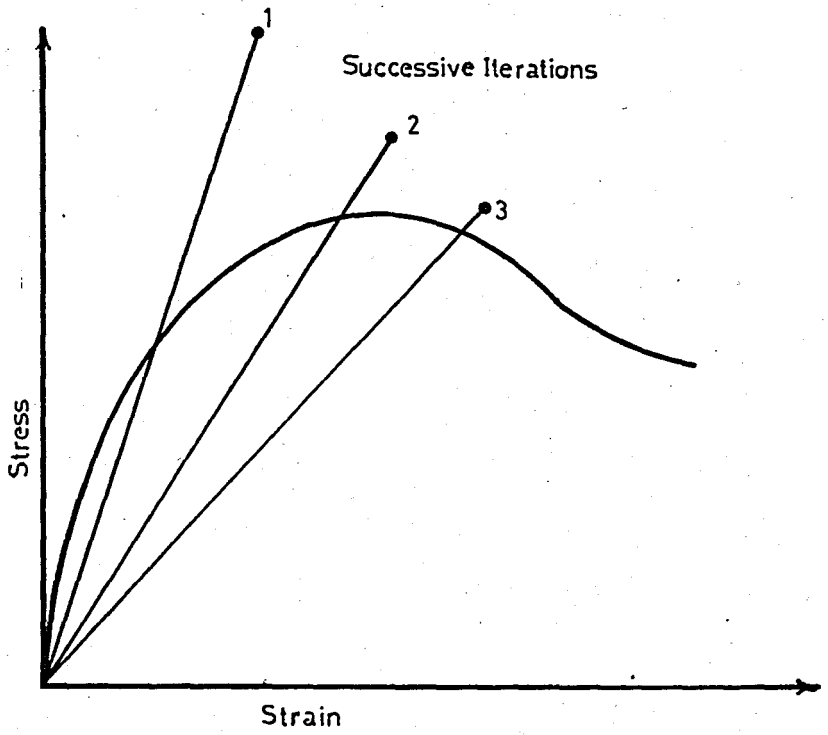

FIGURE (2.11a)

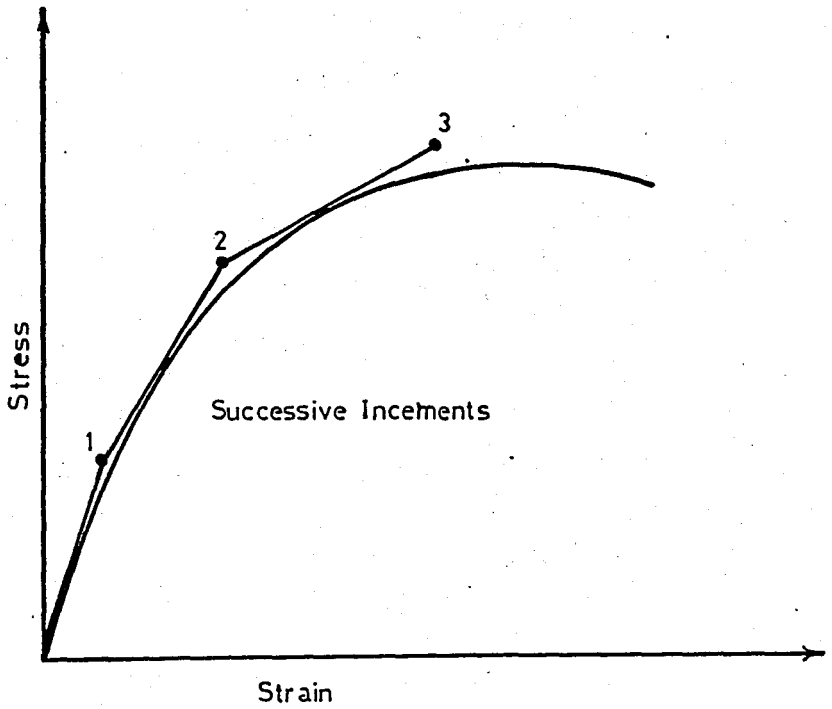

FIGURE(2.11b)

Techniques for Approximating Nonlinear Stress-Strain Behaviour(After Duncan and Chang,1970)

is given for comparison purposes with respect to iterative procedure.

At the beginning of each new increment of loading an appropriate modulus value is selected for each element on the basis of the values of stress or strain in that element. Hence, the nonlinear stress analyses is performed by using series of straight lines. This procedure has been applied to analyses of enbankments by Clough and Woodward, (1967) to analyses of excavated slopes by Dunlop and Duncan, (1968) and to analyses of stresses in simple shear specimens by Duncan and Dunlop (1969).

Both of these procedures have advantages and shortcomings. The main advantage of the iterative procedure is the fact that it is possible, by means of this procedure, to represent stress-strain relationships in which the stress decreases with increasing strain after reaching a peak value. This property may becomes very important because the occurence of progressive failure of soils is believed to be associated with this type of stress-strain behaviour. The shortcoming of the iterative procedure is that it is very difficult to take into account the nonzero initial stresses, which is very important in many soil mechanics problems.

The main advantage of the incremental procedure is that initial stress can be taken into account. At the same time, while analyzing the effects of a given loading, stresses and strains are calculated for smaller loads. For example, if the application of a 50 ton load to a footing was analyzed using 10 steps, or increments, the settlement of the footing, and the stresses and strains in the soil, would be calculated

for footing loads in increments of 5 tons up to 50 tons. The shortcoming of the incremental procedure is that it is not possible to simulate a stress-strain relationship in which the stress decreases beyond the peak.

In order to overcome this shortcoming, negative value of modulus may be used, but this can not be realized in finite element method. The accuracy of the incremental procedure can be improved by analyzing each load increment more than once. Thus, incremental procedure can approximate the nonlinear soil behaviour better.

In program SOIL-STRUCT, iterative technique was used by considering stress-dependent behavioural pattern of soil elements. Because the stress-strain parameters in the formulation developed by Duncan and Chang are stress-dependent, each element in a finite element mesh may have a different modulus value. For a given increment, the modulus value is evaluated for each element in terms of the stresses existing in the element prior to the execution. Iteration may be required if the stress changes within the increment are large relative to the stresses existing within the element prior to execution of the increment.

The criterion assumed to control the use of E_{ur} or E_t , developed by Duncan and Chang(1969) is based upon the maximum previous value of $|\sigma_1-\sigma_3|$. For any value of $|\sigma_1-\sigma_3|$ less than the maximum previous value, the modulus E_{ur} is assumed to be applicable, for any value of $|\sigma_1-\sigma_3|$ greater than the maximum previous value, E_t is assumed applicable.

Laboratory experiments which subjected soil samples to arbitrary stress paths reported by Duncan and Chang (1969) have shown that the proposed modulus relationships could predict the actual stress-strain behavior of the samples to high degree of accuracy.

D. STRESS-STRAIN PARAMETERS

Determination of Hyperbolic Stress-Strain Parameters from Direct-Shear and One-dimensional Consolidation Tests.

For long-term analyses, the stress-strain behaviour of a soil should be determined under drained test conditions. Many clayey soils have such a low permeability that the achievement of fully drained conditions in a triaxial test is not feasible from a practical standpoint because of the time required to conduct the tests.

Direct Shear Test.

Results from the direct shear test provide the data to determine the Mohr-Coulomb strength parameters, $\emptyset'$ and c', which may be employed in the hyperbolic equation of Duncan and Chang (1969). Although the stress-displacement curves from direct shear tests cannot be used to determine stress-strain characteristics of soils, it seems likely that the form of stress-displacement relationship from such a test is qualitatively indicative of the form of the stress-strain relationship, and may be used to establish that the stress-strain behaviour can be reasonably represented by stress-

strain curves of hyperbolic shape. From the results of these test in Port Allen soils, the data fits a straight line closely, indicating that the shear stress versus shear displacement curves are hyperbolic in form. It may be inferred then, that a hyperbolic relationship for the stress-strain behavior is appropriate during primary loading. (See Figure 2.12.a-b)

One Dimensional Compression Tests.

Conventionally, the results of a one-dimensional consolidation test are represented void ratio versus logarithm of the axial pressure plot, as shown in figure (2.13). A change in void ratio represents a change in vertical strain, $\Delta\varepsilon_y$, and figure (2.13) is essentially a stress-strain plot. However, in the consolidation test, the lateral as well as the vertical pressure changes with each load increment, as opposed to a triaxial test in which lateral pressure may remain constant. The lateral stress at any stage of loading in a one - dimensional compression test is defined by-

$$\sigma_x' = K_o \cdot p' \qquad (2.32)$$

The value of K_o has been shown by Brooker and Ireland (1965) to vary with plasticity index and overconsolidation ratio.

Stress-Displacement Data

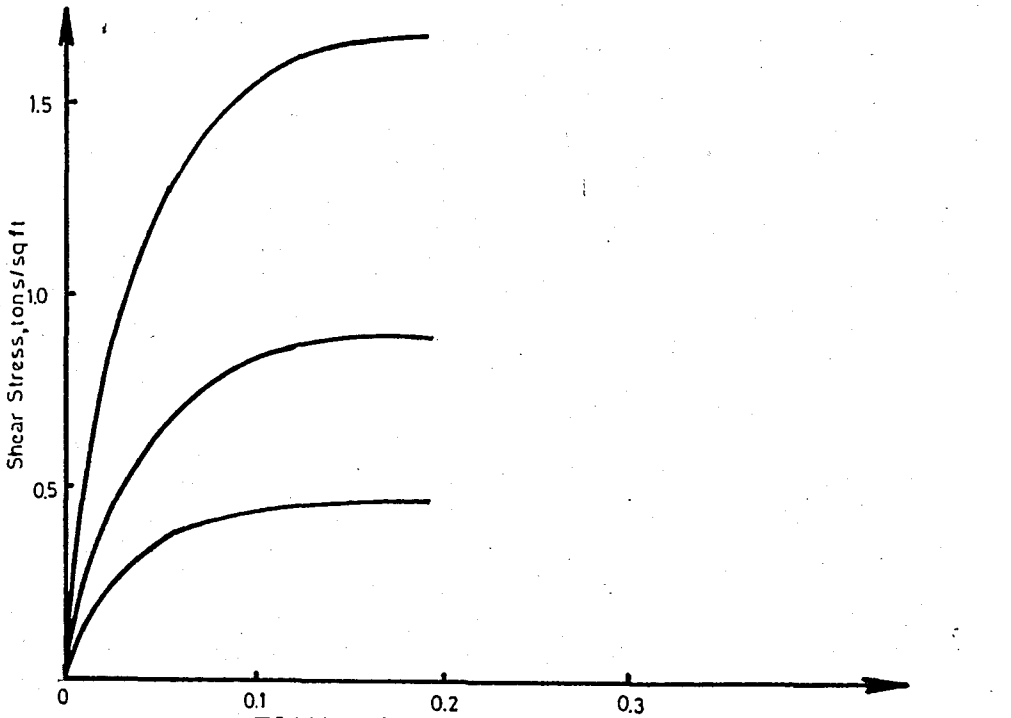

FIGURE (2.12a)

Transformed Linear Hyperbolic Plot

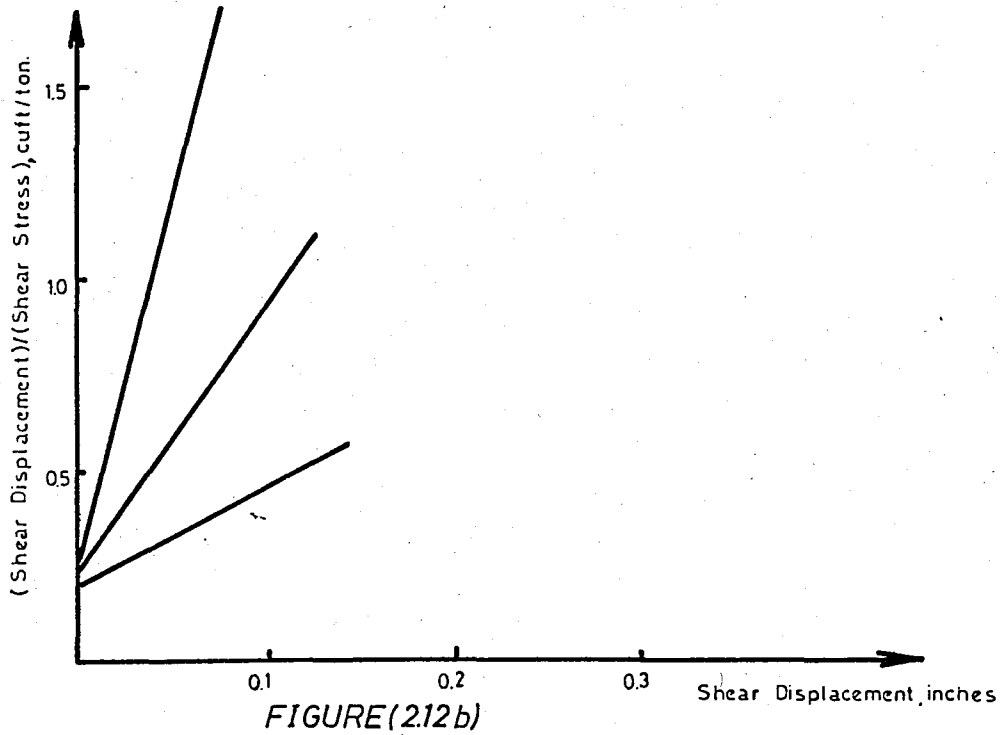

FIGURE (2.12b)

Typical Direct Shear Test Results and Transformed Linear Hyperbolic Plot (After Clough and Duncan, 1969)

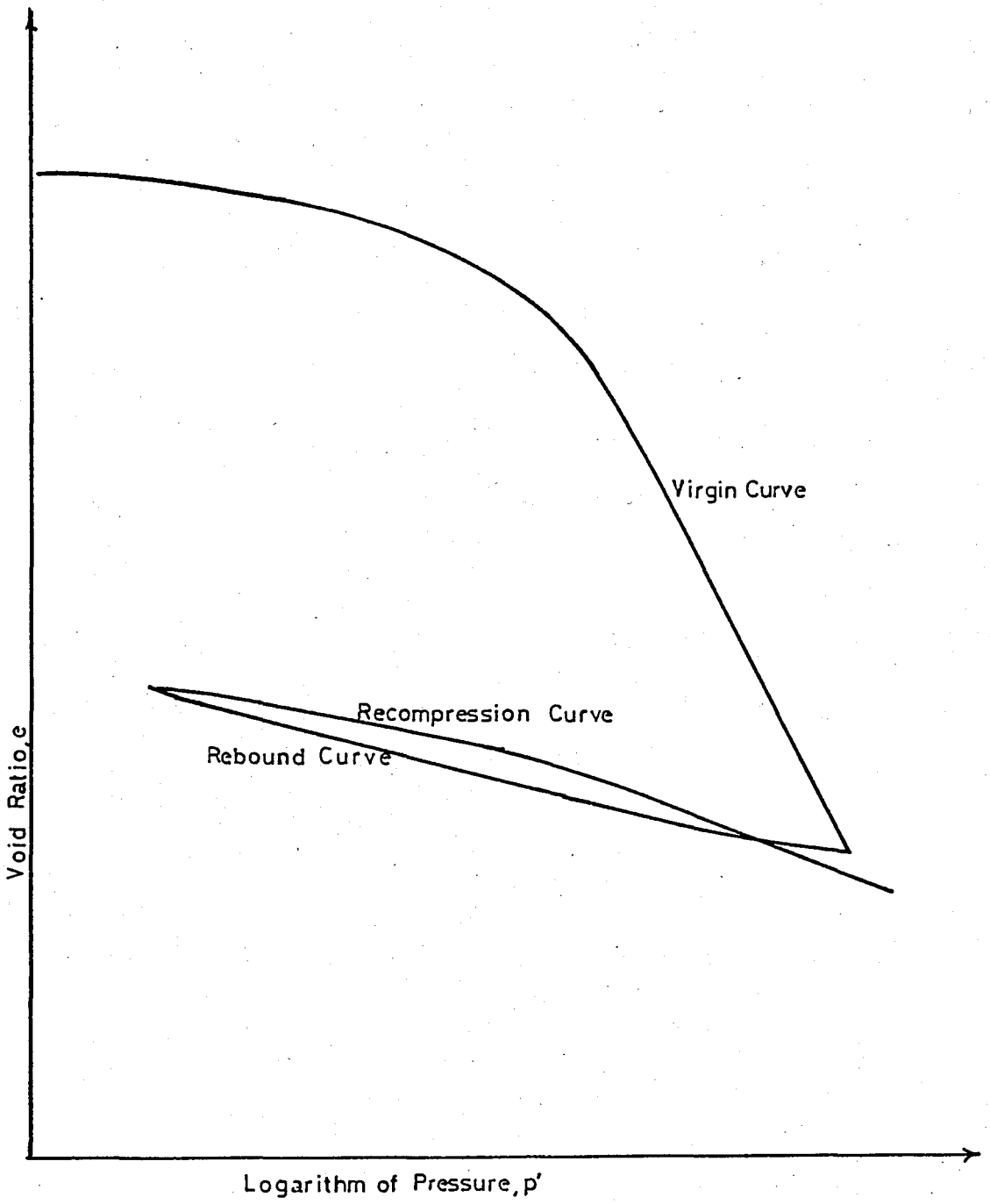

FIGURE (2.13)

Typical Results from One-Dimensional Consolidation Test (After Clough and Duncan, 1969)

Primary Loading

During primary loading (loading beyond the preconsolidation pressure), the overconsolidation ratio is unity, and the value of K_o is constant. Assuming the friction along the sides of a consolidomoter to be negligible and noting that K_o is less than unity for primary loading, the confining pressure for a given axial stress is defined by :

$$\sigma_3' = \sigma_x' = K_o.p' = K_o.\sigma_1' \qquad (2.33)$$

The tangent modulus value from a consolidation test for an increment-loading has been derived by Chang (1969) as,

$$E_t = \frac{1+e_o}{a_v} \cdot \left[1 - \left[\frac{2.\nu^2}{1-\nu}\right]\right] \qquad (2.34)$$

in which e_o is the initial void ratio at the beginning of an increment and a_v is the rate of change of void ratio with change in pressure, p'. Equation(2.34) may also be formulated in terms of coefficient of lateral earth pressure, K_o, using the relationship $K_o = \frac{\nu}{1-\nu}$. The resulting equation is;

$$E_t = \frac{1+e_o}{a_v} \cdot \left[1 - \frac{2.K_o^2}{(1+K_o)}\right] \qquad (2.35)$$

Because the tangent modulus varies with stress level during loading, equation (2.35) defines a tangent modulus at the stress level corresponding to K_o stress conditions. However, values of initial tangent modulus may be determined from the

values of tangent modulus calculated from one dimensional compression test results.

To find E_i from E_t, using equation (2.26), the following equation can be written,

$$E_i = \frac{E_t}{1 - \left[\frac{R_f(\sigma_1 - \sigma_3)}{(\sigma_1 - \sigma_3)f}\right]^2} \qquad (2.36)$$

using the value of E_t from one dimensional consolidation test,

$$E_i = \frac{\frac{1+e_o}{a_v}\cdot\left[1 - \frac{2.K_o^2}{(1+K_o)}\right]}{\left[1 - \frac{R_f(\sigma_1-\sigma_3)}{(\sigma_1-\sigma_3)f}\right]^2} \qquad (2.37)$$

The stress level during primary loading in a consolidation test is determined as follows:

$$\sigma_3' = K_o \cdot \sigma_1 \ldots (2.38) \text{ and } \sigma_1 - \sigma_3 = \sigma_3' \cdot \left[\frac{1 - K_o}{K_o}\right] \qquad (2.39)$$

substituting into the equation for stress level, equation (2.27) for $\sigma_1 - \sigma_3$,

$$\frac{\sigma_1 - \sigma_3}{(\sigma_1-\sigma_3)f} = \frac{\sigma_3'\left[\frac{1-K_o}{K_o}\right]}{\sigma_3'\left[\tan^2\left(45+\frac{\phi}{2}\right)-1\right]+2.c'.\tan\left(45+\frac{\phi'}{2}\right)} \qquad (2.40)$$

This equation can be substituted for E_i into equation (2.36). Thus, initial tangent modulus can be defined in terms of $c', \phi', K_o, R_f, \sigma_3'$. This way initial tangent modulus can be calculated from consolidation test results. In applying this concept to consolidation test results, it has been found that that the exponent ,n, of the variation of E_i with σ_3 is related to the curvature of the virgin curve of the e-log p' plot. Those findings may be summarized as follows :

1. For an e-Log p' curve which is concave downward, typical for silts and sands, n is less than one,

2. For a straight line virgin curve, n is equal to unity. The resulting K_m vaule under these conditions is :

$$K_m = \frac{2.3\ C.(1+e_o)}{C_c.K_o} \qquad (2.41)$$

in which C_c is the compression index (slope of the virgin curve) and C is a constant given as follows,

$$C = \frac{\left[1 - \frac{2.K_o^{\,2}}{1 + K_o}\right]}{\left[1 - \frac{R_f.\ (\sigma_1-\sigma_3)}{(\sigma_1-\sigma_3)f}\right]^2} \qquad (2.42)$$

3. For an e-log p' curve which is concave upward, typical for sensitive clays, n is greater than one.

Unloading-Reloading

Determination of an unloading modulus value from the rebound curve of a consolidation test differs from the procedure used for the primary loading modulus in the following ways :

1. The incremental change in lateral stress is not related to incremental change in axial stress by K_o, but by an incremental coefficient of lateral earth pressure, K_o^{Δ}, which is not equal to K_o.

2. The values of K_o and K_o^{Δ} increase with overconsolidation ratio throughout unloading.

3. The unloading modulus value is independent of stress level. The difference between the values of K_o^{Δ} and K_o during unloading is shown in Figure (2.14) which depicts typical hypothetical results from a one dimensional compression test for one loading and unloading cycle. The value of K_o^{Δ} is represented at point A on the unloading curve, while the value of K_o is the slope of secant line to the same point. These values are not equivalent since the unloading curve does not extend on a straight line through the origin. In this case, the change in lateral stress is related to the change in axial stress by,

$$\Delta\sigma_x' = K_o^{\Delta} . \Delta p' \qquad (2.43)$$

Thus equation (2.35) for the increment tangent modulus from a consolidation test may be changed for the unloading modulus to the following form:

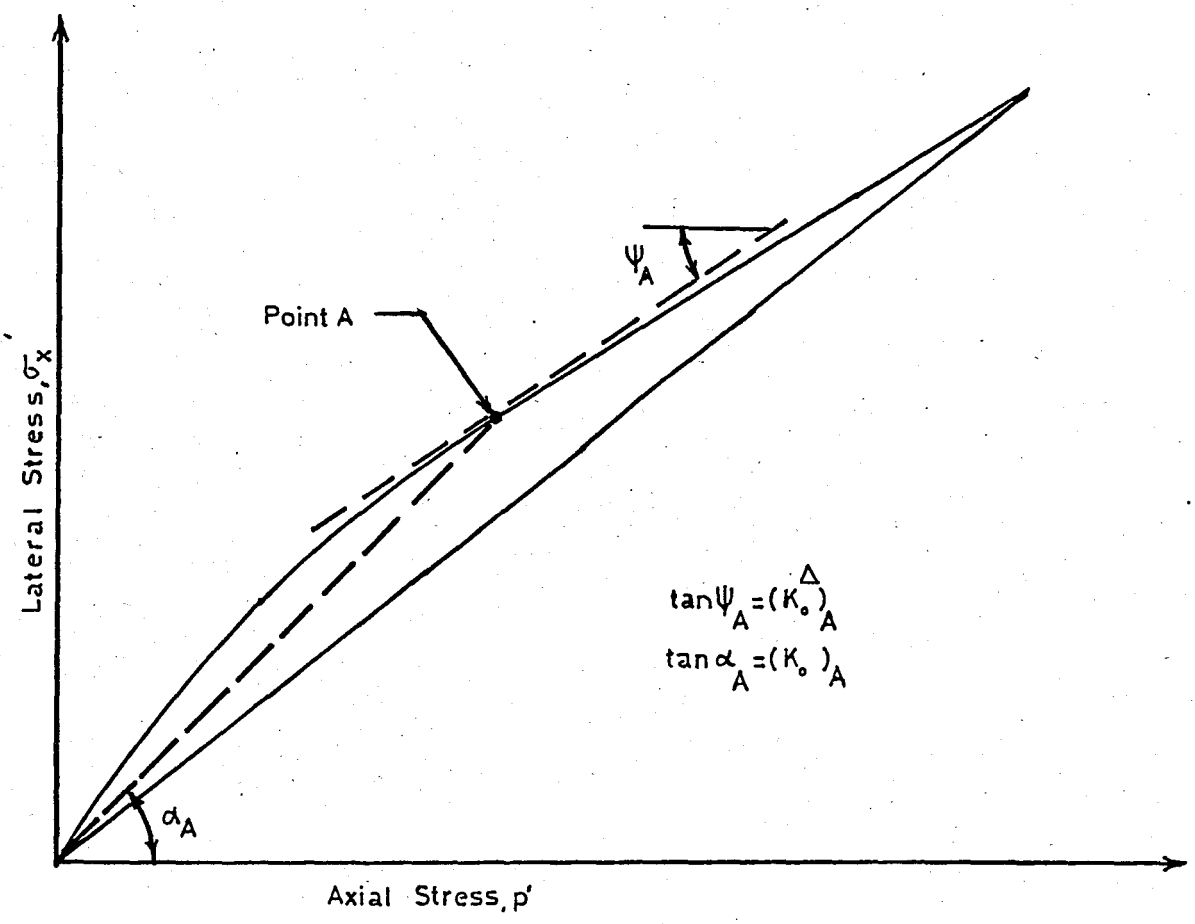

FIGURE (2.14)

Definition of Incremental Coefficient of Lateral Earth Pressure and Coefficient of Lateral Earth Pressure (After Brooker and Ireland, 1965)

$$E_{ur} = \frac{1+e_o}{a_v} \cdot \left[1 - \frac{2.(K_o^{\Delta})^2}{(1+K_o^{\Delta})} \right] \qquad (2.44)$$

The values of K_o^{Δ} and K_o increase with increasing overconsolidation ratio with the value of K_o^{Δ} reaching about 1.0 and the value of K_o reaching about 1.8 at an overconsolidaiton ratio 16. When the value of K_o becomes greater than one, at an overconsolidation ratio in the range of 3 to 6, σ_x' becomes greater than p', and the principal stresses become reoriented with σ_1' equal to σ_x' and σ_3' equal to p'.

Although the value of unloading modulus representing the unloading-reloading hysteresis loop has been assumed to be independent of stress level, the shape of the rebund curve actually varies somewhat with stress level. By examining the behaviour of a triaxial specimen in which the stress level is reduced while the confining pressure remains constant, as shown by the hypothetical stress-strain curve in figure (2.15) the reason for this variation is seen.

At the upper portion of the unloading stress-strain curve, the tangent modulus, E_1, is somewhat higher than the tangent modulus at the lower portion of the curve, E_3. In a consolidation test, the higher value of modulus, similiar to E_1, is determined from the initial portions of the rebound curve, where σ_3' is the highest, and the lower value of modulus, similar to E_3, is determined at the other end of the rebound curve where σ_3' is lowest. Thus, a variation of E_{ur} with σ_3' determined in this manner will exagerrate the effect of σ_3' on E_{ur}.

It can be seen from figure (2.15) that a good approximation to the unloading modulus is represented by the modulus value, E_2, which is determined at about the mid-point of the unloading cycle. A modulus value at one-half of the unloading cycle, similiar to E_2, may be determined from the rebound curve of an e-log p' plot by calculating a tangent modulus value using equation (2.44) at a vertical pressure equal to one-half of the original preconsolidation pressure. The variation of E_{ur} with σ_3 is established by assuming that the exponent, n, from the primary loading is the same as for unloading, as has been shown by Holubec (1968) and Chang (1969). To complete the relationship between E_{ur} and σ_3, equation(2.31)is solved for K_{ur}, as follows

$$K_{ur} = \frac{E_{ur}/p_a}{(\frac{\sigma_3}{p_a})^n} \qquad (2.45)$$

Thus with the unloading modulus value determined by this procedure, the initial tangent modulus determined by equation (2.36), the ϕ', and c' values from the direct shear tests, and the analytical formulation of Duncan and Chang (1969), the stress-strain response of a soil may be established using consolidation and direct-shear test results.

Determination of Parameters from Triaxial Test Results.

To develop techniques for evaluating the parameters K,n, R_f,c and ϕ, and to evaluate the usefulness of Equation (2.30) for representing nonlinear, stress-dependent soil behaviour,

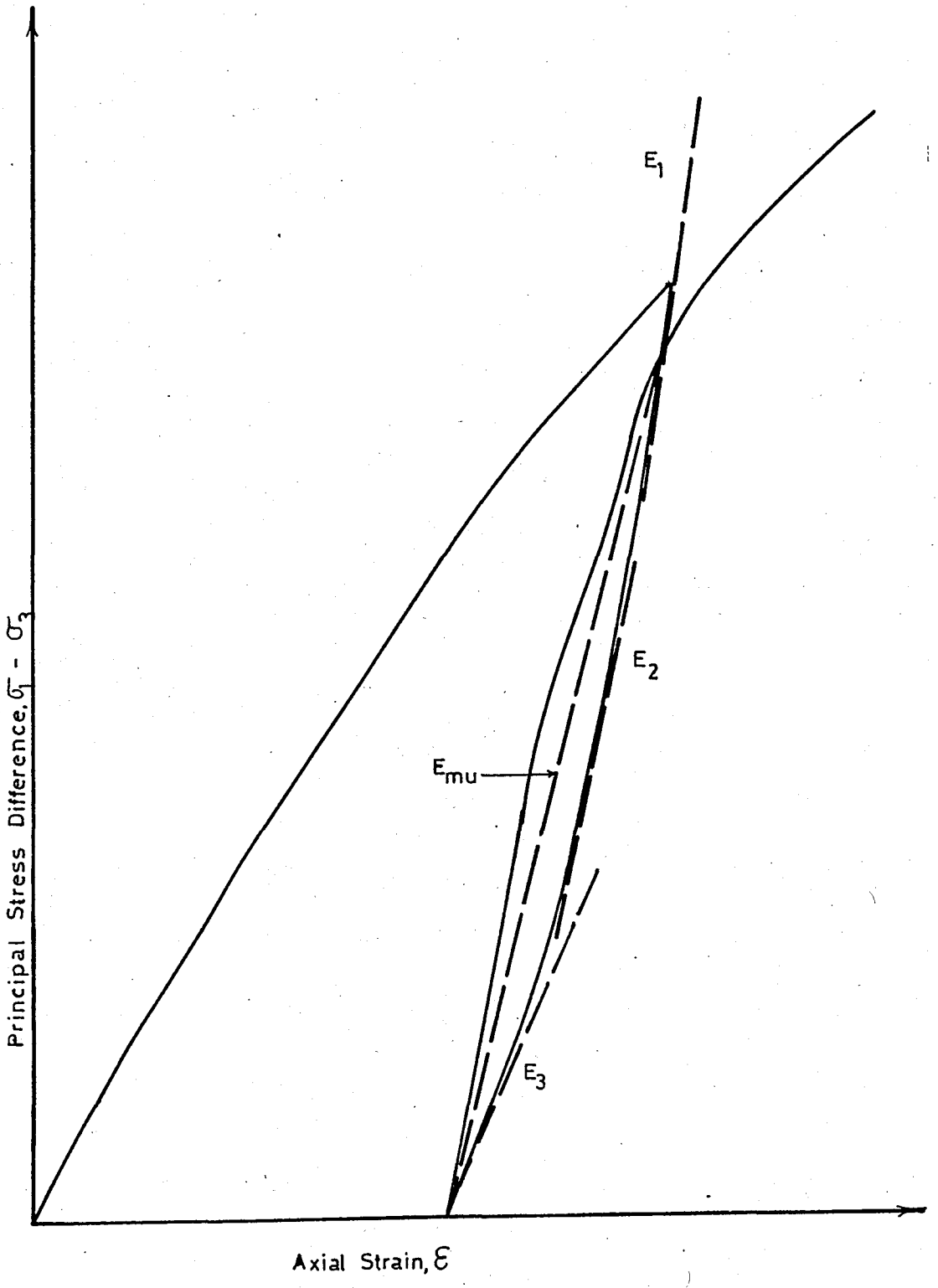

FIGURE(2.15)
Effect of Shape of Unloading Curve on Tangent Modulus Values(After Chang, 1969)

a number of tests have conducted on a uniform fine silica sand by Duncan and Chang(1970). The first of these tests were standard drained triaxial compression tests, which were used to evaluate the parameters representing the behaviour of the sand upon primary loading. Tests were also conducted to find out the stress-strain behaviour of the sand during unloading and reloading.

The sand used in these experiments is a uniform fine silica sand with subangular to subrounded particles. Tests were performed on specimens prepared at two different initial void ratios; Dense, e = 0.50, Dr=100%,which was the lowest void ratio obtainable by vibration in a saturated state; and Loose, e = 0.67, Dr = 38%, which was the loosest condition which can be easily prepared.

In primary loading case, two series of compression tests were conducted, on dense and loose specimens, at effective confining pressure 1 kg per sq cm, 3 kg per sq cm, and 5 kg per sq cm. The variations of stress diffrenece and volume change with axial strain in these tests are shown in Figure (2.16) and (2.17) hypotheticaly. It may be noted that the dense specimens dilated considerably during the test, whereas the loose specimens compressed or dilated very little. The axial strains at failure were 2% to 4% for the dense specimens and 12% to 16% for the loose specimens. The strength parameters determined from these tests were $C_d=0, \phi_d = 36.5^o$ for the dense specimens, and $C_d=0, \phi_d=30.4^o$ for the loose specimens.

The stress-strain data for the dense specimen tested at 5 kg per sq cm have been replotted on transformed axes in figure

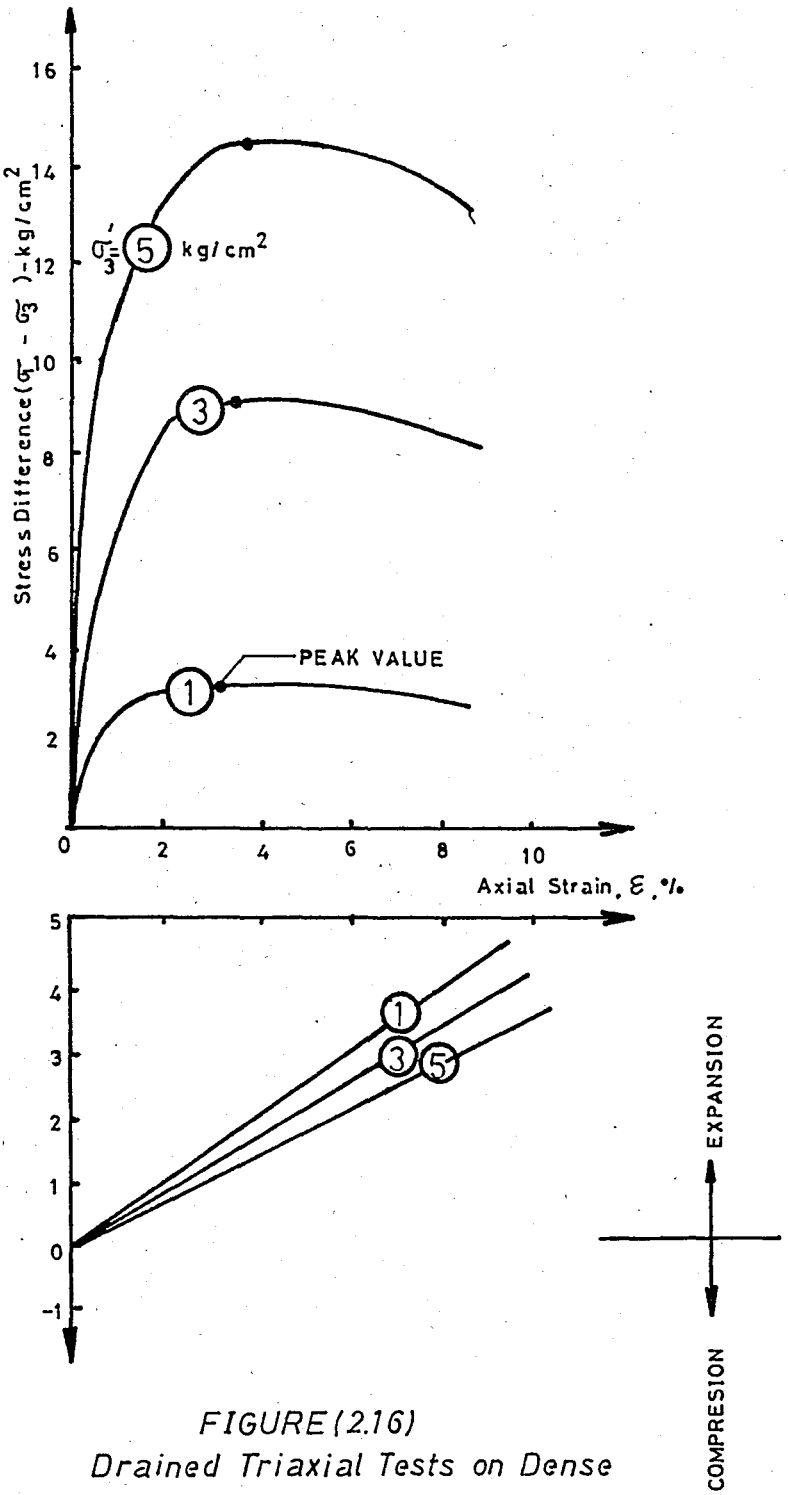

FIGURE (2.16)
Drained Triaxial Tests on Dense Slica Sand (After Duncan and Chang, 1970)

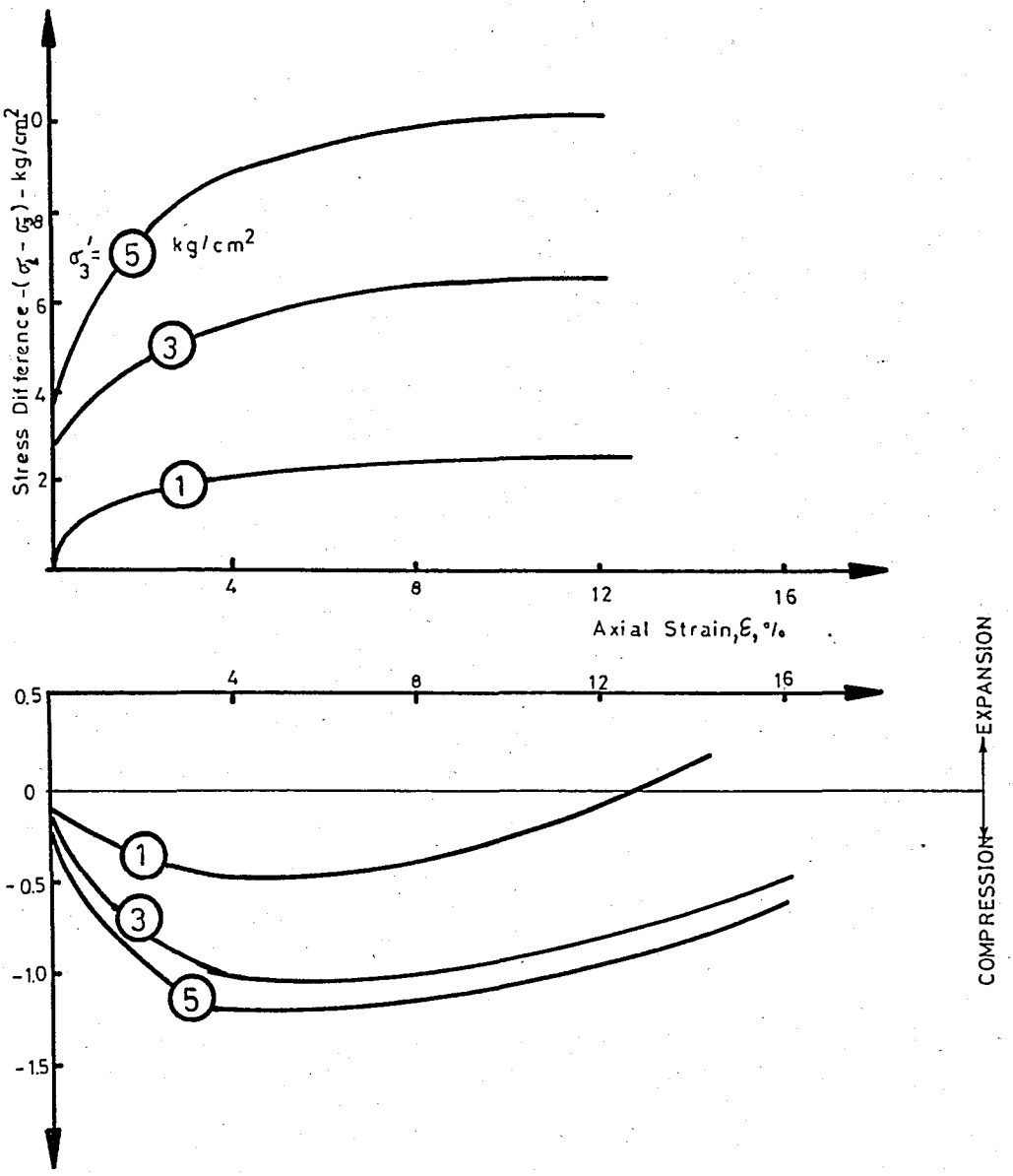

FIGURE (2.17)
Drained Triaxial Tests on Loose Slica Sand
(After Duncan and Chang, 1970)

(2.18 ab) for the purpose of determining the values of E_i and $(\sigma_1-\sigma_3)_{ult}$. It may be noted that data diverge somewhat from a linear relationship at both low and high values of strain, indicating that the stress-strain curve for this test is not precisely hyperbolic in form. However, a hyperbola may be fitted to these data at the origin $[(\sigma_1-\sigma_3)=0, \varepsilon = 0]$ and at two other points. To reduce the degree of subjectivity in this procedure, it was found to be desirable to be consistent with respect to the values of stress level, at which the hyperbolae fits the stress-strain curve. By repeated trials, Duncan and Chang have found that the best choices for overall agreement were S = 0.70 and S = 0.95, or 70% and 95% strength mobilized. This procedure has been found to suit well for a variety of other soils.

The stress-strain data for the loose specimen tested at 5 kg per sq cm has been plotted on transformed axes in figure (2.19). It may be noted that these data diverge from a linear relationship also, but in the opposite way from the dense sand. The relationships depicted in Figure (2.18a) and (2.18b) have been found to be hold in general. The transformed stress-strain data for dense specimens generally lie above the bet fit line at small values of strain, while the data for loose specimens generally lie below the best fit straight line. However, it has been found in every case to be possible to approach the actual stress-strain curve by hyperbolae to a reasonable degree of accuracy.

The values of $(\sigma_1 - \sigma_3)_{ult}$ shown in figure (2.18a) and (2.18b) are somewhat larger than the values of stress difference

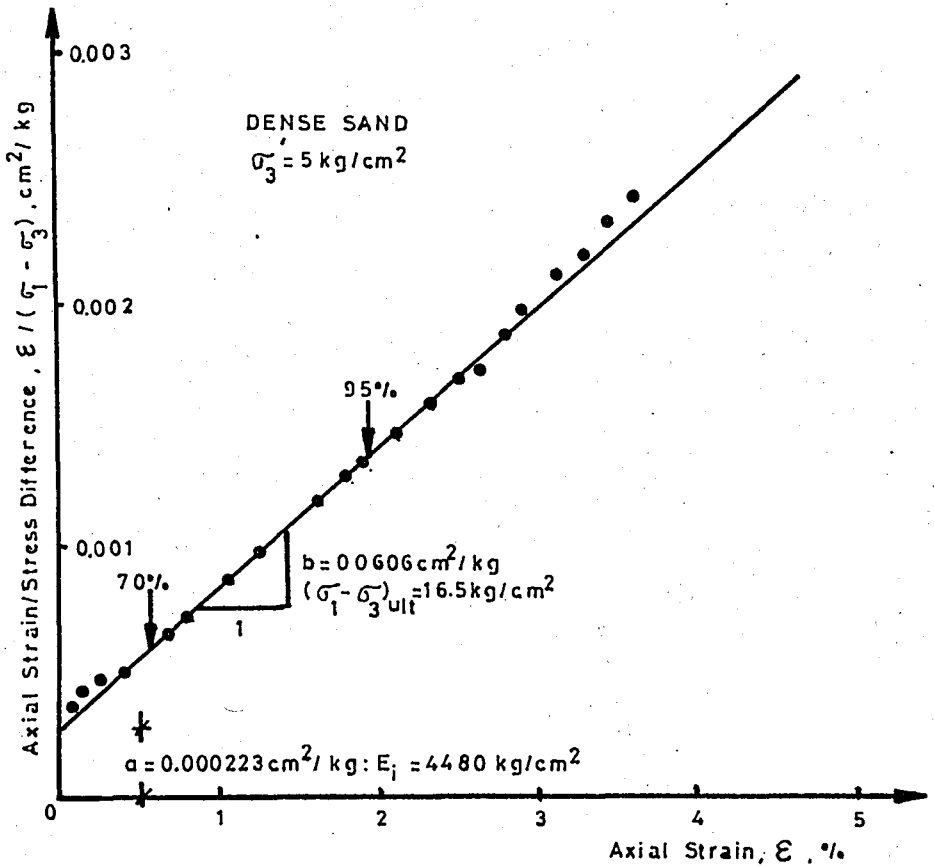

FIGURE(2.18a)
Transformed Stress-Strain Curve for Dense Slica Sand(After Duncan and Chang ,1970)

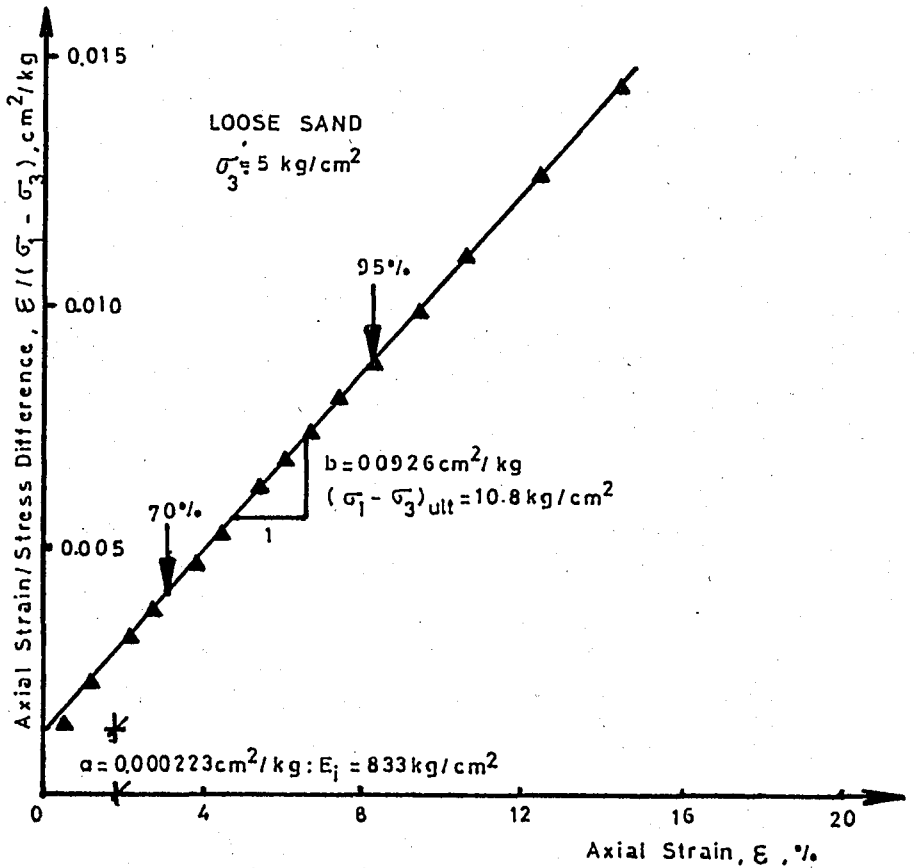

FIGURE(2.18b)
Transformed Stress-Strain Curve for Loose Slica Sand(After Duncan and Chang ,1970)

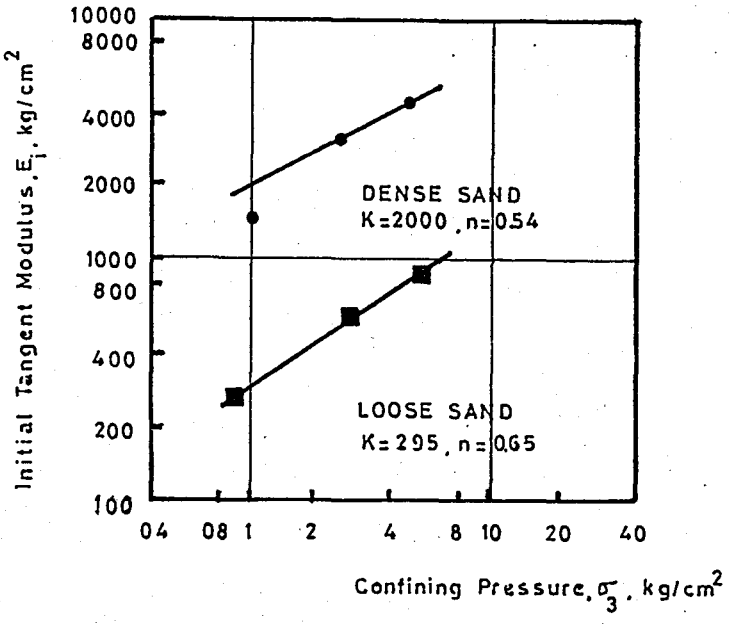

FIGURE(2.19)

Variation of Initial Tangent Modulus with Confining Pressure for Drained Triaxial Tests on Slica Sand(After Duncan and Chang,1970)

at failure in these same tests. The values of R_f, which are a measure of this difference, were found to be 0.91± 0.03 for the dense sand, and 0.90± 0.05 for the loose sand. The values of E_i determined for six tests have been plotted against the corresponding values of σ_3 in figure (2.19), for the purpose of determining the values of K and n. Linear interpretations of these data are shown in Figure (2.19). The straight lines shown correspond to K=2000, n=0.54 for the dense sand, and K=295, n=0.65 for the loose sand.

In loading-reloading case, Davis and Poulos, Makhlouf and Steward, Karst, K_o and Scott, and Holubec have shown that soil is an elasto-plastic material, namely strains occured during primary loading are partially recoverable upon unloading, and when reloaded it behaves nearly elastically. To see this behaviour of the silica sand described herein, additional tests were conducted in which specimens were subjected to one or more cycles of unloading and reloading.

The results of one of these tests on dense sand is shown in figure (2.20) schematically. It may be noted that for cycles of unloading and reloading the sand has a small amount of hysteresis, but is very nearly linear and elastic. Furthermore, the modulus values for both cycles of unloading-reloading are the same, even they occur at different strains and stress levels. Tests conducted on loose specimens of this sand gave similiar results, and similiar behaviour has been found to be characteristic of other soils by Ko ond Scott. On the basis of these observations it seems reasonable to believe that the stress-strain behaviour of soils on unloading and reloading may be

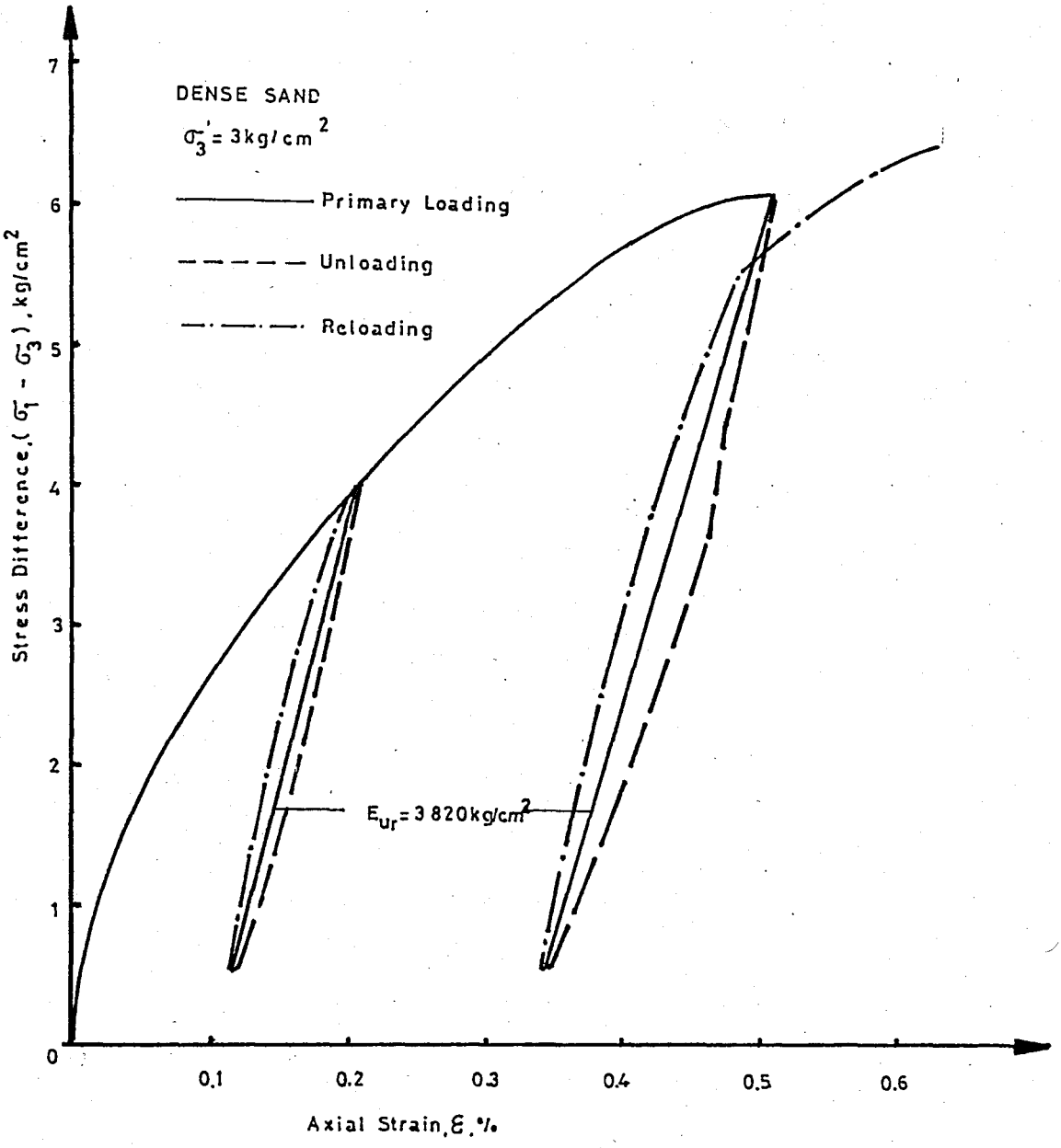

FIGURE (2.20)

Unloading and Reloading of Slica Sand under Drained Triaxial Test Conditions (After Duncan and Chang, 1970)

approximated with a high degree of accuracy as being linear and elastic. Because this linear behaviour is independent of the vaule of stress difference, the representative modulus value is dependent only upon the confining pressure, σ_3. Therefore, the unloading-reloading modulus value, E_{ur}, can be formulated as in equation (2.31). The value of K_{ur} for unloading-reloading, however, is higher than for primary loading. For the slica sand in a dense condition K_{ur} was found to be 2120, and for the Loose condition 1090.

2.6 LOAD-DEFORMATION BEHAVIOUR OF INTERFACE

The finite element analyses is based upon the nodal point displacement compatibility, and do not permit for relative movements between adjacent element, even they are dissimiliar. Due to this fact, an element which provides relative movements is necessary. Since, soil in most of the problems is in contact with other kinds of materials, Goodman, et al., (1968) developed a one-dimensional element capable of undergoing relative displacements which connected the adjacent two-dimensional elements along the entire boundary between the elements.(Fig. 2.21) In order to calculate both normal and shear stiffnesses, it was assumed that both normal and shear displacements vary linearly along the external boundary of the elements and interface element has zero thickness. This kind of displacement variation is suitable with the linear strain triangle used in the program.

The interface element has two kinds of stiffness; normal,

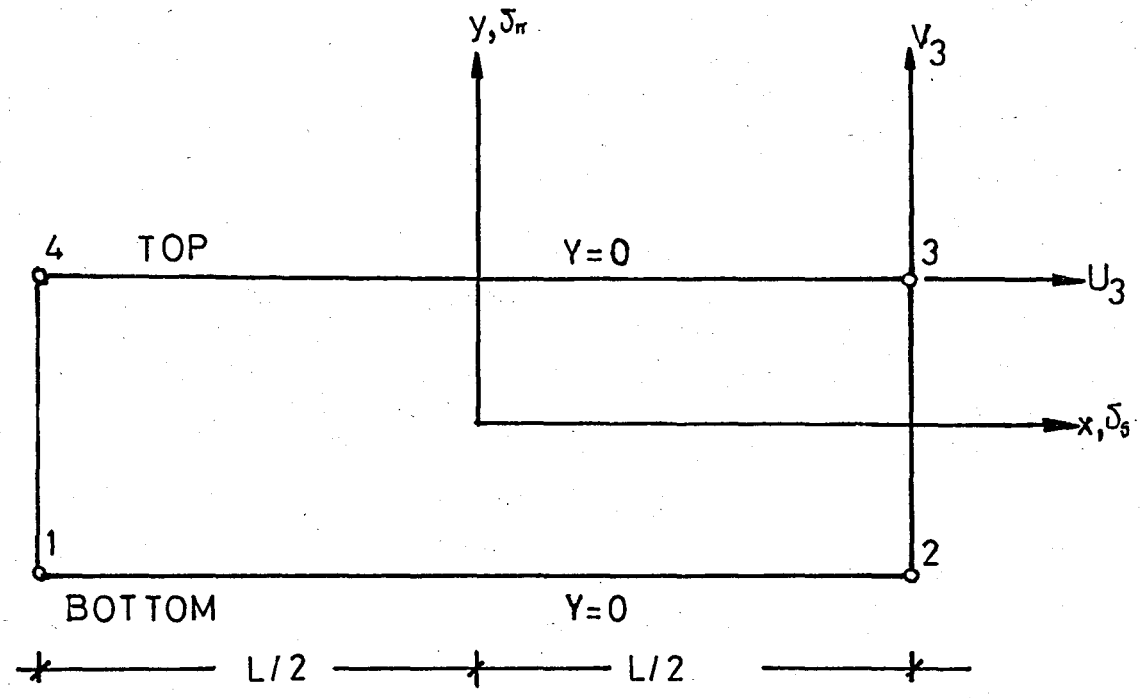

δ_s, δ_n = Relative shear and normal displacements

u = Tangential nodal displacement

v = Normal nodal displacement

FIGURE (2.21)
Interface Element with Zero Thickness (After Goodman, 1968)

k_n, and shear, k_s, stiffnesses. They are related to the corresponding normal stress, σ_n, and shearing stress, τ, acting on the element respectively. The relationship between stiffnesses and stresses are given by the following equations.

$$\sigma_n = k_n . \Delta_n \qquad (2.46)$$

$$\tau = k_s . \Delta_s \qquad (2.47)$$

in which Δ_n is the average relative normal displacement across the element and Δ_s is the average relative shear displacement along the element. The units of σ_n and τ are force/length^2 and units of k_n and k_s are force/length^3.

Possible modes of behaviour of interface element is given in figure (2.22). It can be readily visualized that combined mode and the compressional mode, the adjacent two dimensional elements overlap. This condition occurs due to the fact that compressive stresses require compressive relative displacement across the interface. This kind of behaviour is minimized by using very large normal stiffness which prevents normal displacement of the element considerably.

The mode of behaviour of the interface element of primary interest is the shearing behaviour. The amount of the relative shear displacement and shear stress that develops on an interface element depends upon the shearing stiffness, k_s. For the cases where new layer of soil, such as backfill, is placed, "liquid" condition is assumed. In this case, interface is considered as a frictionless element by assigning a very small

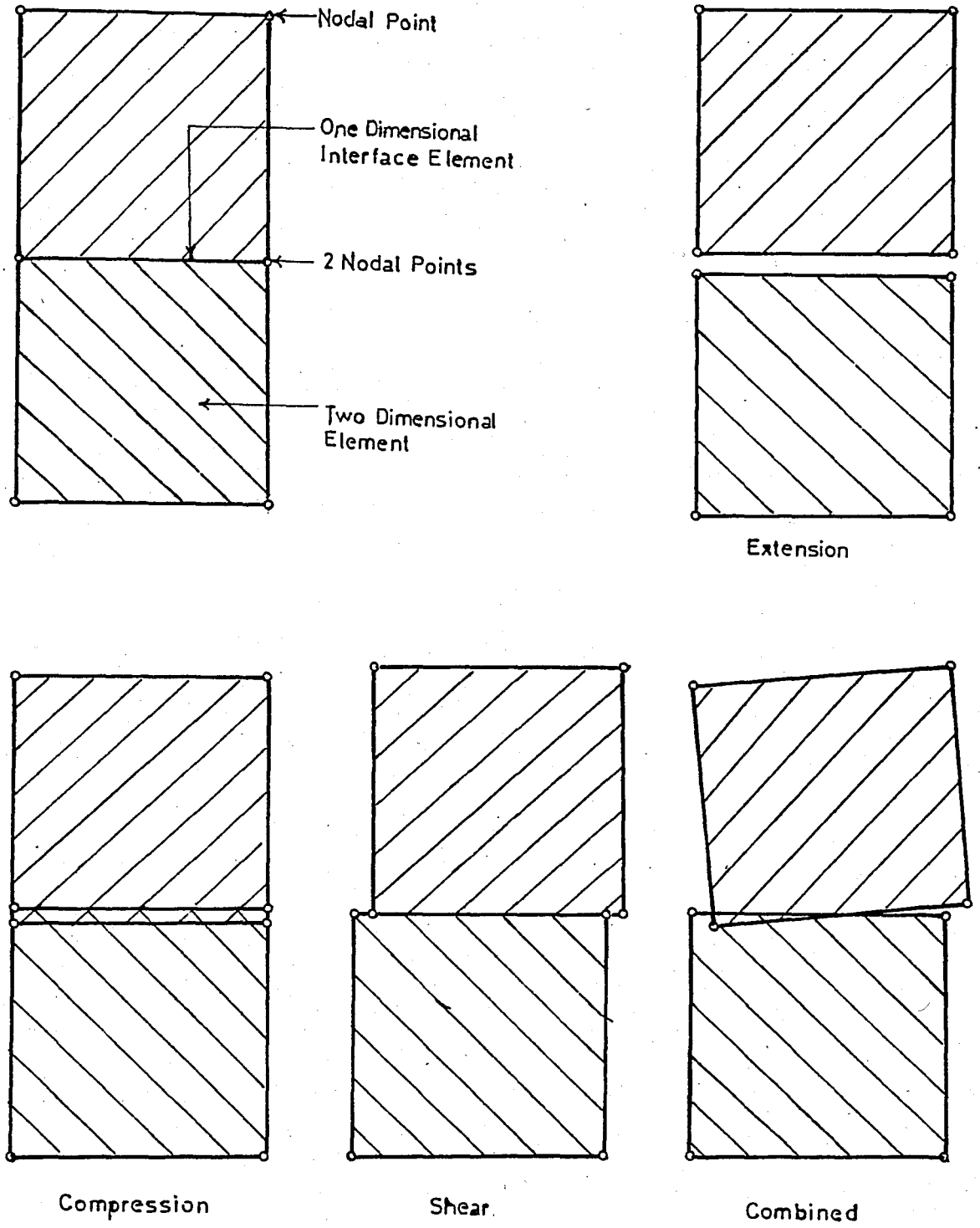

FIGURE(2.22)
Modes of Behaviour of Interface Element
(After Duncan and Goodman, 1968)

shearing stiffness. However, afterwards, when the properties of the two-dimensional soil element are modified to reflect their behaviour during placement of subsequent layers, the properties of the interface elements are also modified to reflect to appropriate stress-displacement characteristics of the interface.

The properties of interface elements can be found in laboratory by conducting interface tests for the sand. A section through the shear box with the specimen in place is shown in figure (2.23).

Because the results of the interface tests showed that the relationship between the shear-stress and relative displacement on the interface was non-linear in form and dependent upon the normal stress on the interface,on analytical simulation of this behaviour was realized using hyperbolic form as in the case of stress-strain behaviour of soils. Terminology to be used in a hyperbolic formulation of this type are shown schematically on the shear stress-relative displacement curve in Figure (2.24).

For a hyperbolic shearing stress versus relative displacement curve, the following equation represents the relationship,

$$\tau = \frac{\Delta s}{a + b.\ \Delta s} \qquad (2.48)$$

where "a" and "b" are constants depending upon the roughness characteristics of the interface and the value of normal stress. Equation (2.48) may be rearranged into a linear form

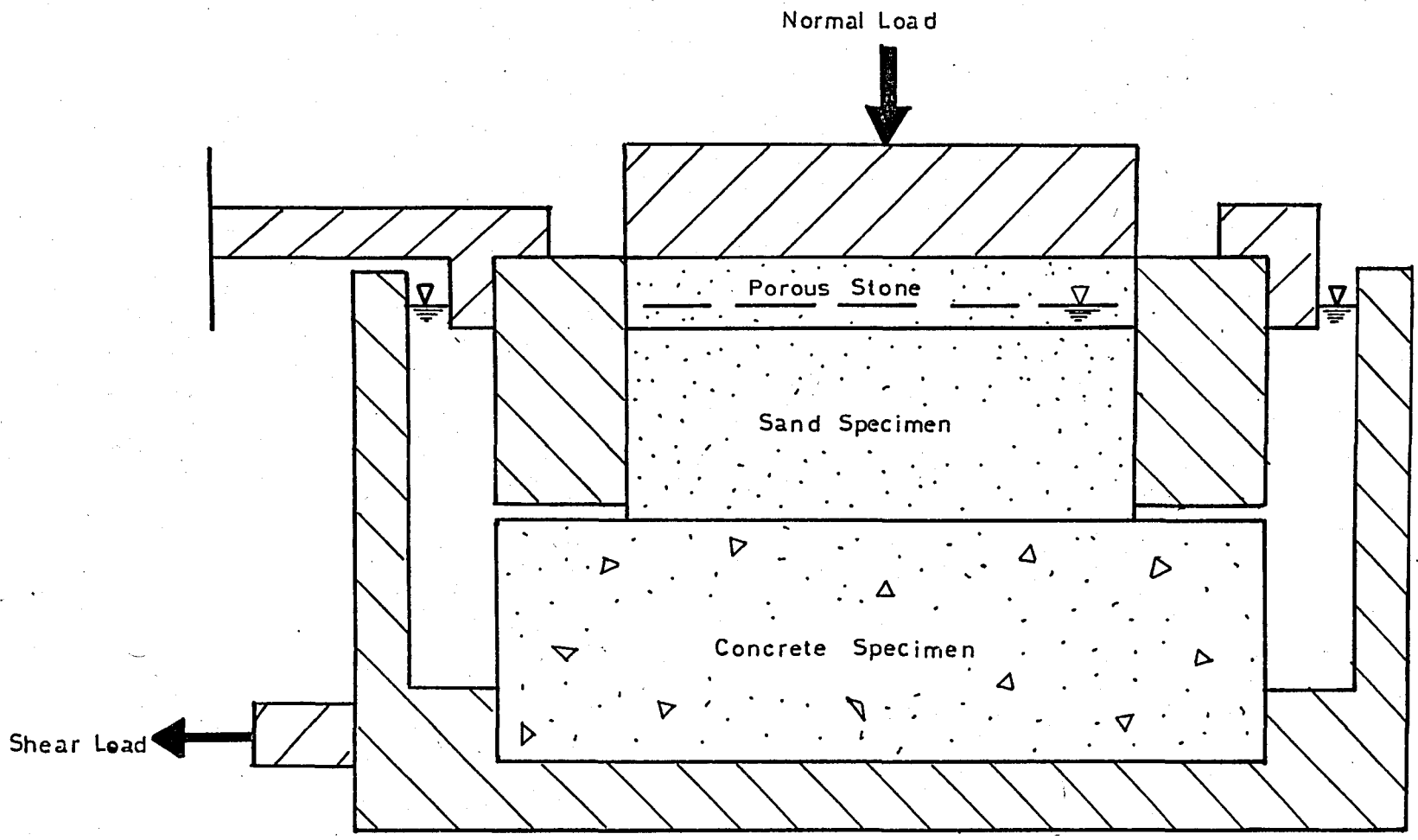

FIGURE (2.23)
Interface Test Arrangement
(After Clough and Duncan,1969)

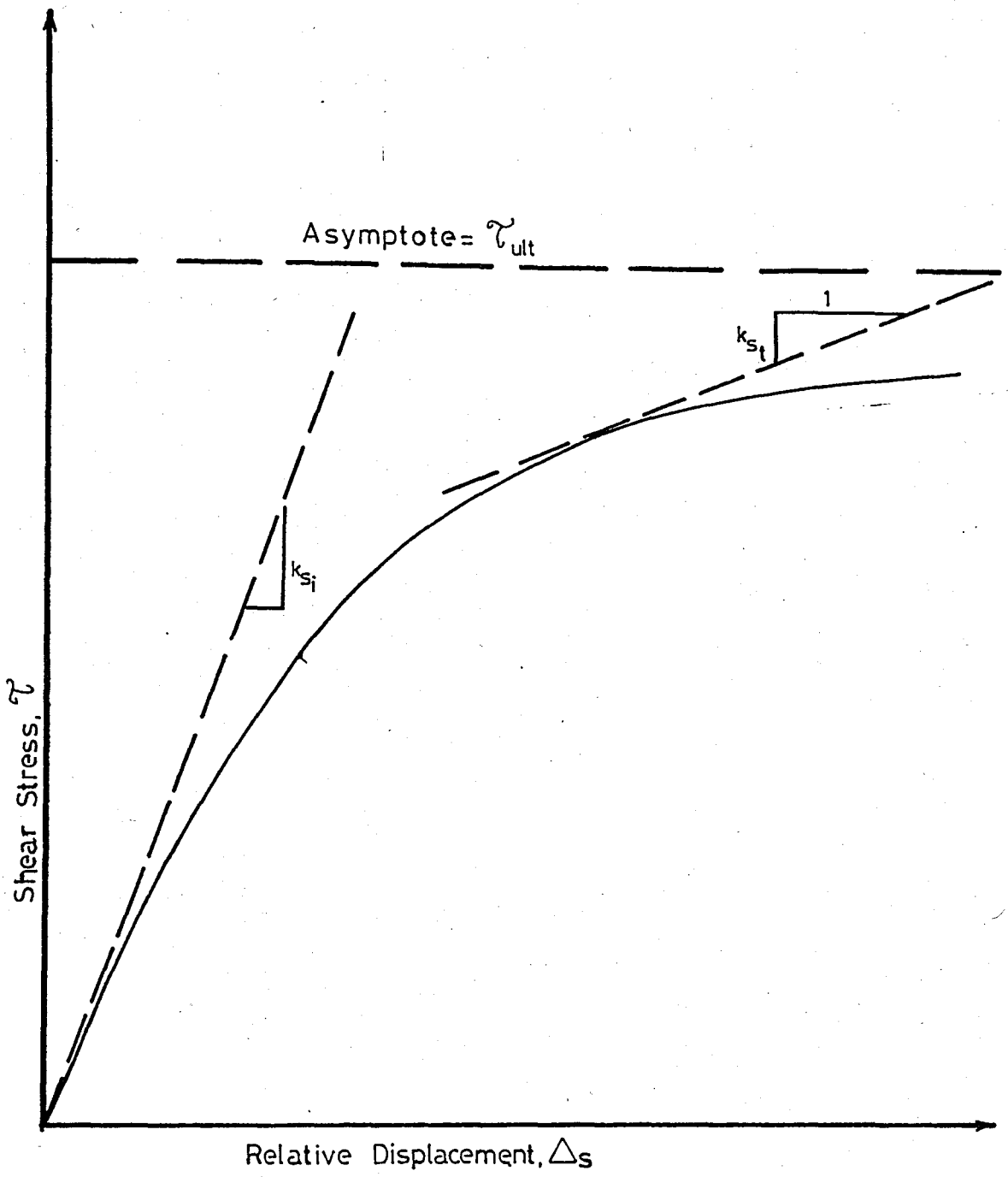

FIGURE(2.24)

Hyperbolic Representation of the Variation of Shear Stress with Relative Displacement(After Clough and Duncan,1969)

as follows

$$\frac{\Delta_s}{\tau} = a + b.\ \Delta_s \qquad (2.49)$$

By plotting test data in the form of equation (2.49), the data should describe a straight line if the relationship is appropriately described by the hyperbolic form. The transformed linear hyperbolic plots is shown in Figure (2.25) As mentioned previously in the description of hyperbolic stress-strain relationship, it was found suitable to determine the straight lines by connecting the points on the curves corresponding to 70% and 95% of shear-resistance mobilized.

The constant "a" in equation (2.48) may be shown to be related to the initial tangent stiffness by the following equation,

$$a = \frac{1}{k_{si}} \qquad (2.50)$$

And by rearranging equation (2.48) into the form,

$$b = \frac{1}{\tau} - \frac{a}{\Delta_s} \qquad (2.51)$$

It may be noted that Δ_s becomes very large when τ approaches to its asymptotic value, τ_{ult}. Therefore,

$$b = \frac{1}{\tau_{ult}} \qquad (2.52)$$

The relationships expressed by equation (2.50) and equation (2.52) may be used to determine k_{si} and τ_{ult} from

the transformed linear hyperbolic plots in figure (2.26),by evaluating "a" and "b"

The tengent shear-stiffness at any point on the hyperbolic curve may be found from equation (2.49) by determining the slope,

$$k_{st} = \frac{d\,\tau}{d\Delta_s} = \frac{a}{(a+b.\sigma_s)^2} \qquad (2.53)$$

An expression for Δ_s can be written from equation (2.48)

$$\Delta_s = \frac{a.\tau}{1-b.\tau} \qquad (2.54)$$

Plugging the values of "a" equation (2.50) and "b" equation (2.52) for Δ_s,

$$\Delta_s = \frac{\tau_{ult}}{k_{si}(\tau_{ult} - \tau)} \qquad (2.55)$$

The values of "a", "b", "Δ_s" from equations (2.50)(2.52), and (2.55), respectively, can be substituted into equation (2.53) for the tangent shear stiffness, the succeding equation is found,

$$k_{st} = k_{si} \cdot \left(1 - \frac{\tau}{\tau_{ult}}\right)^2 \qquad (2.56)$$

Since the value of τ_{ult} overestimates the actual shear stress at failure, τ_f, the ratio between those values is introduced, R_f. Then equation (2.56) is rewritten,

$$k_{st} = k_{si} * (1 - \frac{R_f \cdot \tau}{\tau_f})^2 \qquad (2.57)$$

The value of τ_f can be obtained from figure (2.24b). Since τ_f is related to the normal stress on the interface, σ_n (equation 2.58), the following equation is obtained,

$$\tau_f = \sigma_n . \tan\delta \qquad (2.58)$$

$$k_{st} = k_{si} . (1 - \frac{R_f . \tau}{\sigma_n . \tan\delta})^2 \qquad (2.59)$$

The values of "k_{si}" determined from figure (2.25) are plotted against "σ_n" on Log-Log scales in figure (2.26) where k_{si} changes exponentially with "σ_n" resulting in a relationship between "k_{si}" and "n" of the form,

$$k_{si} = K_j . \gamma_\omega \ (\frac{\sigma_n}{p_a})^n \qquad (2.60)$$

in which "K_j" and "n" are experimentally determined constants and γ_ω is the unit weight of water.

By substituting equation (2.60) for k_{si} into equation (2.59) for k_{st},

$$k_{st} = K_j . \gamma_\omega \ (\frac{\sigma_n}{p_a})^n . \ (1 - \frac{R_f . \tau}{\sigma_n . \tan})^2 \qquad (2.61)$$

Equation (2.61) represents a simplified, practical relationship which describes the nonlinear, stress dependent, stress-displacement behaviour of an interface primarily between sand and concrete. Total stress notation is used

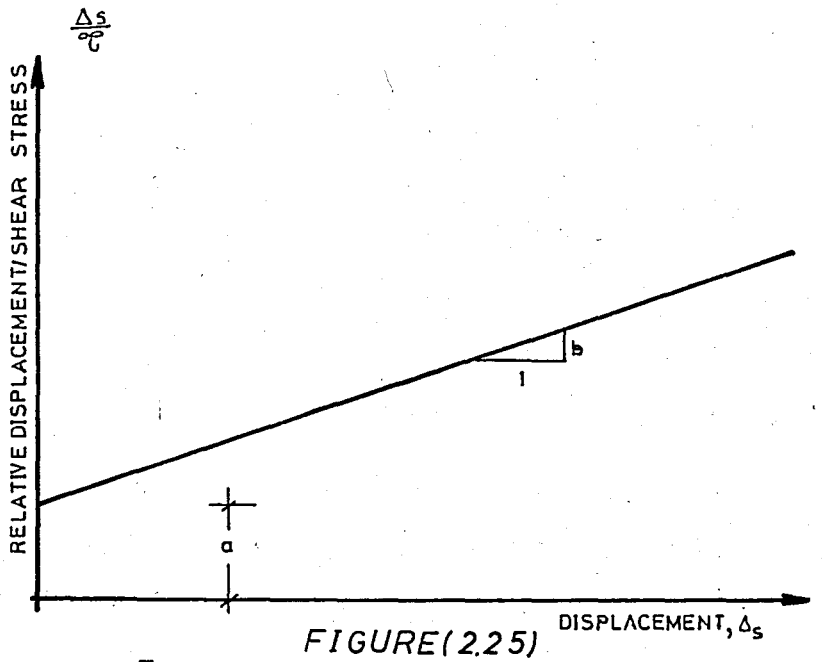

FIGURE(2.25)
Transformed Linear Hyperbolic Plot
(After Clough and Duncan, 1969)

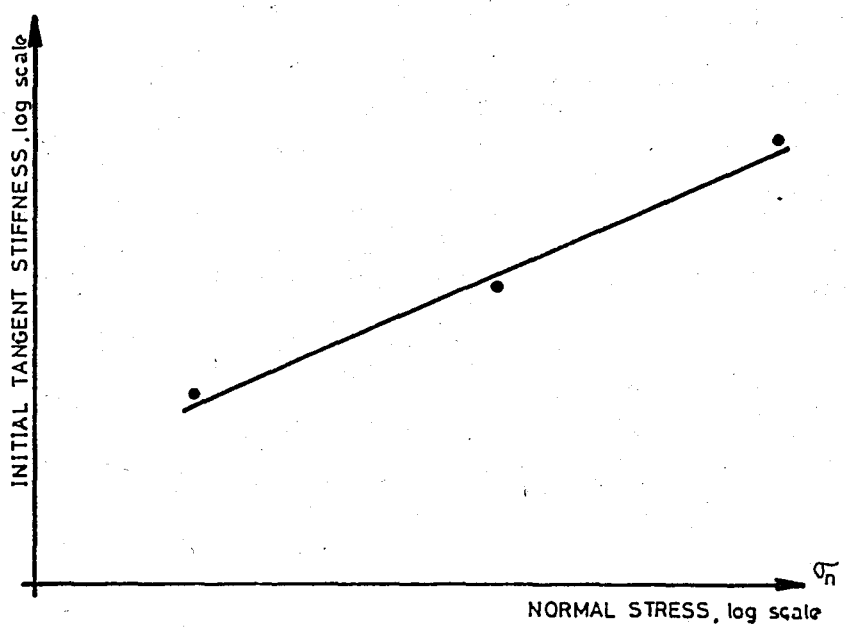

FIGURE(2.26)
Variation of Initial Tangent Stiffness Values with Normal Stress
(After Clough and Duncan, 1969)

throughout in this derivation, but if the interface is under water, then σ_n should replace σ_n in equation (2.58)

The interface element formulation of Goodman, et al., (1968) was used in the incremental finite element program with the hyperbolic shear stress-relative displacement relationship. Because the hyperbolic relationship is stress-dependent, the shear stiffness is evaluated for each increment at the same time modulus values are calculated for the two-dimensional elements.

2.7 SUMMARY

Techniques have been summarized for finite element analyses of following types of incremental loading. For excavation, a method was introduced for elements of arbitrary shape by reversing the initial stresses on the excavation boundary. An interpolation formula was developed to determine the boundary stresses to a high degree of accuracy. The distributed loading due to water pressure changes in pervious soils could be simulated by a technique which was a special case of the excavation bounday loading. Changes of water pressures around the boundaries of elements was also considered. Techniques for placement of concrete and backfill and temperature effects were summarized.

The formulation of the stress-strain behaviour of a soil developed by Duncan and Chang(1969) was presented in detail. The principal factors included in the formulation are the effects of stress dependency, non linearty and inelasticity.

A procedure for determining primary loading and unloading modulus values from consolidation test results was also shown.

At the end of the chapter, the behaviour and formulation of interface elements which is used between the structural material and soil elements was presented.

III. APPLICATION OF SOIL-STRUCT

3.1 INTRODUCTION

In order to show the effectiveness and applicability of program-SOIL-STRUCT, a number of cases is analyzed. From the results of those analyses, the program SOIL-STRUCT is found to be effective and versatile computer program as long as it goes together with detailed investigation of parameters both in laboratory and in site. In laboratory, triaxial test, shear-box and one-dimnsional consolidation test results can be employed by utilizing the procedures developed by Duncan and Chang (1969).

3.2 EMBANKMENT PROBLEM

In order to show the importance of non-linear material behavior and incremental construction with respect to gravity turn-on analyses, an embankment problem is analyzed and results are given in table 3.2 to 3.4. In those tables results are compared with elastic solutions. Attention is given to the vertical and horizontal components of stresses and the shear-stresses developed in the medium under the weight of the embankment. Results are given at the centerline and the toe of embankment in a vertical line. Also, the base pressures underneath the embankment with corresponding elastic solutions are given. Since the elastic solutions are valid for instantaneous loading and elastic material, the comparison can be made between conventional techniques and the incremental finite element analyses.

Table 3.1 Material Properties of Embankment Problem

Material	ν	ν_{ult}	$\gamma(t/m^3)$	R.F	K_o	$\phi(^o)$	n	IDRAIN	K_m	K_{ur}	$c(t/m^2)$	$E_{ult}(t/m^2)$	α
Sand (Foundation)	03	0.45	1.75	0.90	0.45	40.	0.50	1	580.	860.	0	15000.	
Clay (Embankment)	03	0.45	2.00	0.85	0.30	30.	0.85	1	80	200.	2.	7000.	

The material properties used throughout this embankment problem are given in table 3.1. The mesh which is designed to simulate the embankment loading is given in figure 3.1

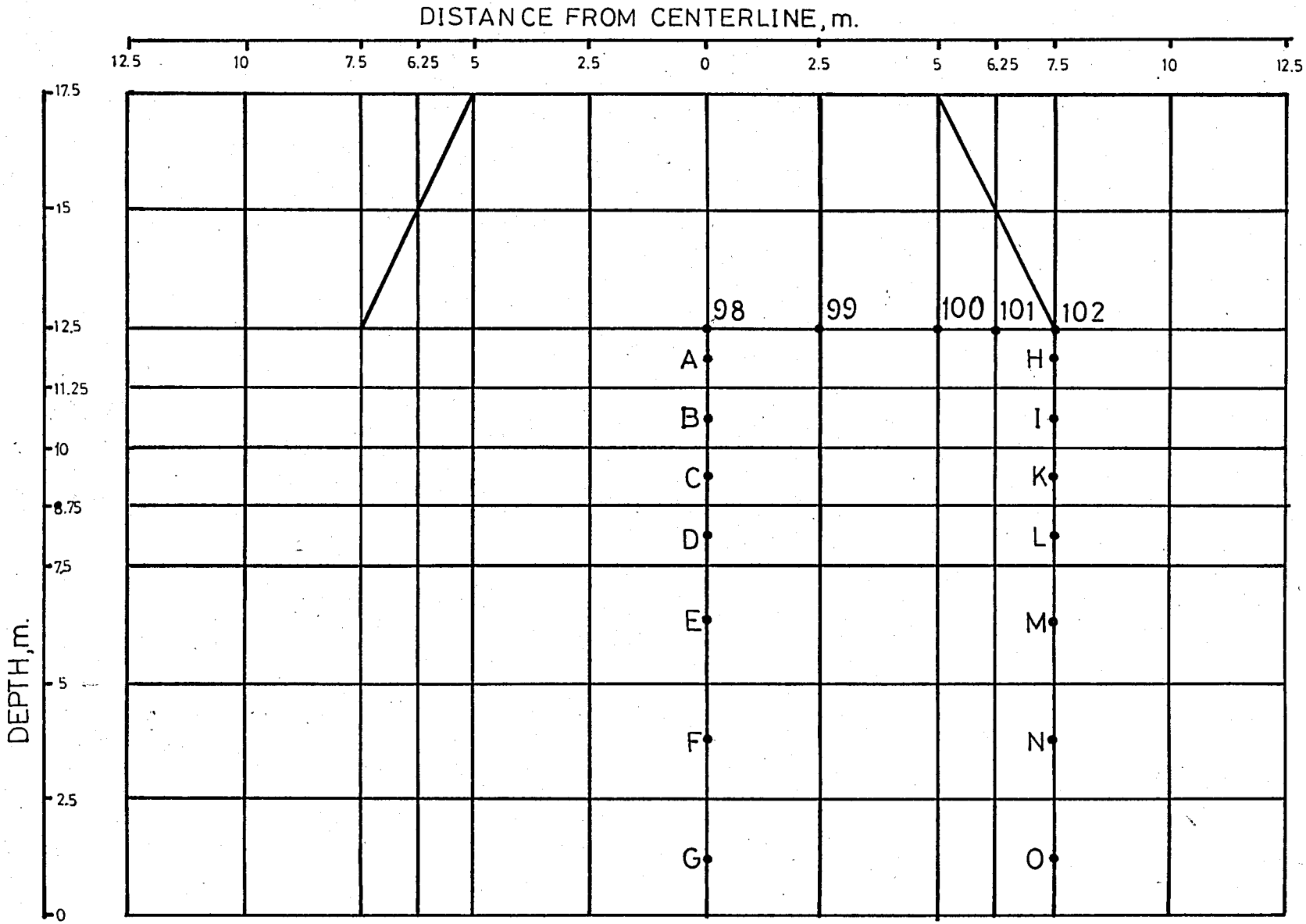

FIGURE (3.1)
The Finite Element Mesh for
The Embankment Problem

In this problem elastic solutions were obtained by Perloff (1967). During the derivation of elastic solutions, the weight of the embankment is assumed to be primary importance. Later these solutions were revised by Verrujit (1969). In elastic solutions, σ_y is independent of Poisson's ratio while σ_x is dependent. Furthermore, the loading of embankment weight is instantaneous.

According to solutions for vertical stress, the effect of incremental construction is seen in the lower portion of mesh at the center of embankment.(table 3.2). On the other hand, at the 'toe' of embankment, the effect of incremental construction is large throughout the medium. The large differences are associated with the nature of non-linear analyses and the variety of parameters used in the program. Since elastic theory uses only two parameters, unit weight, poisson's ratio, but non-linear analyses employ much more parameters for embankment problems. The effect of incremental construction is larger for horizontal stresses, as seem in table (3.3). For shear stresses at the centerline, elastic theory comply with incremental analyses. The differences are due to numeric calculation during the execution of the program. At the toe of embankment, relatively small differences exist in the upper portion, but differences are still large in the lower portion. (see table 3.4)

The only well-correspondence is obtained for the base pressures underneath the embankment(figure 3.2). In general, the highest difference is seen for node 99. which is about 10%. On the other hand, the rest are below 2%.

TABLE(3.2) σ_y Stresses In The Medium Under The Embankment

DEPTH	AT THE CENTERLINE OF EMBANKMENT					AT THE TOE OF EMBANKMENT				
	POINT	FINAL STRESS t/m2	INITIAL STRESS t/m2	THE DIFFERENCE t/m2	ELASTIC THEORY t/m2	POINT	FINAL STRESS t/m2	INITIAL STRESS t/m2	THE DIFFERENCE t/m2	ELASTIC THEORY t/m2
11.875	A	15.640	6.144	9.496	8.2	H	8.342	5.799	2.543	0.9
10.625	B	17.225	8.255	8.970	8.0	I	11.419	8.326	3.093	1.0
9.375	C	18.970	10.506	8.464	7.0	K	13.750	10.352	3.398	2.0
8.125	D	20.645	12.658	7.987	6.2	L	16.395	12.647	3.748	2.2
6.25	E	23.340	15.950	7.390	5.4	M	19.990	15.902	4.008	2.5
3.75	F	27.070	20.314	6.756	4.2	N	24.605	20.312	4.293	2.8
12.5	G	30.970	24.692	6.278	3.5	O	29.175	24.668	4.507	3.0

TABLE(3.3) σ_x Stresses In The Medium Under The Embankment

DEPTH m.	AT THE CENTERLINE OF EMBANKMENT					AT THE TOE OF EMBANKMENT				
	POINT	FINAL STRESS t/m2	INITIAL STRESS t/m2	THE DIFFERENCE t/m2	ELASTIC THEORY t/m2	POINT	FINAL STRESS t/m2	INITIAL STRESS t/m2	THE DIFFERENCE t/m2	ELASTIC THEORY t/m2
11.870	A	6.111	2.765	3.346	1.0	H	6.007	2.610	3.397	2.5
10.625	B	6.999	3.724	3.275	0.8	I	7.367	3.747	3.620	2.0
9.375	C	7.844	4.728	3.116	0.0	K	8.388	4.658	3.730	1.6
8.125	D	8.623	5.696	2.927	-0.2	L	9.462	5.703	3.759	1.2
6.25	E	9.953	7.177	2.776	-0.3	M	11.175	7.156	4.019	0.8
3.75	F	12.040	9.141	2.899	-0.4	N	12.710	9.141	3.569	0.5
1.25	G	14.640	11.112	3.528	-0.4	O	14.370	11.100	3.270	0.4

To sum up, the incementel construction yields relatively different results with respect to elastic analyses due to inelasticity and stress dependency approach. This is due to the fact that incremental analyses needs many parameters with respect to elastic analyses in which only two parameters are used to calculate stresses, polsson's ratio and unit weight of soil.

3.3 CONCENTRATED LOAD PROBLEM

As another example showing the dependability of SOIL-STRUCT according to elasticity theory solutions, a simple case is analyzed. The material is assumed to be sand with a 5 ton single force acting at the surface. This problem consists of one-step incremental analyses. The material properties are given in table (3.5), for purposes of showing the pattern of the distribution of shear-stresses, the shear-stress contours are also plotted in figure (3.4). The results of the problem is tabulated in table (3.6).

In the mesh used, the elements are chosen coarse. But to converge the actual values, at the tip of the load, relatively finer elements should te chosen.

The solutions of the analyses indicate that satisfactory results one obtained at element 6 due to the distance far enough from the point of application of load. At element 5, convergent values are obtained except the shear stress value. This is due to the boundary condition chosen at the lower boundary where restrain in x-direction does not exist.

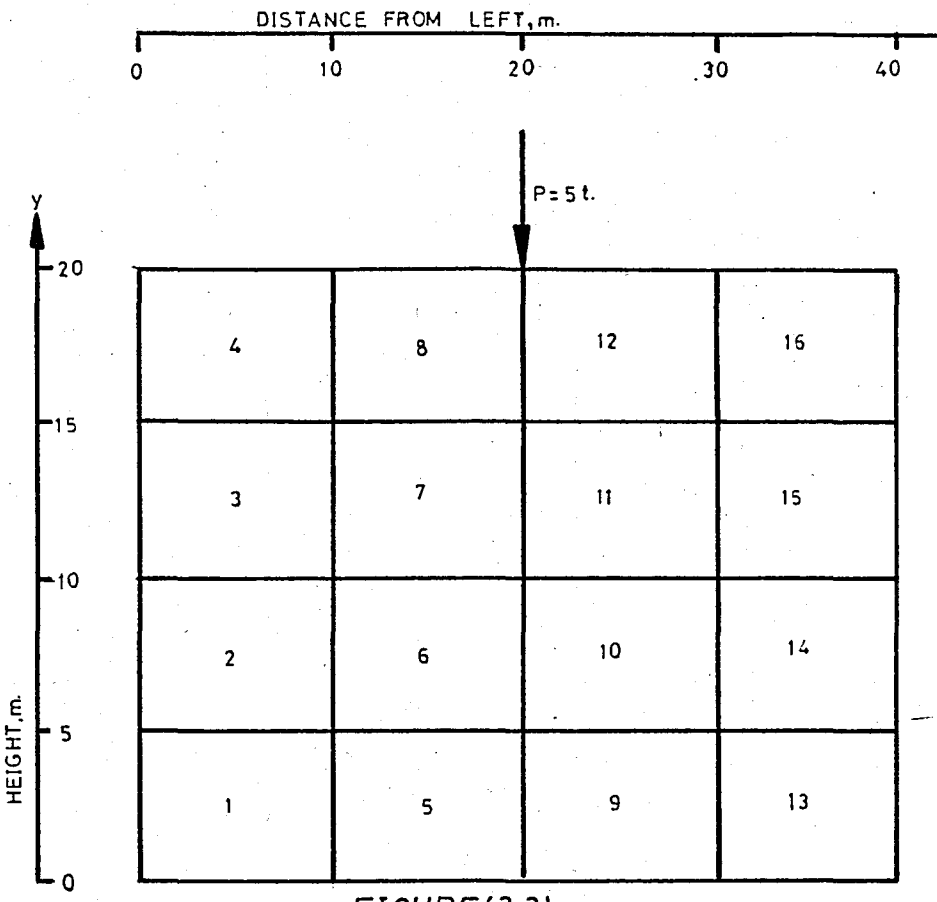

FIGURE(3.3)

The Finite Element Mesh Used In The Simulation Of Concentrated Load Problem With Element Numbers Indicated.

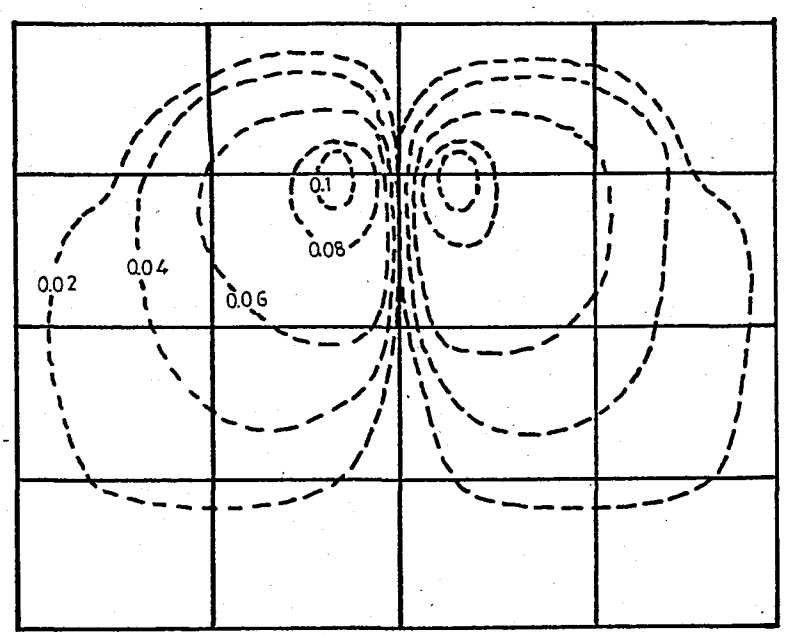

FIGURE(3.4)

τ_{xy} *Stresses Within The Medium.*

TABLE(3.6) Stresses Due To Concentrated Load

ELEMENT	HEIGHT m.	DISTANCE m.	STRESS	INITIAL STRESS t/m2	FINAL STRESS t/m2	THE DIFFERENCE t/m2	ELASTIC THEORY t/m2
8	17.50	15	σ_y	4.650	4.955	0.305	0.0247
			σ_x	3.360	3.505	0.145	0.101
			τ_{xy}	0.000	0.121	0.121	0.050
7	12.50	15	σ_y	13.950	14.200	0.250	0.198
			σ_x	10.080	10.130	0.050	0.086
			τ_{xy}	0.000	0.102	0.102	0.131
6	7.50	15	σ_y	23.250	23.450	0.200	0.208
			σ_x	16.800	16.830	0.030	0.033
			τ_{xy}	0.000	0.057	0.057	0.053
5	2.50	15	σ_y	32.550	32.730	0.180	0.175
			σ_x	23.520	23.550	0.030	0.024
			τ_{xy}	0.000	0.018	0.018	0.049

At the upper elements, such as element 7 and 8 , σ_y stresses are diverged, since finer element is to be used near stress concentration regions. More convergent results can be obtained with much finer elemets. Here also, τ_{xy} stresses differs in great amount. This can be attributed to the same reason as well. In general SOIL-STRUCT gives reasonable results relating to elastic solutions even employing very coarse elements. Then, it can be inferred that SOIL-STRUCT can be employed in the solution of elastic problems, by choosing correct parameters involved in non-linear analyses.

Table (3.5) Material Properties of Concentrated Load Problem

Material	ν	ν_{ult}	$\gamma(t/m^3)$	R.F	K_o	$\phi(^o)$	η	IDRAIN	K_m	K_{ur}	$c(t/m^2)$	$E_{ult}(t/m^2)$	$\alpha(1/^o$
Sand	0.35	0.49	1.86	0.65	0.40	40	0.43	0	1000.	1200.	0	3000.	0

3.4 SEEPAGE THROUGH EMBANKMENT

In order to show the usage and the interpretations of the results of seepage-option of SOIL-STRUCT, a sample problem is chosen to simulate the behaviour of an embankment in which the water level is assumed to be lowered 2 meters. For seepage option, the necessary data is given both when defining the nodal points and the new level of phreatic line. In nodal point cards, the pore pressures must be given for every nodes by calculating from Bernoulli equation in head of water. If the boundaries of flow lines are not known, such as phreatic line of embankment problem, the boundaries must be determined. In the example,

here, the seepage-phreatic lines, both for present and future levels, are obtained utilizing the sine method. Afterwards, flow lines with corresponding equipotential lines are drawn, then the pore pressures necessary to be indicated in nodal points cards are calculated. The mesh used and future and present levels of phreatic lines are shown in figure (3.5). The material properties are tabulated in table (3.7). The results of this problem are shown in figure (3.6)-(3.7)-(3.8).

Table (3.7) Material Properties for Seepage Problem

Material	ν	ν_{ult}	$\gamma(t/m^3)$	R.F.	K_o	$\phi(^o)$	n	IDRAIN	K_m	K_{ur}	$C(t/m^2)$	$E_{ult}(t/m^2)$	$\alpha(1$
Clay	0.30	0.49	2.00	0.85	0.43	30.	0.50	1	80.	200.	8.00	7000.	

The procedure is summarized below,

1. Determine the boundaries of the seepage field. If unknown boundary, such as seepage-phreatic line, exists, establish the boundary by appropriate technique.

2. Draw equipotential lines and flow lines using flow-net technique.

3. Utilizing Bernoulli equation, find pore pressures in head of water.

4. Step 1 through 3 should be repeated for the new-water level, or the coordinates of seepage phreatic-line should be presented in seepage option.

As can be seen from figure (3.7), at the upstream face

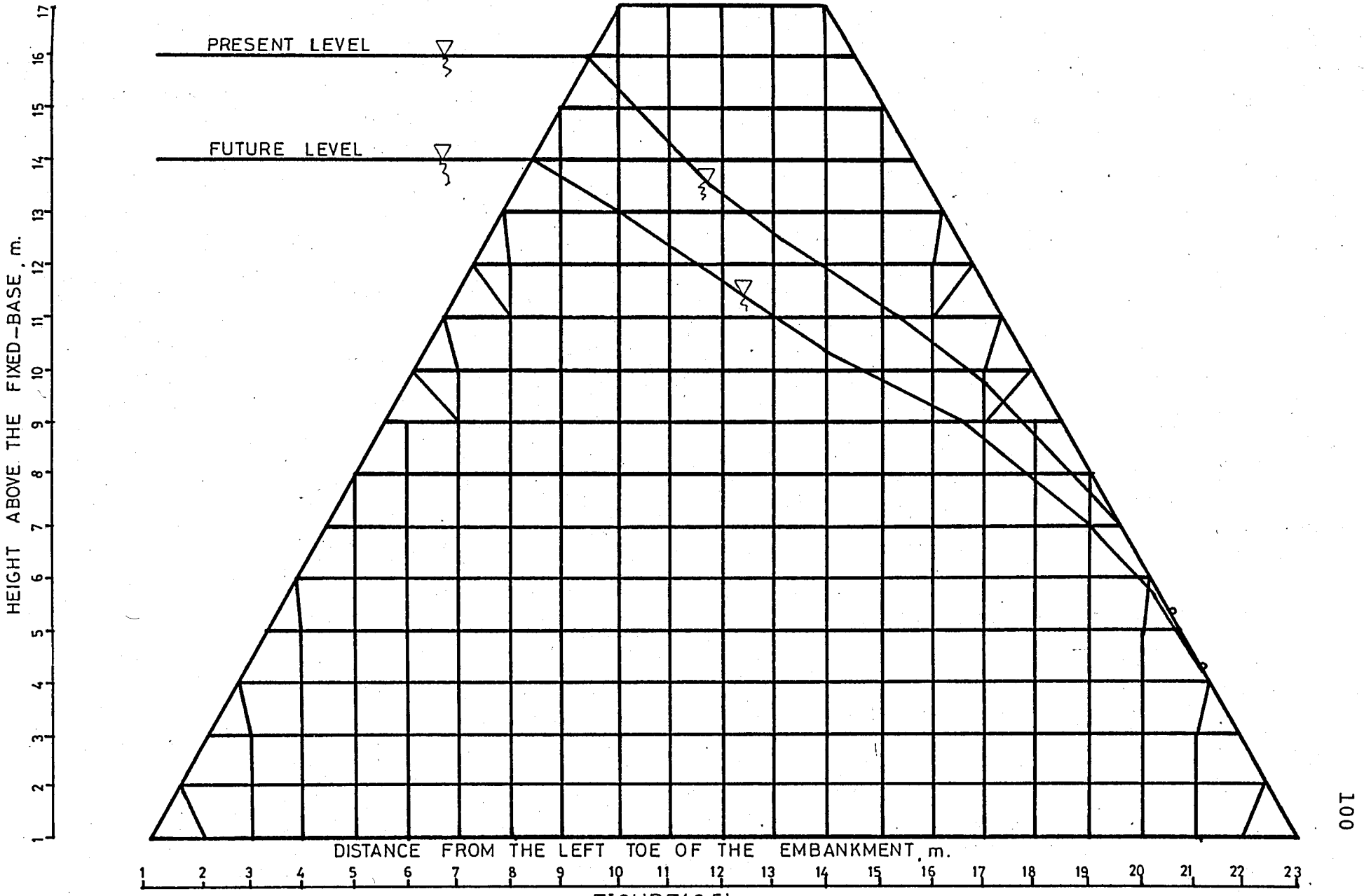

FIGURE(3.5)

Finite Element Mesh for Seepage Problem and the Lines of Seepage for Present and Future Levels.

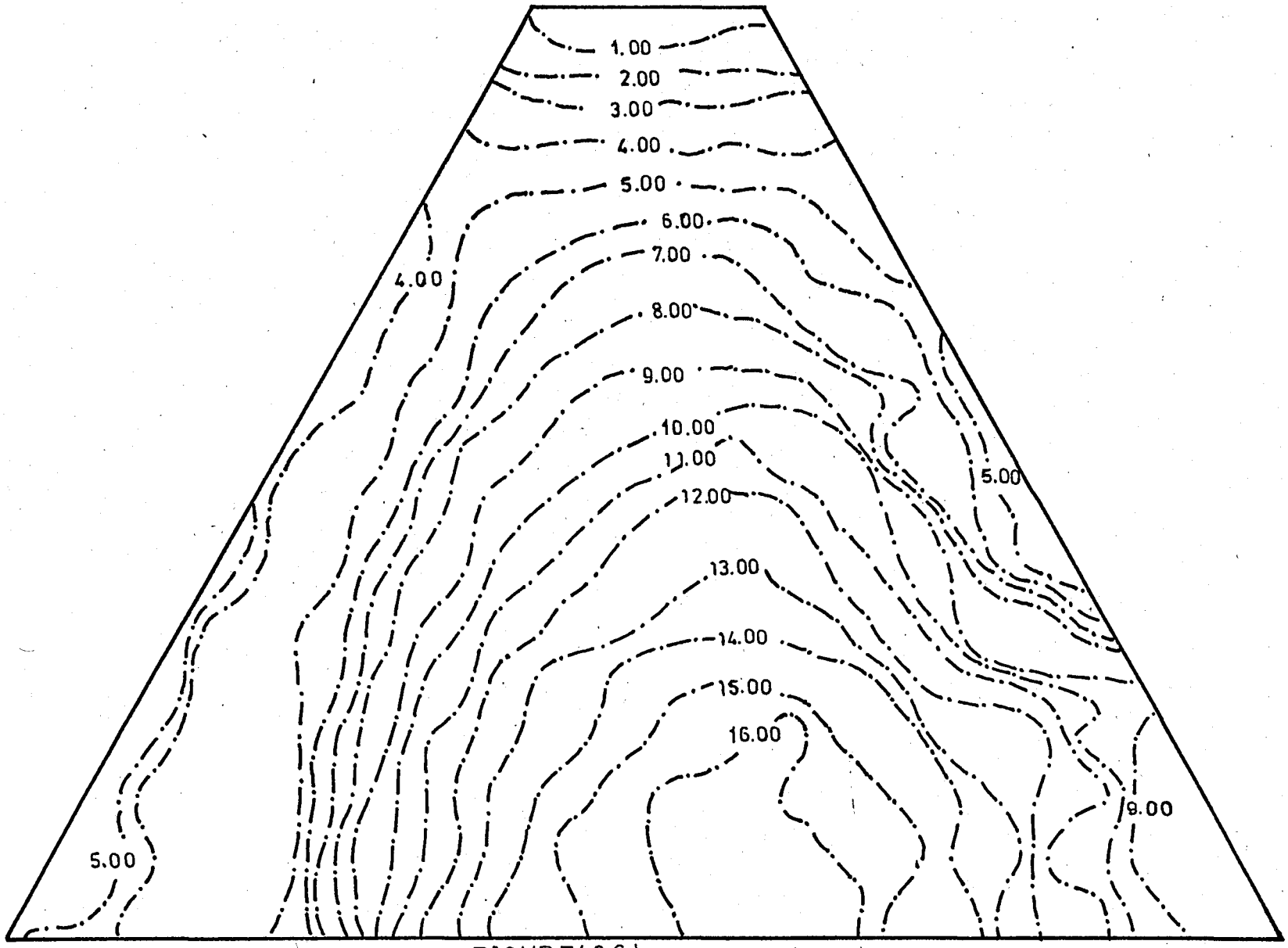

FIGURE(3.6)

The Major Principal Stress Countours, t/m^2

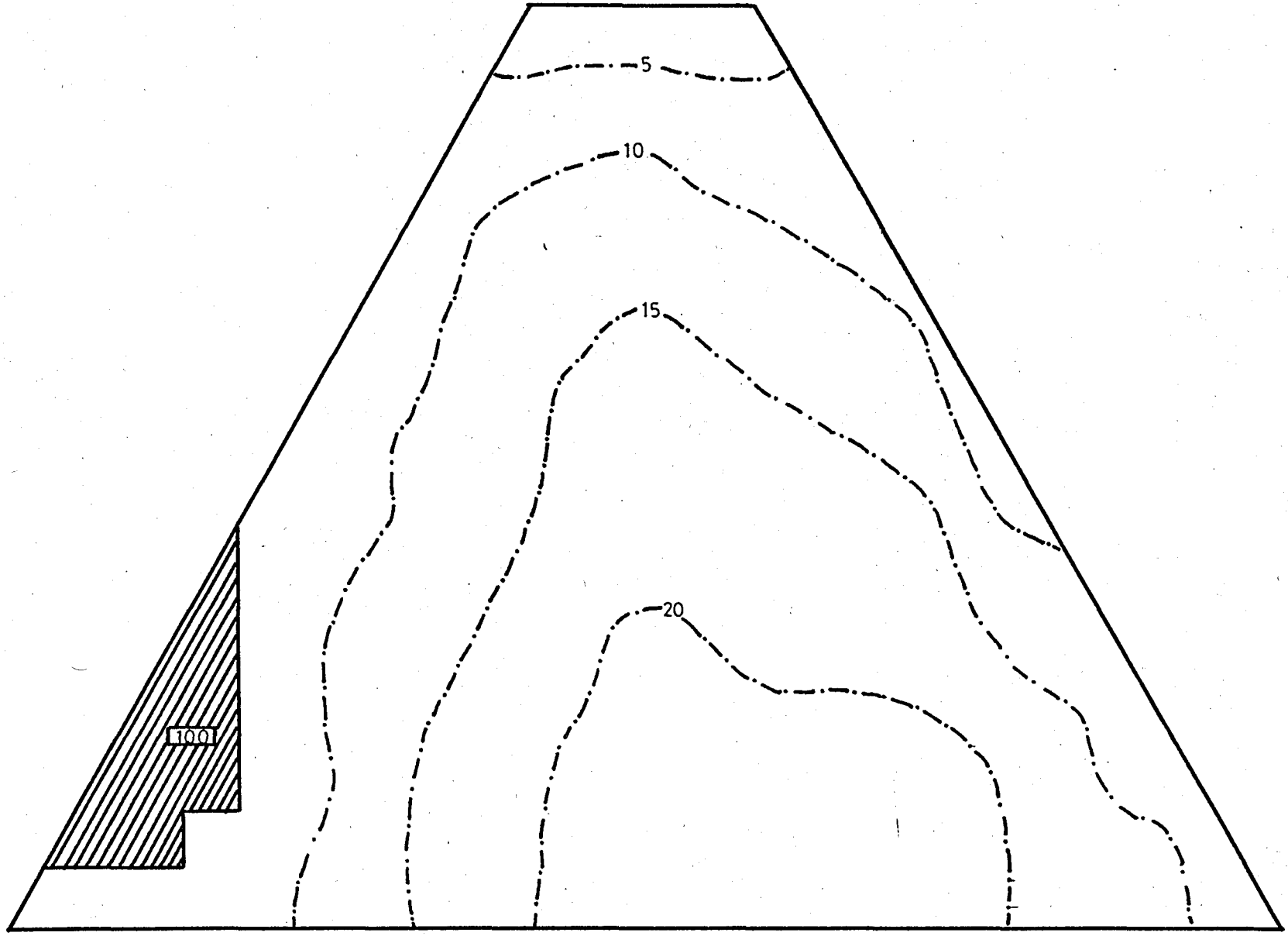

FIGURE(3.7)
The Stress Levels Developed During The Decrease of Water Level Elevation, %

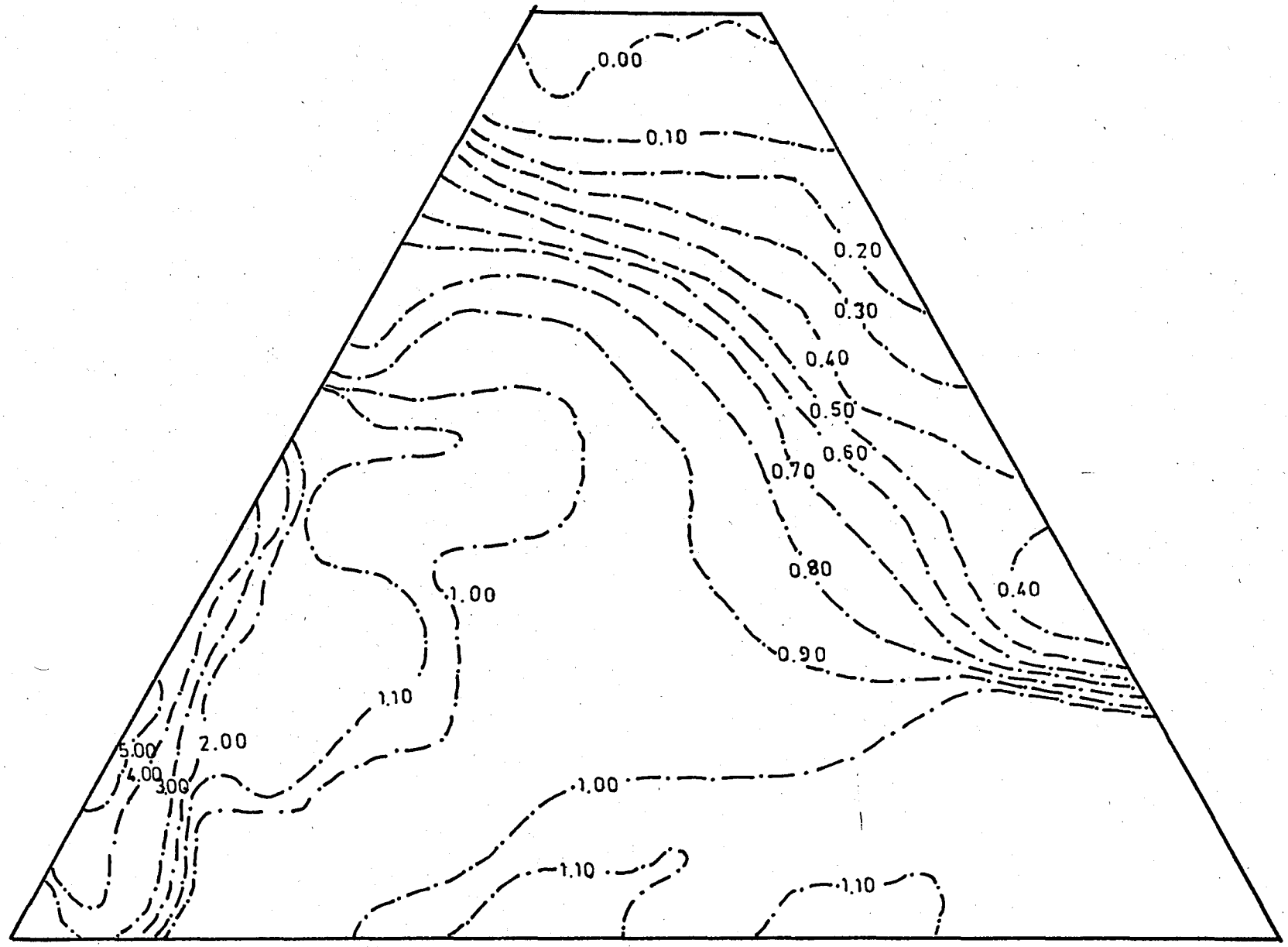

FIGURE(3.8)

The Shear Stresses Developed During the Decrease of Water Level Elevation, t/m²

of the embankment many elements fail. From the elastic solution given by Clough and Woodward (1967), it is known that the most-critical parts of embankments are their slopes if water does not exist. When the water pressure and the seepage flow occurs, the upstream face become much more critical. This is true in terms of stress level, vertical, horizontal and shear stresses. In fact, like stress-level, shear stress and gradients of shear-stresses have higher values in those regions (figure 3.8). On the other hand, stress levels are also concentrated at the base of embankment but they do not have ciritical values. Accordingly, it can be inferred that stress levels are ciritical at the upstream face where pore pressures are high and, less importantly, at the base of embankment.

In figure (3.6), the contours of major principal stress are depicted. From this figure, the maximum values of major principal stresses and maximum gradient of major principal stresses are seen at the lower-portion of the embankment. This may be related to the gravity turn-on type of analyses assumed in the problem where gravity loads increase with the depth of the embankment. Therefore, in embankment problems, instead of using gravity turn-on analyses or instantaneous loading, incremental construction procedures, namely layered system, should be employed to show the shape of contours of major principal stress in a more correct way.

The shear-stresses are critical at the upsteam-face of the embankment where the stress levels are high. In general, the shear-stresses have higher values in those regions where pore pressure has considerable magnitude. The effect of pore pressure

can also be seen at the down-stream face of the embankment. In this region, the contours of shear-stresses are following the path of seepage-phreatic line. At the exit point, all contours are concentrated. Thus, it can be stated that the level and variation of phreatic line influence the magnitude and gradient of shear stresses importantly. To sum up, shear stresses, developed within the embankment, have higher values where pore pressures are effective and the upstream and downstream faces of embankment.

During the investigation of stress-levels, it is seen that two meter lowering of water level elevation at the upstream face of embankment causes up to 5% increment in stress levels. Also, it is found that it causes up to 11 cm. horizontal movements at the top of embankment and 3 cm. downward movement at the point where initial level of water touches the upstream face. Those relative movements may get much higher and critical values when the level of water is completely dropped. Then, this kind of behaviour should be considered in the design in terms of displacements.

3.5 Summary

In this chapter, the utilities provided by computer-program SOIL-STRUCT are tested. Classic types of soil mechanics problems are chosen and the results are compared with the elastic theory. The problems employed in this chapter are concentrated load on elastic medium, embankment loading and seepage analysis. The results obtained during this study, in general, compare well with the theoretical solutions. Thus, the problems of soil mechanics even if including very complex geometries and loading conditions with diverse material properties can be solved efficiently by incremental finite element technique.

IV. SUPPORTED EXCAVATION IN CLAY

4.1 Introduction

Design of a temporary braced excavation in an urban area requires a knowledge of the movements expected to be caused by the excavation in surrounding street and building areas. Traditionally, prediction of movements in such cases has been made purely on the basis of experience. However, the finite element method now provides a tool which has the capabilities to allow analytical movement predictions to be made. Unfortunately, the state of the art in this area is not well-established, and to the uninitiated engineer the available literature often is conflicted and confusing as to how such an analysis should be performed and whether or not it will provide reliable information.

On the analytical side, the interested engineer will find a number of different methods used to simulate excavation effects and various constitutive models employed to simulate soil behiaviour. The question of howmuch the different solution techniques affect the predicted behaviour has not been answered. On the practical side, the engineer

will find authorities often pointing out that analytical predictions of behaviour of temporary excavations are subject to distrust because,

- soil-strength and deformation parameters are difficult to reliably define, and,
- construction sequence, which affects behaviour significantly, is often subject to change during construction, after analysis is usually complete.

Thus, on the basis of both analytical and practical considerations, questions can be raised as to how the finite element method should be applied to temporary excavations and how reliable the predicted results are. It is the purpose of this chapter to deal with these questions and to provide a way which gives the consistent and reliable usage of the finite element method in analysis of temporary excavations. In order to show the application of finite element method in supported excavations, a real project, Braced Excavation System of Istanbul Metro Construction, is studied and the results are presented in following pages.

4.2 Project Descriptions

The purpose of this study is to predict the movements of supported retaining wall structure and the performance of surrounding soil using Finite Element Method within the framework of a consulting project of Istanbul Metro System being constructed by cut and cover technique. The computer

program SOIL-STRUCT, capable of making incremental finite element analysis, was developed by Cloung and Duncan(1969), This program is adapted to CDC Cyber 170/815 system at Computer Center, Boğaziçi University, Istanbul during this study. Program listing and User's manual are given in Appendix. The principal advantages of incremental finite element analysis are that the soil and the structure can be considered interactively and both design loads and expected displacements are studied. Thus, it is possible to compare various system designs for minimizing displacements within an analytical rather than empirical framework. The finite element type employed to represent the soil and wall materials is an isoparametric linear strain quadrilateral developed by Doherty (1969). This element is particularly accurate in simulating bending behaviour for structural elements. In an incremental finite element analysis, strength and modulus values for each element in the finite element mesh are to be adjusted at each stage of construction so as to account for nonlinearity and stress-reorientation.

The zone of construction consists of two types of different soils. An artificial fill is underlain by fully-saturated homogeneous clay stratum. The material properties of those soils are given in Table (4.1).

TABLE 4.1 Material Properties of the Supported Excavation Problem

Material	ν_{ult}	ν	γ (t/m^3)	R_f	K_o	ϕ (°)	n	K_m	K_{ur}	c (t/m^2)	α (1/°C)	E_{ult} (t/m^2)	IDRAIN
Steel	0.45	0.25	4.	0.	0.	0.	0.	0.	0.	0.	0.	1.5×10^7	1
Clay	0.45	0.35	2.	0.75	0.5	0.	0.7	200.	250.	15.	0.	1000.	0
Artificial Fill	0.45	0.35	1.8	0.75	0.5	30.	0.7	300.	400.	0.	0.	50.	1

The Metro System requires excavations up to 9.5 meter-depth through artifical fill into the clay-substratum. The excavation is fullfilled in two layers. Construction sequences are shown in figure (4.1). As can be seen from this figure, 7-step incremental analysis is employed. These steps are summarized below.

1. Surcharge Loading

At the upper part of the finite element mesh, surcharge load of 1 ton per square meter is applied.

2. Pile Installation

A Sheet Pile, which is 12 meter-long and 10 centimeter-thick, is driven into the soil so as to start the excavation and strut installation. The embedment depth and the thickness of wall are selected on the basis of initial static calculations. Wall thickness is selected assuming 1 meter-long planar element which has the same moment of inertia with the original sheet-pile obtained from statics.

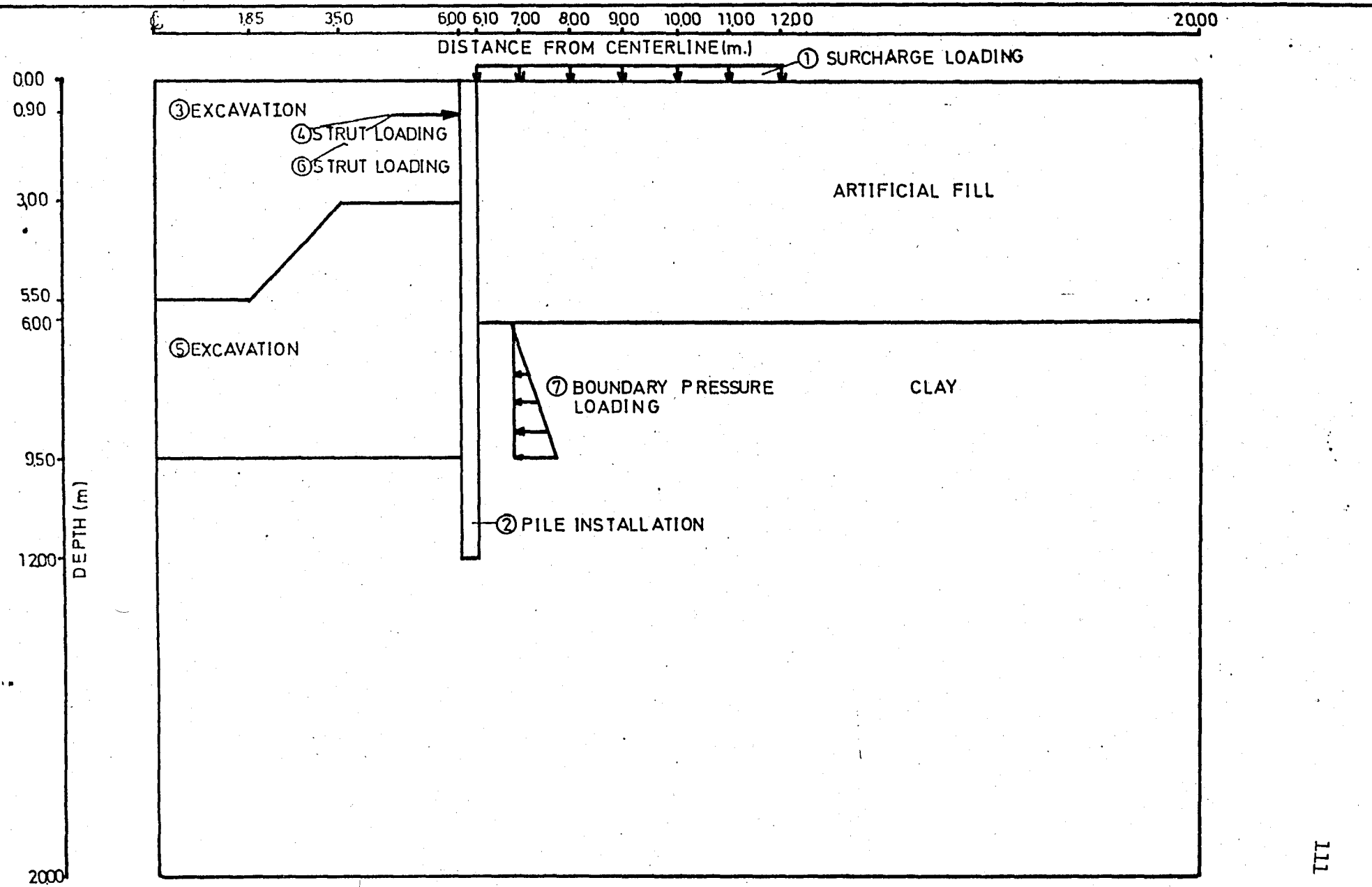

FIGURE(4.1)
The Construction Sequences of Supported Excavation

3. Excavation

First layer of excavation is performed up to 5 meter-depth at the center, 3 meter-depth at the edges of excavation. For the ease of performance of machinery a trench is left with a slope of 3 vertical on 2 horizontal.

4. Strut Loading

Some portion of final strut load is applied to the sheet pile wall at 0.9 meter-depth. Final strut load is computed from initial static calculations.

5. Excavation

Second layer of excavation is depened into 9.5 meter. This final excavation has flat base-surface.

6. Strut Loading

The rest of total strut load is acted at 0.9 meter-depth due to the increased depth of excavation.

7. Boundary Pressure Loading

In order to take into account the groundwater behind the wall, boundary pressure loading coming from lateral pressure of ground water is applied at the middle part of sheet pile.

After deciding the construction sequences, the finite element mesh is designed, with 408 elements and 448 nodes. The selected finite element mesh is shown in figure (4.2).

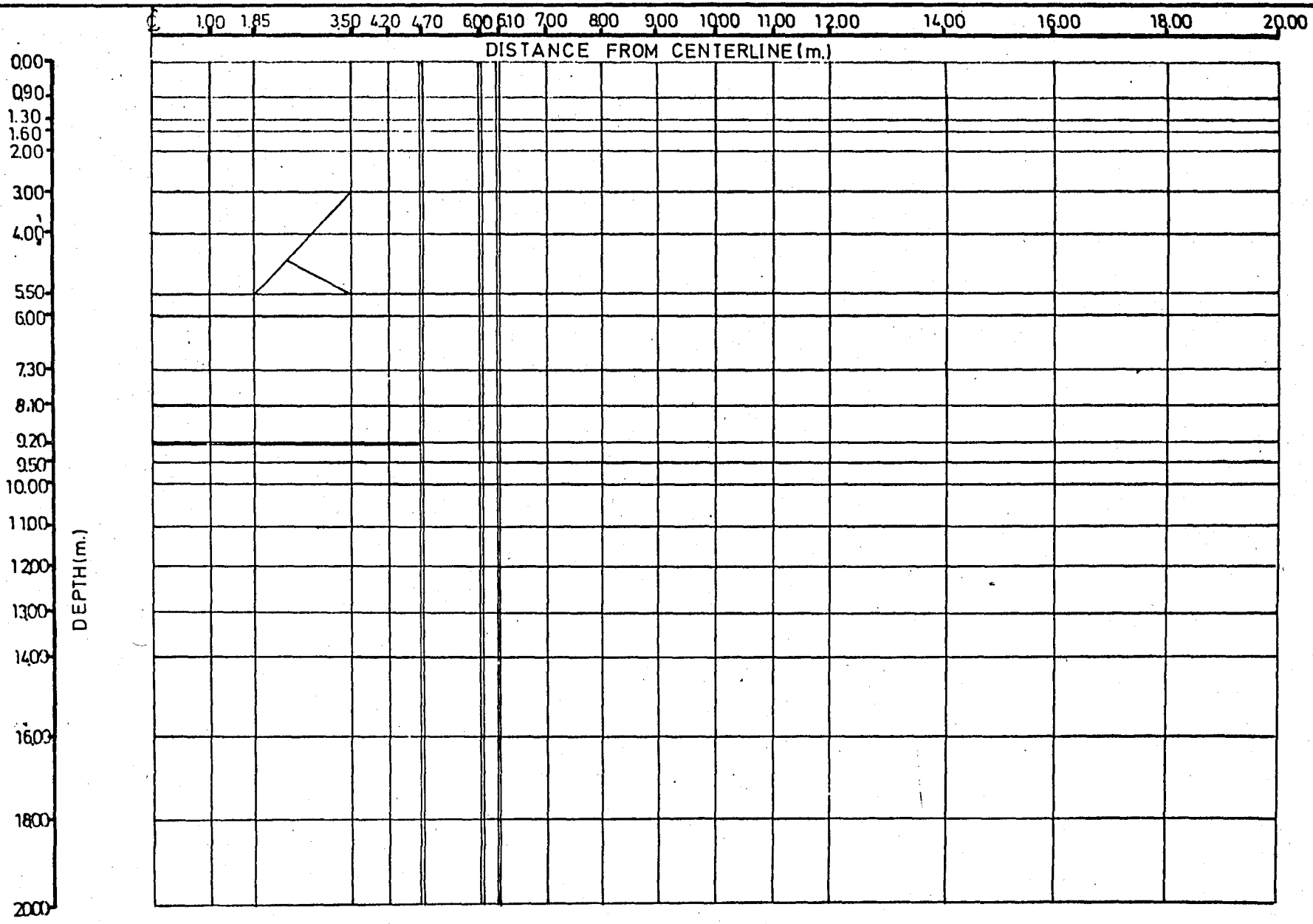

FIGURE (4.2)
The Finite Element Mesh of Supported Excavation.

65 interface elements are used in the analysis to simulate the interaction between soil and structural elements.

In this analysis, the lowermost horizontal boundary is assumed to be fixed against both horizontal and vertical movements due to the assumption that stiff substratum is reached. Beside this, left and right vertical boundaries are selected to be fixed against horizontal movements and allowed free against vertical movements. Rightmost vertical boundary is located far enough from excavation zone so as not to influence movement pattern. The utilized system properties are summed up in Table (4.2)

TABLE 4.2 System Properties of the Supported Excavation

EXCAVATION GEOMETRY	
The width of Excavation,m.	12.00
Final depth of Excavation,m.	9.50
Initial depth of Excavation,m.	3.00
Number of Excavation Layers	2
The depth of Strut,m.	0.90
Spacing between Struts,m.	4.00
Section modulus of Sheetpiles,cm^3	1600.00
FINITE ELEMENT MESH	
Number of Nodal Points	448
Number of Elements(including interface elements)	408
Number of Interface Elements	65
Number of Material Types	3

The plan view of sheet piling and bracing-system is depicted in figure (4.3).

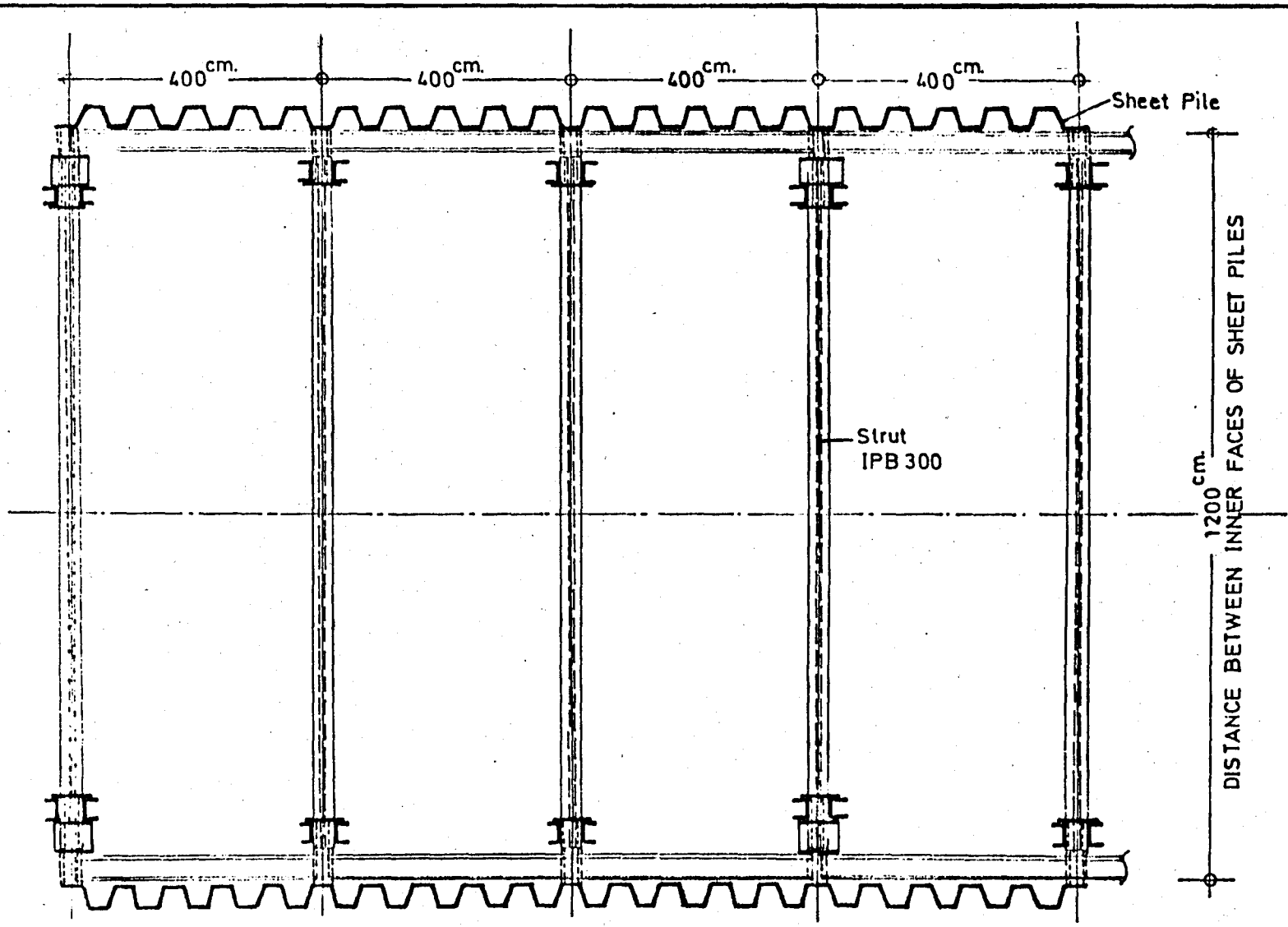

FIGURE(4.3)
Sheet Piling and Bracing System
Plan for Supported Excavation.

4.3 Evaluations of the Results.

The evaluations of the results obtained from finite element analysis of braced-excavation will be considered interms of the three criteria. These are stress levels mobilized within the soil media, passive and active earth pressures acting on the sheet-pile wall and the displacements of sheet-pile wall system and the top of artificial fill. Furthermore, the difference in displacements of wall system will be thought before the strut loading at 1st level of excavation and after the 2nd level of excavation.

Stress Levels

The most critical part of soil media, interms of stress levels, is the excavation base which is shown in figure (4.1). In general, in most of the soil-structure interaction problems including excavations, this zone yields stress-levels just above 100%. That is because, unloading of the area causes the soil to swell, as well as the stress difference between minor and major principal stresses to increase. The increase in deviatoric stress leads to the increase in stress-levels. Beside this, those regions where horizontal and vertical boundaries coincide as junctions create stress-concentrations. All of above mentioned points cause the soil excavation base to fail.

Another critical region develops at the behind of wall where maximum lateral displacement of sheet pile occurs. This critical zone extends as it goes away from the sheet pile

system, as shown in figure (4.4). This zone is completely failed. The reason for this is that the largest lateral displacement of sheet-piling which is on the order of 2.5 centimeter occurs in this region. Moreover, the artificial fill does not move as much as the sheet-pile wall which leads to the failure of backfill. In other regions of the finite element mesh, stress levels are generally below %50 that is assumed to be normally accepted state of stress in non-failed soils. Thus, the stress-levels are in good aggrement with predicted results and the soil can support the loads on and around the system. The movement of artificial fill can be prevented by the strut installation which exerts compression load on the backfill.

Lateral Earth Pressures

The lateral earth pressures acting on the sheet-pile wall are depicted in figure (4.5). The values of lateral earth pressures are obtained from the normal stresses developed within the interface elements. As can be seen from the general trend of active earth pressures, relatively higher active pressures can be obtained at the upper part of sheet pile wall where the strut loading is performed. Naturally, this result can be expected. From this zone to the final level of excavation, earth pressures are decreased a little, due to the fact that sheet pile wall displaces laterally much more than the surrounding soil. In other words, the soil can not have a chance to exert higher pressures to the sheetpiling. In this zone, earth pressures drop below the original

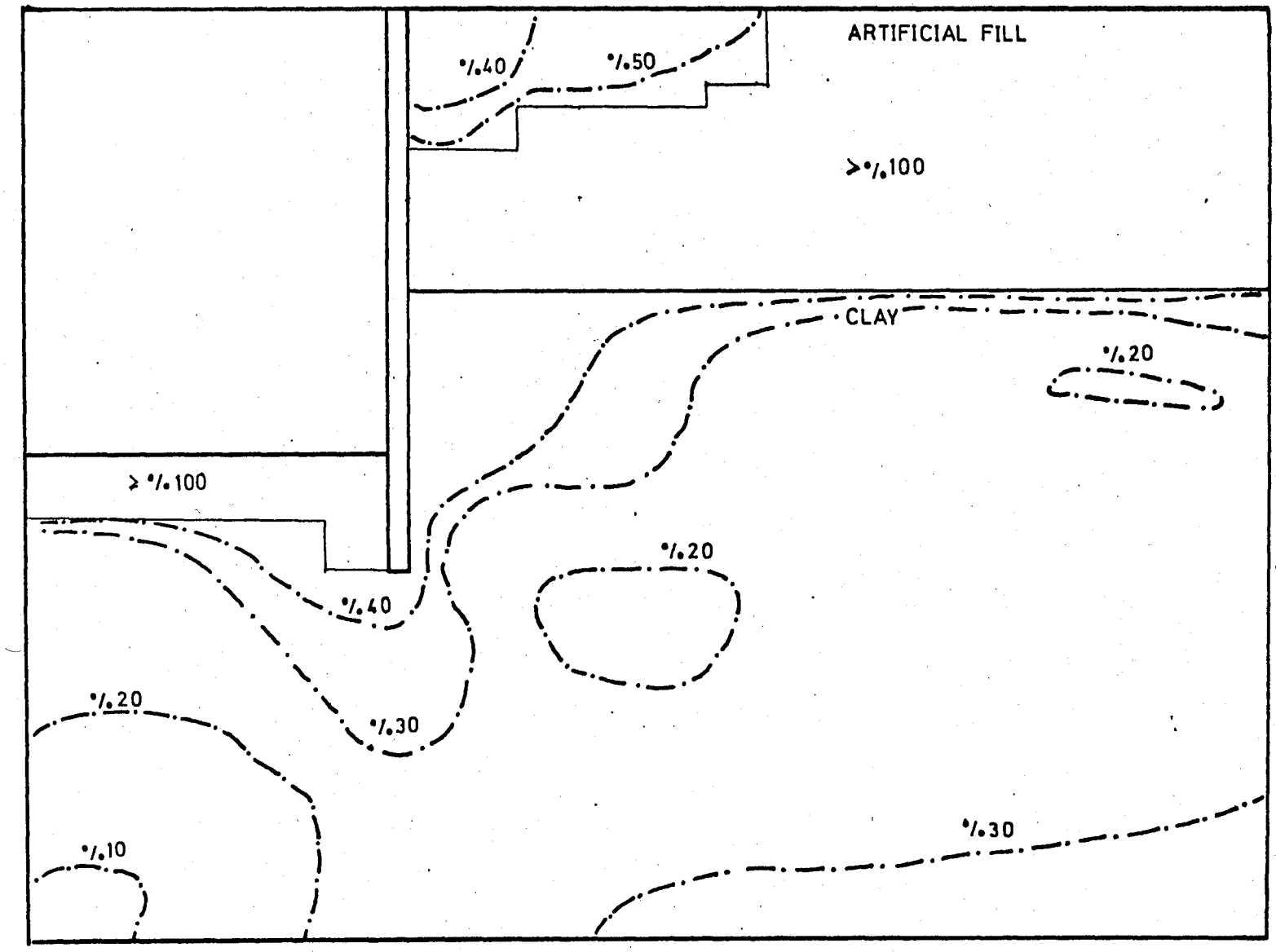

FIGURE(4.4)
The Stress Level Contours of Supported Excavation

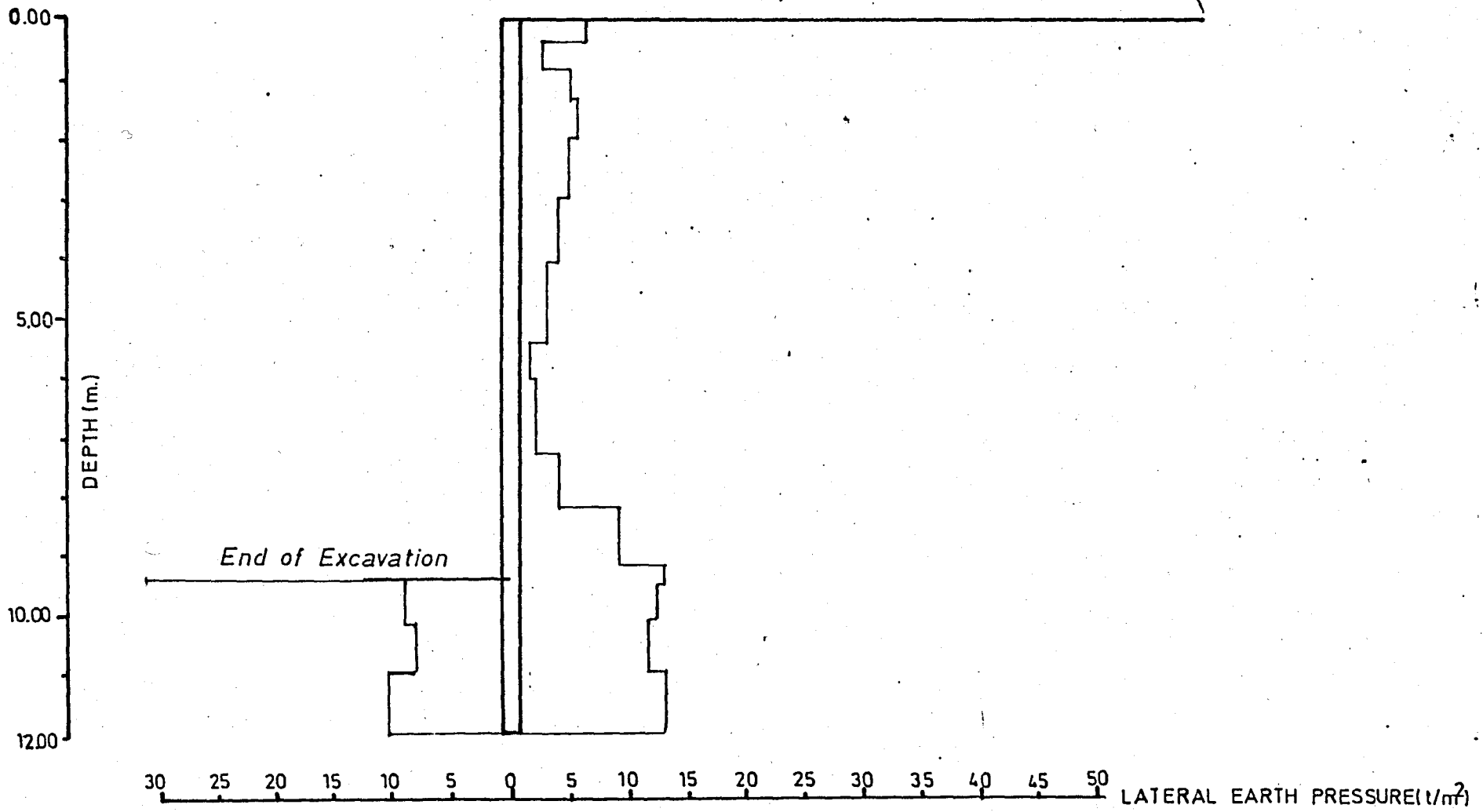

FIGURE(4.5)
Lateral Earth Pressures acting on The Wall

at rest pressures but do not fully reach active earth pressures. This is consistent with the fact that, although large percentages of the strength of the soils are in some instances mobilized, few elements just behind the wall actually fail and thereby develop active pressures. Full mobilization of active pressures will, infact, lead to excessive deformations in a braced system. This kind of behaviour can also be attributed to the flexibility of wall and the fixing of the lower part of sheet-pile. The latter reasons cause the sheetpile wall to displace easily with respect to surrounding soil, then the soil can not exert higher pressures. After getting into the clay stratum, active eartpressures increase again due to the small displacement and fixing of lower part of sheet-pile. One important point to be stated is that the compression values is given in the clay are presented interms of effective pressures.

On the passive side of sheet piling, the earth pressures resemble to the generally predicted results in case of flexible walls. Consequently, lateral earth pressures obtained from the finite element analysis compare well with assumed pressures in the initial static calculations. But, the strut load of 12 tons found from statics is decreased to 9 tons due to the flexibility of wall and non-mobilized active pressures to get reasonable displacement pattern of sheet-pile wall.

Displacements

In figure (4.6), the displacement values around the excavation system are shown. At the top of artificial-fill the vertical displacements increases along the surcharge region gradually, but after the surcharge effect is disappeared, displacements decreases reaching an asymptotic value. This kind of behaviour is expected, since the effect of excavation decreases as the distance from the sheet-pile system increases. The general profile of deflections is quite similar to the other projects and observed behaviours.

Lateral displacements of wall-system are considered interms of two aspects. Firstly, the displacements after 1st level of excavation and before strut loading are investigated. Here, the behaviour completely agrees well with predicted, because the wall makes its maximum displacement at the top like cantilever wall, which is about 0.5 centimeter. Secondly, the displacement after 2nd level of excavation is detected so as to see the probable system movements and if there exists any large deflection within the excavation system. After 2nd level of excavation, maximum displacement occurs just above the base of excavation which is about 2.5 centimeter. This amount of displacement can be considered reasonable considering the material properties of clayey substratum. In general, the displacement patterns comply with the observed studies and finite element analysis conducted by G.W.Clough and others. In all the analyses of

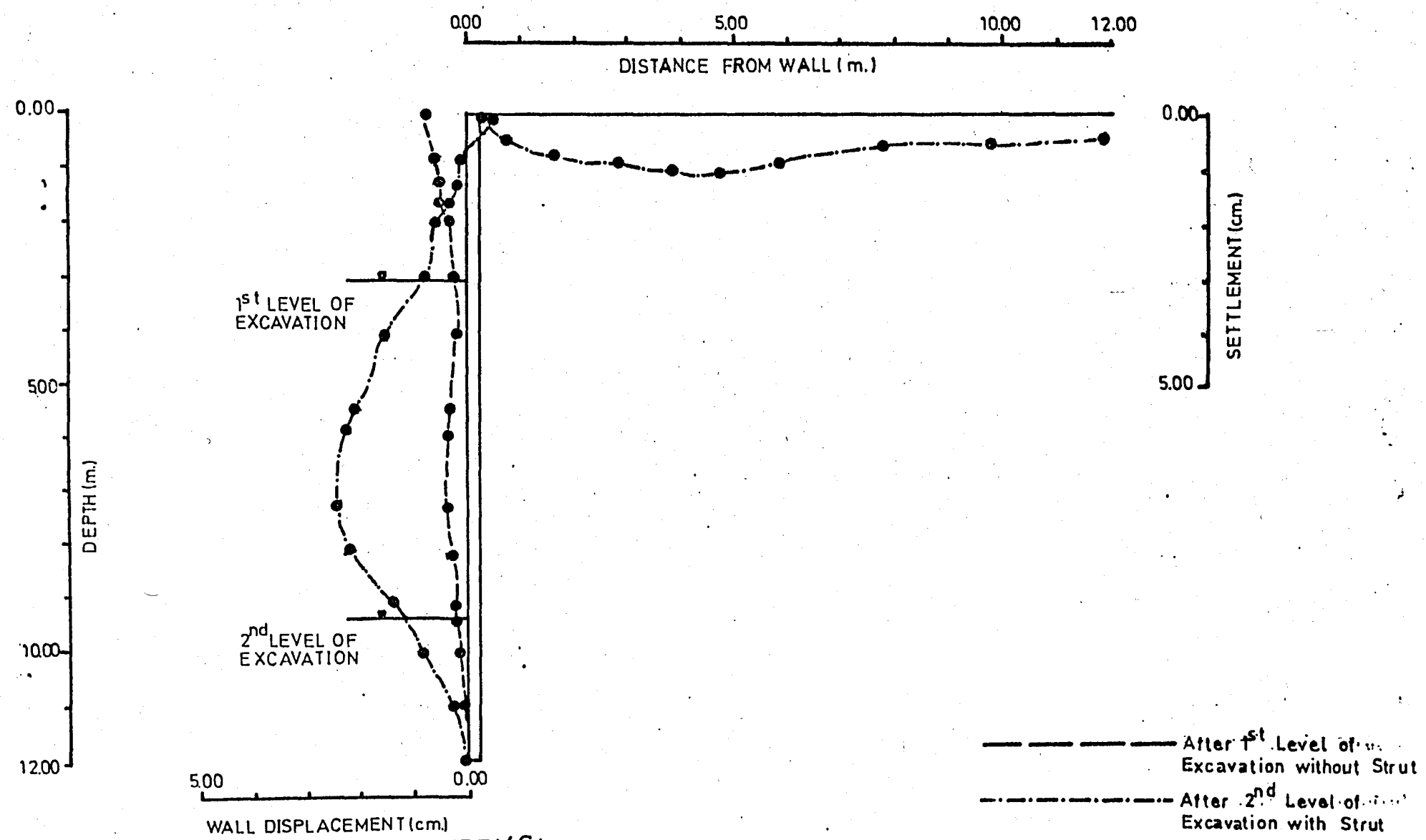

FIGURE(46)
The Movements of Supported Excavation System.

practice, the maximum displacement is obtained around the base of excavation where yielding of passive zone soils occur. Hence, it can be stated that both the displacement patterns and displacement magnitudes of sheetpile system and that of top of artificial fill are in expected range with suitable displacement pattern.

4.4 Summary and Conclusion

In this chapter, the finite element analysis of braced excavation within framework of project of Istanbul Metro System is performed. The results are discussed interms of stress levels, developed active and passive pressures and system-movements. It is shown that finite element modelling provides a rational alternative to emprical means for prediction of above-mentioned criterias. For stress levels, obtained results are in good agreement with previously conducted analyses and behaviour of many projects. Earth pressures are also acceptable for both active and passive cases. Utilization of finite element analysis also lead to accurate and reliable predictions of the movements of excavation system which are compatible with the behaviour of observed projects. This point can be considered very encouraging in getting useful design information and accurate performance predictions for temporary excavations in clay.

Based on the analysis presented herein, it is possible to conclude that finite element modelling can be a useful

and economic design tool. Its successful implementation requires reliable data relative not only to soil characteristics but also to construction sequences. Finite element modeling also serves as a natural supplement to instrumentation data. If the tools are used interactively, it is possible to adjust parameters based on behaviour, during the early stages of construction and thus afford great economies in a "design as you go" framework.

V. CONCLUSION

In this study, the computer program SOIL-STRUCT, developed by Clough and Duncan (1969), is shown to be applicable to different soil mechanics problems, especially to supported excavation systems. This computer program uses incremental finite element technique which takes into account both irregular and complex geometries and different construction sequences assumming nonlinear stress-dependent stress-strain behaviour of soil. The basic input is the definition of mesh of problem chosen and material properties. The latter is the most difficult part of data preparation, which are supplied by utilizing shear-box tests, one-dimenisonal consolidation tests or triaxial tests. The test should be conducted in the range of pressures anticipated and under the drainage conditions appropriate for the cases to be analyzed. In cases where it is impractical to conduct drained triaxial or plane-strain tests on silty or clayey-soil due to their low-permeability, it appears to feasible to determine the required parameters from results of drained shear-tests or one-dimensional consolidation tests.

The program SOIL-STRUCT is studied interms of two aspects in this thesis. Firts, general problems of soil mechanics, such as loading on elastic media, embankment loading and seepage through dam, are discussed and presented in Chapter (III). It is concluded that SOIL-STRUCT is an efficient tool in the solution of soil mechanics problems. Secondly, a real project, The Braced Excavation System of Istanbul Metro, is chosen to show the validity of computer program in order to predict the behaviour of braced excavations in clays. The results of this analysis also indicate that this program can be utilized in the prediction of behaviour of braced system and surrounding soil as comparing with the other studies and experience obtained so far.

The following results are obtained from the application of SOIL-STRUCT to various practical problems of soil mechanics realized in this thesis.

. For the solution of simple problems of which results are available from the theory of elasticity, SOIL-STRUCT gives reasonable results where gravity loads are of primary importance, such as the base pressures of embankments. Although, the shear-stress are not as similiar as vertical stresses to the solutions of elastic theory, they are still found to be in an acceptable range. The differences may be attributed to a very few number of parameter used in the derivation of elastic theory solutions to represent soil behaviour, namely poisson's ratio and unit weight of soil, with respect to non-linear incremental finite element analyses where 13

parameters are defined for each single soil type. It should also be noted that the comparisons can be made between elastic solutions, where instantaneous loading is used, and incremental analyses in order to see the effect of construction sequences.

. In the sample problem where the effect of single concentrated load is analyzed, it should be stated that stress concentration regions occur where the behaviour of medium can not be predicted. For this reason, the vicinities of single loads, the vertical and horizontal boundaries of excavations, and slopes should be facilitated with much finer elements.

. The program SOIL-STRUCT can also be applied to the seepage problems where the flow of water is time-independent. The input for seepage option is supplied by porepressures of nodal points, and the water level changes represented either by the definition of phreatic-line or the pore-pressures developed for the changed level of watertable. It is found that the change in water level elevation is primarily important for the shear stresses and the displacements. Shear stress are quite high at the regions where the water level change is high and at the exit points where the seepage phreatic line goes out from embankment. At the exit points, the contours of shear-stresses follow the seepage-phreatic line in a close interval causing high stress gradients.

Another important phonemena which is inferred from seepage analyses is the magnitudes of displacement. When the

changes of water level elevation is high, the displacements may get large values. Thus, the decrease and increase of water level elevation should be considered in design to prevent large displacements. Large displacements of embankments can be prevented using appropriate fill material, with suitable elastic properties.

. SOIL-STRUCT is also efficient in the solution of excavation problems, such as supported excavations. Since the primary aim of this thesis is to apply SOIL-STRUCT to supported excavation problems, a real project which is the bracing system of excavation of Istanbul Metro, is taken, then SOIL-STRUCT is applied to predict the system and surrounding soil-behaviour. In this study, soil properties and construction sequences are estimated at first so as to approach reasonable system behaviour as reported by other studies. After initial analysis, material properties are changed to find out real material properties looking at system behaviour. The changes of material properties is repeated until accurate system behaviour is obtained. The shear-strength and modulus values for softclays are difficult to define for finite element studies ingeneral. Because of difficulties in selecting soil parameters and anticipating construction changes, the finite element analysis should be incorporated into an observational procedure which allows for reanalysis to be performed so as to accommodate better soil parameter estimates and construction changes. Updated soil parameters are best obtained by comparisons of early observed performance and comparable finite element predictions. The behavi-

our of soil is based on the nonlinear elastic model. The non-linear elastic model allows the soil modulus to be adjusted consistently with the shear-stress levels in each element. The form of the stress-strain curve is assumed to by hyper-bolic up to failure where upon the shear modulus is reduced to near zero.

The problem analyzed is a braced, sheet-pile supported excavation. The problems involved in defining soil parameters and construction sequence make "pure prediction" of the be-haviour of temporary excavations by finite element analysis very difficult. In certain instances it may be possible,but in general this will not be the case. Fortunately, there is an approach which obviates many of the questions shrouding the "pure prediction" technique.

The results obtained from the finite element analysis of supported excavation problem of Istanbul Metro are evalu-ated interms of three aspects; stress levels, earth pressures, and displacements.

Stress levels mobilized within the soil medium show that the base of excavation fails due to the swelling of soil and increment in deviatoric stress ofter the removal of soil. But this kind of behaviour is predicted, since most of the finite element analysis conducted by many other scientists have such base failures in clays. Another critical region is just behind the wall where maximum displa-cement of wall occurs. In the other regions of the finite

element mesh, stress level are generally around 50% that is mostly assumed as normally accepted magnitude in soil media.

Lateral earthpressures acting on the sheet-pile are investigated whether they comply with general pressure trends. It should be stated that active pressures are higher than Rankine's active pressures at the upper part of wall where strut loading is performed. Below the strut level, earth pressures decrease due to the fact that sheetpile wall displaces more than the artificial fill laterally. In the clay stratum, active earth pressures increase again. On the passive side of sheet-pile wall, earth pressure generally consistent with predicted results.

Displacements of excavation system are generally within the acceptable and reasonable magnitudes for both of displacements of sheet pile wall and that of the top of artificial fill. At the top of backfill, the vertical displacements decreases as the distance from the wall increases. Lateral displacements of sheet-pile wall has the maximum value just above the base of excavation which is very sensible as compared with the other studies done so far. In general, the trend and the magnitudes of displacements aggree well with the observed results and other finite element analyses.

As a result, the finite element analysis of supported excavation of Istanbul Metro gives reasonable braced system and soil medium behaviour. But, in order to obtain exact results, reanalysis should be conducted regarding to the behaviour of excavation system. Thus, exact values of material

parameters which are very difficult to estimate at first attempt can be found. It can be said that SOIL-STRUCT can be utilized in the prediction of supported excavation problem provided that analysis is conducted with observational procedure. When property utilized, a finite element analysis can be expected to yield useful design information and accurate performance predictions for temporary excavations in soft clay.

REFERENCES

1 Brooker,E.W. and Ireland,H.O.(1965), "Earth Pressures at Rest Related to Stress History," Canadian Geotechnical Journal, Ontario, Vol.2,No.1, pp.1-15.

2 Chang,C.V.(1969), "Finite Element Analyses of Soil Movements Caused by Deep Excavation and Dewatering," Thesis Presented to the University of California, Berkeley, in 1969, in Partial Fulfillment of the Requirements for the Degree of Doctor of Philosophy.

3 Clough,R.W.(1960), "The Finite Element Method in Plane Stress Analysis," Proceedings of the 2nd ASCE Conference on Electronic Computation, Pittsburg, Pa.

4 Clough,R.W. and Hansen,L.A(1981), "Clay Anisotropy and Braced Wall Behaviour," Journal of the Soil Mechanics and Foundations Division,ASCE, Vol.107, No GTT, Proc Paper 19391, July.,1981, pp.893-913.

5 Clough,R.W. and Woodward, R.J.(1967) "Analyses of Embankment Stresses and Displacements," Journal of the Soil Mechanics and Foundations Division, American Society of Civil Engineers, Vol.93, No.SM4, Proc.Paper 5329, July, 1967,pp. 529-550.

6 Diboj,M. and Penzien, I.(1969), "Response of Earth Dams to Travelling Seismic Waves," Journal of the Soil Mechanics and

Foundations Division American Society of Civil Engineers, Vol. No.95, No.SM2, Proc Paper No.6453, March,1969, pp.541-560.

7 Domaschuk,L. and Wade,N.H. (1969), "A Study of Bulk and Shear Moduli of a Sand," Journal of the Soil Mechanics and Foundations Division, American Society of Civil Engineers, Vol.No.95, No.SM2, Proc.Paper No.6461, March, pp. 561-581.

8 Duncan,J.M. and Chang, C.Y.(1970), "Nonlinear Analysis of Stress and Strain in Soils," Journal of the Soil Mechanics and Foundations Division, American Society of Civil Engineers, Vol.96, No.SM5, Proc.Paper 7513, September, 1970, pp.1629-1653.

9 Duncan J.M., and Clough,G.W.(1969). "Finite Element Analyses of Port Allen and Old Rher Locks," Report No.TE 69-3,0 Office of Research Services, University of California, Berkeley, September, 1969.

10 Duncan, J.M. and Dunlop,P.(1969), "Slopes in Stiff-Tissured Clays and Shales," Journal of the Soil Mechanics and Foundation Division, ASCE, Vol.94, No.SM2, Proc.Paper 6449,March,1969, pp.467-492.

11 Dunlop,P., Duncan, J.M. and Seed,H.B.(1968), "Curved Isoparametric, Quadrilateral Elements for Finite Element Analysis." International Journal of Solids and Structures, Vol.4,1968, pp.31-42.

12 Duncan,J.M., Monismith,C.L. and Wilson,E.L.(1968), "Finite Element Analyses of Pavements," Proceedings of the 1968 Annual Meeting of the Highway Research Board.

13 Ergatoudis,I., Irons,B.M., Zienkiewicz,O.C.(1968),"Curved Isoparametric, Quadrilateral Elements for Finite Element

Analysis," International Journal of Solids and Structures, Vol.4,1968,pp.31-42.

14 Ergatoudis,I.,Irons,B.M. and Zienkiewicz,O.C.(1968),"The Dimensional Analysis of Arch Dams and their Foundations, "Symposium on Arch Dams,Institute of Civil Engineers, London, March.

15 Felippa,C.A.(1966),"Refined Finite Element Analysis of Two-Dimensional Structures," Structural Engineering Laboratory Report 66-2, University of California, Berkeley, California, October.

16 Girijavallabham,C.V. and Reese,L.C.(1967), "Finite Element Method for Problems in Soil Mechanics," Journal of Soil Mechanics and Foundations Division, American Society of Civil Engineers, Vol.No.94,SM2,Proc. Paper No.5864, March,1968,pp. 473-496.

17 Goodman,L.E. and Brown,C.B.(1966) "Dead Load Stresses and the Instability of Slopes," Journal of the Soil Mechanics and Foundations Division, American Society of Civil Engineers, Vol.89, No.SM3, May,1966, pp.103-134.

18 Goodman,R.E., Taylor,R.L. and Brekke,T.L. (1968),"A Model for the Mechanics of Jointed Rocks," Journal of the Soil Mechanics and Foundations Division,American Society of Civil Engineers, Vol.94, No.SM3, May, pp. 637-668.

19 Holubec,I.(1968),"Elastic Behaviour of Cohesionless Soils," Journal of the Soil Mechanics and Foundations Division, American Society of Civil Engineers, Vol.94,No.SM6,Proc. Paper 6216,November, pp.1215-1231.

20 Idriss,I.M. and Seed,H.B.(1967), "Analysis of Soil Liquifaction : Niigata Earthquake," Journal of the Soil Mechanics and Foundations Division, American Society of Civil Engineers Vol.93, No.SM3, May, pp.83-108.

21 King,I.P.(1969), "On Finite Element Analysis of Two Dimensional Stress Problems with Time Dependent Properties,"Thesis presented to the University of California, in 1969, in Partial Fulfillment of the Requirements for the Degree of Doctor of Philosophy.

22 Konder,R.L./1963),"Hyperbolic Stress-Strain Response-Cohesive Soils," Journal of the Soil Mechanics and Foundations Division, American Society of Civil Engineers, Vol.80.No. SM1, 1963, pp. 115-143.

23 Konder,R.L. and Zelasko, I.S.(1963), "A Hyperbolic Stress Strain Formulation fon Sands," Proceedings, 2nd Pan American Conference on Soil Mechanics and Foundation Engineering,Vol. 1, 1963.

24 Konder,R.L. and Zelasko,IS.(1963), "Void Ratio Effects on the Hyperbolic Stress-Strain Response of a Sand," American Society of Testing Materials, STP No.361, Laboratory Shear Testing of Soils, Ottawa, pp.250-257,1963.

25 Perlof,W.H., Baladi,G.Y. and Harr,M.E.(1967) Stress Distribution within and under Long Elastic Embankments," High, Res. Record No.181, p.12.

26 Sandhu,R., Wilson,E.L. and Raphael,J.E.(1967), "Two Dimensional Analysis with Incremental Construction and Creep," Structural Engineering Laboratory Report No.67-74,University of California, Berkeley, California, December.

27 Vesic, A.S. and Clough,G.W.(1968), "Behaviour of Granular Materials Under High Stresses," Journal of the Soil Mechanics and Foundations Division, American Society of Civil Engineers, Vol.94,No.SM3, May, pp. 661-668.

28 Verrüjit,A.(1969), "Stresses Due to Gravity in an Elastic Half-Plane with Notches or Mounds," Drukkerij Wed.G.Wan Soest N.V.,Amsterdam.

29 Wilson,E.L.(1963),"Finite element Analysis of Two-Dimensional Structures," Thesis presented to the University of California, Berkeley, in 1963, in Partial Fulfillment of the Requirements for the Degree of Doctor of Engineering.

30 Woodward,R.J. (1966), "Analysis of Stresses and Displacements in Embankments with Non-Linear Material Properties, "Thesis presented to the University of California, Berkeley, in 1966, in Partial Fulfillment of the Requirements for the Degree of Doctor of Philosophy.

31 Zienkiewicz,O.C, Wallioppan,B.E. and King, I.P. (1968), "Stress Analysis of Rock as a 'No-Tension' Materials," Geotechnique, Vol.18,pp.56-66.

APPENDIX A

USER's MANUAL FOR PROGRAM, SOIL-STRUCT
INPUT DATA SEQUENCE

I. IDENTIFICATION CARD - FORMAT (17A4)

Cols. 2-80 Descriptive title of run

II. CONTROL CARD - FORMAT (1315, F5.1, F10.3)

a) Mesh Information

Cols. 3-5 NUMNP - Total number of nodal points in mesh (maximum 620)

Cols. 8-10 NUMEL - Initial number of elements in mesh including interface elements(max.620) Shoring elements (to be added during execution) are not included in NUMEL

Cols.13-15 NUMJT - Total number of interface elements (maximum 350)

b) Material type information

Cols.19-20 NUMMAT - Total number of material types required during execution of program including interfaces (maximum 30)

Cols.24-25 NUMSOL - Total number of material types for elements other than interface elements (maximum 20)

c) Job control parameters

Cols.26-30 NC - Number of loading and construction steps in analysis

Col. 35 NMOD - Code for type of modulus specification input NMOD=0 modulus specification to be input as per Section IV;NMOD=1 modulus specification to be input as per Sec.V

Col. 40 INIT - Code describing how initial stresses for the run are to be obtained
INIT=1 calculated by computer from a gravity turn-on analysis
INIT=0 read from cards placed after element cards in input data deck (see Section XV)

Col. 45 KI - Code for interface element activation during initial stress calculation (INIT=1)
KI=1 interface elements activated
KI=0 interface elements not activated

Col. 50 IHORIZ - Code for level or sloping initial surface
IHORIZ=1 sloping ground surface, stresses calculated from gravity turn-on assuming linear elastic response of soil
IHORIZ=0 horizontal ground surface, vertical stresses computed from gravity turn-on; horizontal stresses may be modified to arbitrary values through k_o specified for material, otherwise they will equal $\left[\nu/1-\nu\right].(\sigma_y)$

d. Printout Parameters

Col. 55 ITRD - Code for printout of results
ITRD=1 results for every iteration are printed out

ITRD=0 only results for final iteration are printed out.

Col. 60 ILIST - Code for printout of nodal point and and element card data
ILIST=1 data printed out
ILIST=0 printout suppressed

Col. 65 IPUNCH - Code for punchout of results of analysis (stresses,etc.) which are ordinarily used as input for subsequent stages of analysis(INIT=0)
IPUNCH=1 results punched on cards
IPUNCH=0 no cards punched

e) Basic parameters

Cols.66-70 GAMW - Unit weight of water

Cols.71-70 PATM - Atmospheric pressure

III.MATERIAL ALLOCATION CARD - FORMAT 5(I10)

Cols. 1-10 NATYP - Material type number for air (50 if not used)

Cols. 11-20 NCTYP - Material type number for structural material (50 if not used)

Cols.21-30 NBITYP - Material type number for backfill type 1 (50 if not used)

Cols.31-40 NB2TYP - Material type number for backfill type 2 (50 if not used)

Cols.41-50 NBAR - Material type number for one-dimensional strut or anchor bar material (50 if not used)

IV. LOADING INFORMATION CARD-FORMAT (415,15A4)

One card is supplied for each loading step. One or two different loading, types can be executed simultaneously for each loading step .

Col. 5 KCS(N,1) First loading type code

The codes used to denote the different loading types are as follows:

1 - Excavation

2 - Build-up

3 - Seepage loading

6 - Boundary pressure loading

7 - Temperature loading

8 - Concentrated force or displacement loading

9 - Change of material type

Col. 10 KCS(N,2) - Second loading type code (Codes are same as for KCS(N,1). Set to zero if there is no second loading phase in the current loading step.

Cols.11-15 NUMIT(N) - Number of iterations for each loading step (may be different for different steps.

Col. 20 MOD(1,N) - Modulus calculation code for the loading step. This code is only applicable if NMOD=0; set to zero if NMOD=1. Consult Sec. V for case of NMOD=1. The MOD codes used are as follows:

1-loading modulus to be calculated for all elements

2-unload-reload modulus to be calculated for all elements

0-computer decides type of modulus for each element depending on whether the most recently calculated maximum shear stress exceeds all previous shear stresses calculated for the element or not. If they are exceeded, a loading modulus is calculated for the next loading step, otherwise an unload-reload modulus is used.

Cols.21-80 HED(1)-Description of the nature of the loading step-use alphabetic characters if desired.

V. MODULUS SPECIFICATION CARDS FORMAT (40I2)

These cards are required only when NMOD=1

Cols. 2,4,6,8,10,.. - Modulus calculation codes for each material type (1 to NUMSOL) for the first loading step. The modulus calculation codes are the same as those defined on the Loading Information Card in Section IV.

Use a new card to specify the modulus calculation codes for each loading step (1 to NC).

VI.MATERIAL PROPERTY INFORMATION CARD NO 1-FORMAT (F10.5)-I10

Material property information cards nos.1 and 2 are placed one after the other in the input deck for each material type.

Cols. 1-10 GUI(N) - Poisson's ratio (before failure)

Cols. 11-20 GUF(N) - Poisson's ratio (at failure-no greater than 0.49)

Cols. 21-30 GAM(N) - Total unit weight (always specified regardless of drained or undrained material behavior)

Cols. 31-40 FR(N) - Correlation factor; ratio of strength at failure to ultimate strength from hyperbolic stress strain curve.

Cols.41-50 AO(N) - K_o-coefficient of lateral earth pressure at rest.

Cols.51-60 PHI(N) - Friction angle (degrees)

Cols. 61-70 XXP(N) - Exponent n (zero for simple elastic material)

Col. 80 INDRAIN(N) Code defining drainage conditions
1=drained material behavior
0=undrained material behavior

VII. MATERIAL PROPERTY INFORMATION CARD NO 2-FORMAT (3F10.3, F20.5, F20.10)

Cols. 1-10 HCOEF(N) Coefficient K_m in equation expressing values of initial tangent modulus as a function of confining pressure

$$E_i = P_a K_m \left(\frac{\sigma 3}{P_a}\right)^n$$

Cols. 11-20 ULCOEF(N) Coefficient K_{ur} in equation expressing values of unload-reload modulus as a function of confining pressure

$$E_{ur} = P_a K_{ur} \left(\frac{\sigma_3}{P_a}\right)^n$$

Cols. 21-30 COHE(N) - Cohesion

Cols. 31-50 E(N) - Tangent modulus at failure nonlinear (nonelastic) materials. Typical value= 100 psf OR Young's modulus for structural or simple elastic materials.

Cols. 51-70 ALPHA(N)- For structural element material specify coefficient of linear thermal expansion.For bar or strut element material, specify the cross sectional area of the bar or strut element divided by the horizontal spacing. Zero otherwise

Note: The stiffness of the struts (tie-backs) are computed as $\frac{EA}{L}$ in the program. For elements with different x-sectional areas from that specified in ALPHA(N) the strut (tie-back) length may be artificially adjusted to produce the correct stiffness when calculated in the program.

VIII.INTERFACE PROPERTY CARD-FORMAT (3F10.5)

One card is supplied for each interface material type. For the case of no interface material types, no cards are required.

Cols. 1-10 PHJ(N) - Interface friction angle (degrees)

Cols. 11-20 RKS(N) - Shear stiffness before failure

Cols. 21-30 COJ(N) - Cohesion

IX.NODAL POINT CARD - FORMAT (I10,4F10.2)

One card is supplied for each nodal point

Cols. 1-10 N - Nodal point number

Cols. 11-20 X(N) - X-coordinate, + to right

Cols. 21-30 Y(N) - Y-coordinate, + upwards

Cols. 31-40 PP(N) - Pore prussure in head of water Zero otherwise (pore pressures need not be specified for undrained materials but must be for drained materials)

Cols 41-50 DP(N) - Change in pressure in head of water for soil elements; change in temperature for structural material
Zero otherwise

Nodal point numbers may be omitted, in which case those omitted are generated automatically at equal spacings between the nodal points specified. The first and last nodal points must always be specified.

X.BOUNDARY CONDITIONS CARD NO - FORMAT (3I10)

Cols. 1-10 NOY - Number of nodal points fixed against Y movement only

Cols. 11-20 NOX - Number of nodal points fixed against X movement only

Cols. 21-30 NOXY - Number of nodal points fixed against X and Y movement

Specific nodal point numbers should not be included in NOY or NOX and in NOXY, but are specified in the following cards.

XI. BOUNDARY CONDITIONS CARD NO. 2-FORMAT (8I10)

Cols. 1-10 IC(N) - First nodal point number to be fixed against Y Movement.

11-20 IC(N) - Second nodal point number to be fixed against Y movement.

Repeat for next six fields and continue on additional cards if necessary. Nodal point numbers should be sequential.

XII. BOUNDARY CONDITIONS CARD NO.3 - FORMAT (8I10)

Cols. 1-10 IC(N) First nodal point number to be fixed against X movement.

Repeat for next seven fields and continue on additional cards if necessary. Nodal point numbers should be sequential.

XIII. BOUNDARY CONDITIONS CARD NO. 4 FORMAT (8I10)

Cols. 1-10 IC(N) First Nodal point number to be fixed against X and Y movement

Repeat for next seven fields and continue on additional cards if necessary. Nodal point numbers should be sequential.

XIV. ELEMENT CARD-FORMAT (6I10)

One card is supplied for each element.

Cols. 1-10 N Element number

11-20 IL(N,1) Number of nodal point I

21-30 IL(N,2) Number of nodal point J

31-40 IL(N,3) Number of nodal point K

41-50 IL(N,4) Number of nodal point L

51-60 IL(N,5) Material type number

No bar or strut elements are to be included in these cards. These elements are added later during incremental loading.

Interface elements whould be numbered first; the other elements follow.

The nodal point numbers must be specified proceeding counterclockwise around the elements. The first and last nodal point numbers for interface elements must be adjacent nodes.Triangular shaped two dimensional elements having 4 nodal points may not be used. The first and last nodal points of a triangular element should be the same. The nodal point numbers fon any element may not differ by more than 30. For convenience, element numbers may be omitted, in which case those missing will be generated by incrementing the nodal point number by one and assigning the same material type number as the last element specified. The first and last elements must always be specified.

XV.CONTINUATION OR INITIALIZATION CARDS

These cards are supplied if INIT=0 and would normally be obtained as punched output from the previous part of the analysis. This option is provided principally so that an incremental analysis sequence may be stopped at intermediate steps and restarted from that step without redoing the whole analysis. However, these cards may also be used to supply particular initial values of these variables without using the gravity turn on procedure followed with INIT=1.

FIRST CARD FORMAT (2I5)

Cols. 1-5 NUMEL - Total number of elements including interface elements and strut and bar elements added in the intermediate steps in the analysis.

6-10 IQ - Number of elements excluding strut and bar elements already added in the analysis.

SECOND CARD FORMAT (8F10.2)

Different information is specified on each card depending on whether the element is a 2-dimensional, interface or strut or bar element.

Cols. 1-10 SIG(N,1)- X-stress value for 2-dimensional element. Shear stress for interface element. Force for 1-dimensional element.

11-20 SIG(N,2)- Y-stress value for 2-dimensional element. Normal stress for interface element. Length for 1-dimensional element.

21-30 SIG(N,3)- X-Y shear stress value for 2-dimensional element. Zero for interface element. Cos α for anchor or bar element(where α is the engle the element makes with the horizontal axis).

31-40 SIG(N,4)- Maximum previous shear stress value 2-dimensional element. Zero for interface element. Sin α for anchor or bar elemen

Use the next 4 fields for the following element. Continue on additional cards spacifying two elements per card.

THIRD CARD FORMAT (9F8.3)

Cols. 1-8 DISP(N,1) X displacement

9-16 DISP(N,2) Y displacement

17-24 PP(N) Pore pressure in head of water.

Use the next 6 fields for the following 2 nodes. Continue on additional cards specifying 3 nodal points per card.

FOURTH CARD FORMAT (1515)

Cols. 1-5 IL(N,5) Material type number

Use the next 14 fields for the material type number of the following 14 elements. Continue on additional cards specifying 15 material type numbers per card.

FIFTH CARD FORMAT (1515)

These cards are supplied only if IQ ≠ NUMEL

Cols. 1-5 IL(N,1) First nodal point of first bar or strut element installed in previous part of the analysis.

6-10 IL(N,2) Second nodal point of first bar or strut element installed in previous part of the analysis.

Use the next 13 fields for the following elements and continue on additional cards if necessary.

SIXTH CARD FORMAT(8E10.4)

Supply these cards only if NUMJT ≠ 0

Cols. 1-10 STFS(N) Shear stiffness for interface element 1.

11-20 STFN(N) Normal stiffness for interface element 1.

Use the next 6 fields for the shear and normal stiffnesses of the following 3 elements. Continue on additional cards specifying 2 stiffnesses for 4 elements per card.

XVI. LOADING AND CONSTRUCTION STEP CARDS (supplied only if NC ≠ 0)

(A) EXCAVATION CARDS

These cards are supplied only if KCS(N,1) or KCS(N,2)=1

FIRST CARD - FORMAT (I10)

cols. 1-10 NEL Number of elements to be excavated

SECOND CARD - FORMAT (8I10)

Cols. 1-10	LUL(N,1)	Element to be excavated (also the first interpolation element)
Cols. 11-20	LUL(N,2)	Second interpolation element
Cols. 21-30	LUL(N,3)	Third interpolation element
Cols. 31-40	LUL(N,4)	Fourth interpolation element
Cols. 41-50	LUL(N,5)	Loading code for node I 0 - node I is not loaded by excavation forces 1 - node I is loaded by excavation forces

Loading codes for nodes J,K, and L are specified in the next 3 fields. The loading code should be set to 1 only if the node is common to both an excavated and an unexcavated element.

The interpolation elements are numbered in criss-cross fashion.

If the element to be excavated has no cmmon boundary with an unexcavated element then only the element number, LUL(N,1), needs to be specified on the card-the interpolation elements and loading codes ned not be specified. Interpolation elements and loading codes are never required for excavated interface elements.

The cards for the excavated elements should be ordered as follows:

(1) Interface elements

(2) 2-D elements which have no common boundary with unexcavated elements

(3) 2-D elents which have a common boundary with unexcavated elements.

If possible the cards for the excavated elements should be ordered so that the cards of elements with common boundaries are adjacent to one another.

(B) FILL OR CONCRETE PLACEMENT STEP CARDS

These cards are supplied only if KCS(N,1) or KCS(N,2)=2

FIRST CARD - FORMAT (1615)

Cols. 1-5 NLEL Total number of elements to be placed including interface elements

Cols. 6-10 LEL(N) Element number to be pleced

Cols. 11-15 LEL(N) Element number to be placed

Use the next 13 fields for the following 13 elements to be placed. Continue on additional cards if necessary.

The elements should be read in by material type numbers according to the following sequence:

1) Structural elements
2) Elements of backfill type 1
3) Elements of backfill type 2
4) Interface elements to be "activated"
5) Interface elements to be left "inactive" but to be placed between elements of like materials.

SECOND CARD - FORMAT (15)

Cols. 1-5 NJ - Number of elements to be placed less the number of "inactive" interactive elements to be placed

THIRD CARD - FORMAT (1615)

Cols. 1-5 NONP - Number of nodal points within the newly

placed layer(s) to be assigned zero displacements. This includes all nodal points of the elements to be placed except those nodal points in common with the already existing element.

Cols. 6-10 NP(N) Nodal point number to be assigned zero displacement

Cols. 11-15 NP(N) Nodal point number to be assigned zero displacement

Use the next 13 fields for the following 13 nodal points to be assigned zero displacement. Continue on additional cards if necessary.

Nodal point numbers should be in sequential order.

FOURTH CARD - FORMAT (2I10,F10.2)

Cols. 1-10 NCE Number of structural material elements to be placed.

11-20 NBIE Number of backfill type 1 elements to be placed.

21-30 HTB New Y coordinate on top of backfill.

(C) SEEPAGE LOADING STEP CARDS

These cards are supplied only if KCS(N,1) or KCS(N,2)=3.

FIRST CARD - FORMAT (I10)

Col. 10 NCODE Code specifying option for reading in seepage loading data.

0-Seepage loadings are specified by DP(N) on Nodal Point Cards.

No further seepage loading cards are required. 1-Seepage loading is specified by change in phreatic surface and the seepage loading data must be read from the SECOND and THIRD CARDS described subsequent

SECOND CARD - FORMAT (I10)

Cols. 1-10 NWAT Number of levels required to approximate the new phreatic surface.

THIRD CARD - FORMAT (3F10.2)

Cols. 1-10 XW(L) X coordinate bounding the levels PREL(I) and FUEL(I) on the right hand side

11-20 PREL(I) Present level of phreatic surface

21-30 FUEL(I) New level of phreatic surface

Continue on new cards from 1 to NWAT for each different surface level approximating the phreatic surface.

(D) BOUNDARY WATER PRESSURE STEP CARDS

These cards are supplied only if KCS(N,1) or KCS(N,2)=6

FIRST CARD - FORMAT (I10)

Cols. 1-10 NWPF Number of elements loaded with boundary pressures.

SECOND CARD - FORMAT (3(2I8,F8,2))

Cols. 1-8 IBC(L) Nodal point on the left on the element boundary when viewed in the same direction as the applied pressure.

Cols. 9-16 JBC(L) Nodal point on the right of the element boundary when viewed in the same direction as the applied pressure.

Cols. 17-24 PR(L) Average normal pressure (always positive).

Use the next six fields for the following two elements and continue of additional cards if necessary.

(E) TEMPERATURE LOADING STEP CARDS

Temperature loadings are generated only when

KCS(N,1) or KCS(N,2) = 7

On additional cards are necessary. Tempetarure loadings must be specified through PP(N) on the NODAL POINT CARDS.

(F) CONCENTRATED FORCE OR DISPLACEMENT STEP CARDS

These cards are supplied only if KCS(N,1) or KCS(N,2)=8

FIRST CARD - FORMAT (I10)

Cols. 1-10 NCL Number of concentrated forces or displacements to be specified.

SECOND CERD - FORMAT (2(I10,2F10.5))

Cols. 1-10 N Nodal point

Cols. 11-20 FX(N) Component of concentrated force of displacement in X direction. (+ and to the right)

Cols. 21-30 FY(N) Component of concentrated force or displacement in Y direction (+ and upwards)

Use the next three fields for the following concentrated force or displacement. Continue on additional cards if necessary.

(G) MATERIAL TYPE ALTERATION STEP CARDS.

These cards are supplied only if KCS(N,1) or KCS(N,2)=9.

The material type alteration is made before the execution of the loading step on which it is specified.

FIRST CARD - FORMAT (I10)

Cols. 1-10 NELCH Number of elements to be altered to a new material type number.

SECOND CARD - FORMAT (16I5)

Cols. 1-5 LUL(I,1) Element number

Cols. 6-10 LUL(I,2) New material type number

Use the next 14 fields for the following seven elements and continue on additional cards if necessary.